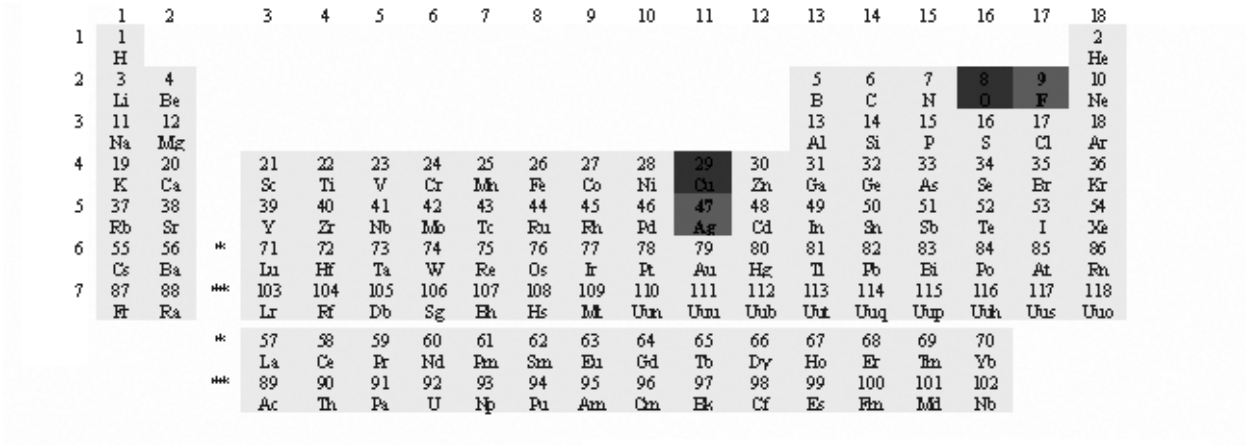


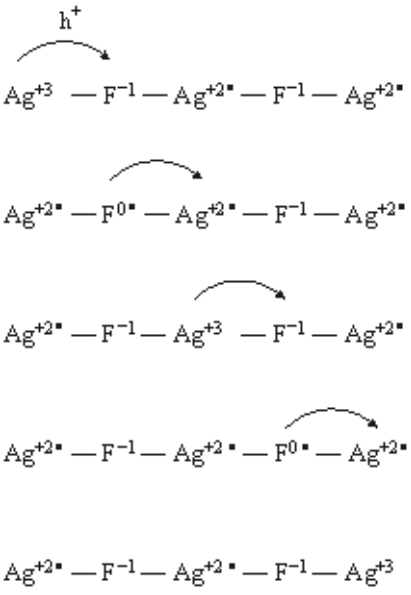


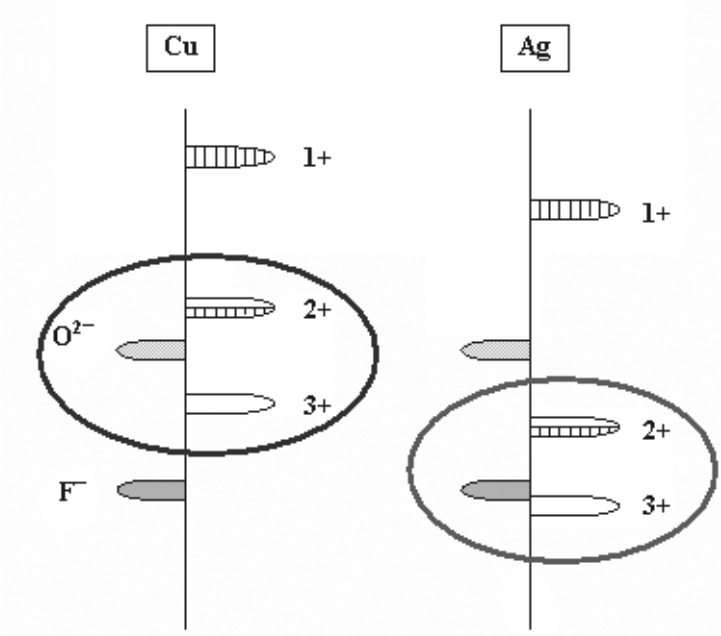


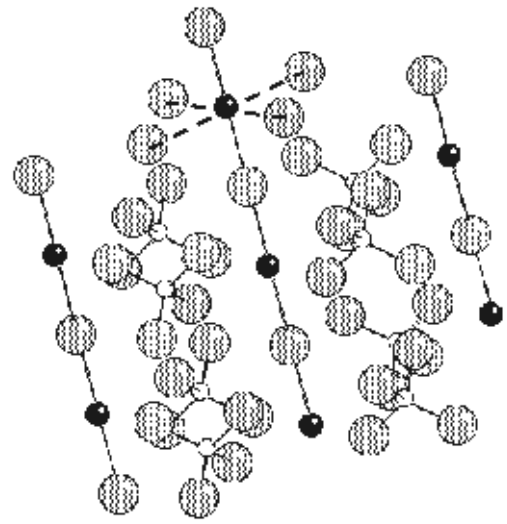

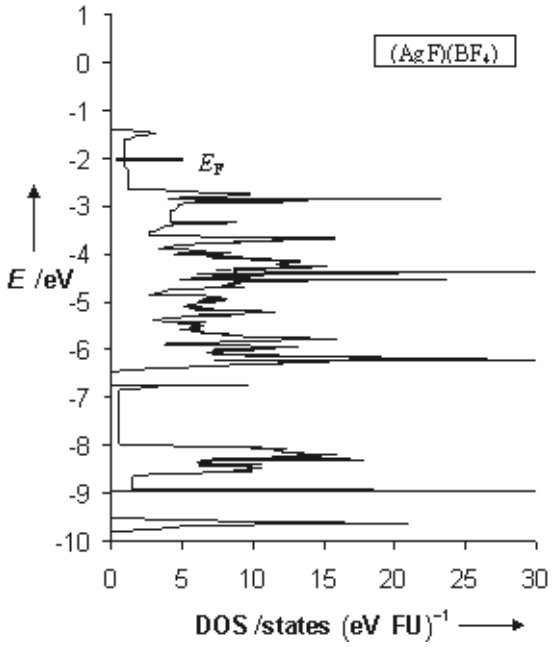

# Real and Hypothetical Intermediate-Valence $Ag^{II}/Ag^{III}$ and $Ag^{II}/Ag^{I}$ Fluoride Systems as Potential Superconductors

**Wojciech Grochala and Roald Hoffmann***

*Dedicated to Professor Neil Bartlett,*
*with our deep admiration for his chemistry—he made molecules which were unimaginable*

With the aim of gauging their potential as conducting or superconducting materials, we examine the crystal structures and magnetic properties of the roughly one hundred binary, ternary, and quaternary $Ag^{II}$ and $Ag^{III}$ fluorides in the solid state reported up to date. The $Ag^{II}$ cation appears in these species usually in a distorted octahedral environment, either in an $[AgF]^+$ infinite chain or as $[AgF_2]$ sheets. Sometimes one finds discrete square-planar $[AgF_4]^{2-}$ ions. The $Ag^{III}$ cation occurs usually in the form of isolated square-planar $[AgF_4]^-$ ions. Systems containing $Ag^{III}(d^8)$ centers are typically diamagnetic. On the other hand, the rich spectrum of $Ag^{II}(d^9)$ environments in binary and ternary fluorides leads to most diverse magnetic properties, ranging from paramagnetism, through temperature-independent paramagnetism (characteristic for half-filled band and metallic behavior) and antiferromagnetism, to weak ferromagnetism. $Ag^{II}$ and $Ag^{III}$ have the same d-electron count as $Cu^{II}(d^9)$ and $Cu^{III}(d^8)$, respectively. $F^-$ and $O^{2-}$ ions are isoelectronic, closed-shell ($s^2p^6$) species; both are weak-field ligands. Led by these similarities, and by some experimental evidence, we examine analogies between the superconducting cuprates ($Cu^{II}/Cu^{III}-O^{2-}$ and $Cu^{II}/Cu^{I}-O^{2-}$ systems) and the formally mixed-valence $Ag^{II}/Ag^{III}-F^-$ and $Ag^{II}/Ag^{I}-F^-$ phases. For this purpose we perform electronic-structure computations for a number of structurally characterized binary and ternary $Ag^{I}$, $Ag^{II}$, and $Ag^{III}$ fluorides and compare the results with similar calculations for oxocuprate superconductors. Electronic levels in the vicinity of the Fermi level ($x^2-y^2$ or $z^2$) have usually strongly mixed Ag(d)/F(p) character and are Ag–F antibonding, thus providing the potential of efficient vibronic coupling (typical for $d^9$ systems with substantially covalent bonds). According to our computations this is the result not only of a coincidence in orbital energies; surprisingly the Ag–F bonding is substantially covalent in $Ag^{II}$ and $Ag^{III}$ fluorides. The electron density of state at the Fermi level ($DOS_F$) for silver fluoride materials and frequencies of the metal–ligand stretching modes have values close to those for copper oxides. The above features suggest that properly hole- or electron-doped $Ag^{II}$ fluorides might be good BCS-type superconductors. We analyze a comproportionation/disproportionation equilibrium in the hole-doped $Ag^{II}$ fluorides, and the possible appearance of holes in the F(p) band. It seems that there is a chance of generating an $Ag^{III}-F^-/Ag^{II}-F^0$ "ionic/covalent" curve crossing in the hole-doped $Ag^{II}-F^-$ fluorides, significantly increasing vibronic coupling.

**Keywords:** conducting materials · electronic structure · fluorides · silver · superconductors

## 1. Introduction

This paper builds to a claim and a prospect. Both are based on theoretical considerations and chemical reasoning. The claim is that the Ag–F bonding in $Ag^{III}$ and (to lesser extent) $Ag^{II}$ fluorides is substantially covalent. The prospect is that such high oxidation-state silver fluorides might be superconducting, if modified in certain ways. But before we get to the evidence and argument, some beautiful synthetic and structural work on the known binary and ternary $Ag^{II}$ and $Ag^{III}$ fluorides has to be reviewed.[1]

About a hundred binary, ternary, and quaternary silver fluorides are known, among them six binary species: $Ag_2F$, AgF, $AgF_2$, $Ag_2F_5$, $Ag_3F_8$, and $AgF_3$. The reasons for interest in silver fluorides in various oxidation states vary. For $Ag_2F$ (silver subfluoride) its metallic conductivity[2, 3] and super-

[*] Prof. Dr. R. Hoffmann, Dr. W. Grochala
Department of Chemistry and Chemical Biology
and Cornell Center for Materials Research
Cornell University, Ithaca NY, 18453-1301 (USA)
Fax: (+1) 607-255-5707
E-mail: rh34@cornell.edu

  1433-7851/01/4015-2743 $ 17.50+.50/0 

conductivity[4] have been the focus, while AgF has been studied in context of $Ag^+$ ion diffusion,[5] phase transitions under elevated pressure,[6–10] and with relevance to photographic development.[11] On the other hand, $Ag^{II}$ compounds are of interest because of the enormous oxidizing properties of $Ag^{II}$ centers,[12, 13] as well for the disproportionation of $Ag^{II}$ to $Ag^{I}$ and $Ag^{III}$. For example, $AgF_2$ is known in both the disproportionated (high-temperature) $Ag^{I}[Ag^{III}F_4]$[14] and nondisproportionated (low-temperature) $Ag^{II}F_2$ form.[15] The higher silver fluorides ($Ag_2F_5$, $Ag_3F_8$, and $AgF_3$) were first prepared in 1991;[16] all of them have been structurally characterized.[17–19]

$Ag^{II}$ is a unique species. It is peculiar to fluorine systems,[20] and disproportionates to $Ag^{I}$ and $Ag^{III}$ in oxides.[21–23] The $Ag^{II}$ ion is also an extremely strong oxidizing agent, one of the most powerful known. For example, cationic $Ag^{II}$ in anhydrous HF solutions oxidizes $Xe^0$ to $Xe^{II}$.[24, 25] The $Ag^{III}$ ion is common to fluoride systems, as well, in agreement with the rule that fluorine stabilizes high oxidation states of most elements. Cationic $Ag^{III}$ in anhydrous HF solutions is an even stronger oxidizing agent than $Ag^{II}$; it oxidizes $[MF_6]^-$ (M = Pt, Ru) to $MF_6$.[26] Solvated $Ag^{III}$ is an oxidizer of unsurpassed power, better than $Kr^{II}$,[27] and (together with solvated $Ni^{IV}$) probably the best oxidizing agent available in inorganic chemistry.

In the last two decades, the chemistry of $Ag^{II}$ and $Ag^{III}$ fluoride systems has developed significantly. New, previously unknown systems such as $Ag^{I}[Ag^{III}F_4]$,[14] $[Ag^{II}F]^+[SbF_6]^-$,[28] and $[Ag^{II}F]^+[BF_4]^-$[29] (the latter is probably metallic) have been synthesized. The chemistry of $Ag^{II}$ and $Ag^{III}$ has recently inspired the first successful efforts to stabilize the rare $Au^{II}$ center in fluoride complexes.[30] The chemistry of another powerful oxidizer, $Ni^{IV}$, has also developed.[31]

$Ag^{II}$ is isoelectronic with $Cu^{II}$ ($d^9$ configuration). $F^-$ and $O^{2-}$ are isoelectronic ions, closed-shell species; both $F^-$ and $O^{2-}$ are weak-field ligands. These similarities inspired our theoretical investigations. Given the existence of the superconducting cuprates ($Cu^{II}/Cu^{III}-O^{2-}$ systems), one might be naturally interested in the analogous $Ag^{II}/Ag^{III}-F^-$ solids. As we will show, $Ag^{II}$–$F^-$ bonds are substantially covalent (similar to $Cu^{II}$–$O^{2-}$ bonds), thus providing potentially large values of a vibronic coupling constant in a crystal.[32]

To investigate theoretically the possible occurrence of superconductivity in one-dimensional (1D) and two-dimensional (2D) Ag–F nets, we compute density of states (DOS) and the composition of states near the Fermi level for some selected Ag–F systems and compare these with corresponding calculations for the cuprate superconductors. Subsequently we look at $Ag^{I}$, $Ag^{II}$, and $Ag^{III}$ fluoride systems analogous to the isoelectronic fluorides, chlorides, and oxides of Cu and Au. We also consider hypothetical intermediate-valence (comproportionated) $Ag^{II}/Ag^{I}$ or $Ag^{II}/Ag^{III}$ systems and the mixed-valence (disproportionated, Peierls-distorted) ones. The design of class III[33] or class II[33] $Ag^{II}/Ag^{I}$ or $Ag^{II}/Ag^{III}$ fluoride systems might eventually provide us with an understanding of the conditions for strong dynamic band-gap opening at the Fermi level, possibly leading to superconductivity. We show, however, that such intermediate-valence $Ag^{II}/Ag^{I}$ and $Ag^{II}/Ag^{III}$ systems will not be easy to reach in practice. In a separate contribution we will propose a number of so-far unknown quaternary, possibly intermediate-valence $Ag^{II}/Ag^{III}$ and $Ag^{II}/Ag^{I}$ fluorides.

## 2. Contents

The Review is organized as follows: in Sections 3.1 and 3.2 we review the experimental data on the known binary and ternary $Ag^{II}$ and $Ag^{III}$ fluorides. In Section 3.3 we present

*Roald Hoffmann was born in 1937 in Złoczów, Poland. He came to the USA in 1949 and studied chemistry at Columbia University and Harvard University (Ph.D. 1962). Since 1965 he has been at Cornell University, now as the Frank H. T. Rhodes Professor of Humane Letters. He has received many of the honors of his profession, including the 1981 Nobel Prize in Chemistry (shared with Kenichi Fukui). He also has a career as a writer, that profession sometimes overlapping his chemistry, sometimes not. He writes poems, essays, nonfiction, and plays. His interest in chemistry was stimulated by the life of Maria Skłodowska Curie, and he has learned nearly all he knows about silver fluorides from another Pole, his coauthor.*


R. Hoffmann


W. Grochala

*Wojciech Grochala was born in Warsaw (Poland), in 1972. He received his Ph.D. degree from the University of Warsaw in 1998, and came to Cornell University (US) as a postdoctoral fellow in 1999. His studies on resonance Raman spectroscopy with Prof. Jolanta Bukowska initiated his interest in vibronic coupling. He studied chemical aspects of this phenomenon with Prof. Roald Hoffmann, with support from The Kosciuszko Foundation. His research then focused on prediction of new superconducting materials in the solid state. He is currently working with Prof. Peter P. Edwards as a Royal Society Fellow at the University of Birmingham (UK), searching for experimental evidence of superconductivity in doped $Ag^{II}$ fluorides.*

results of density functional theory (DFT) band-structure calculations for a selection of the experimental structures. In Section 3.4 we examine analogies and differences in geometric and electronic structure between well-known superconducting oxocuprates and Ag–F systems. We also look here at $Ag^{I}$, $Ag^{II}$, and $Ag^{III}$ fluorides from the perspective of analogous fluorides, chlorides, and oxides of Cu and Au. In Section 3.5 we analyze our DFT electronic-structure calculations for several structurally characterized binary and ternary $Ag^{II}$ and $Ag^{III}$ fluorides in the context of potential superconductivity in these systems. We also discuss the comproportionation–disproportionation equilibrium in the hole- and electron-doped $Ag^{II}$ fluorides. Finally, in Section 3.6 we briefly discuss a general "chemical" strategy to obtain intermediate-valence $Ag^{II}/Ag^{III}$ and $Ag^{II}/Ag^{I}$ silver fluoride compounds.

## 3. Results and Analysis

### 3.1. Review of Structural Data for Binary and Ternary $Ag^{II}$ and $Ag^{III}$ Fluorides

We begin by looking at the structure and magnetic properties of all experimentally known binary and ternary $Ag^{II}$ and $Ag^{III}$ fluorides. This is not just a review, but a reasoned preparation for an exploration of the suitability of Ag–F chemistry for expanding the known repertoire of inorganic superconductors.

#### *3.1.1. Structures Containing Magnetically Isolated $Ag^{II}$ Centers*

There are known over twenty ternary and quaternary fluorides containing magnetically isolated $Ag^{II}$ centers.[34] They belong to five principal types:

a) $Ag^{II}[MF_4^-]_2$, M = Ag,[16] Au;[19, 35]
b) $Ag^{II}[MF_6^-]_2$, M = Bi,[28] Sb,[36, 37] Ru/Bi,[28] Nb,[38] Ta;[38]
c) $Ag^{II}[MF_6^{2-}]$, M = Ge,[39] Sn,[18, 39, 40] Pb,[39, 40] Ti,[18, 39] Zr,[39, 40] Hf,[39] Rh,[39] Pd,[18, 39, 41] Pt,[18, 39, 41] Mn[42] Cr[43]
d) $Ag_3M_2F_{14}$, M = Hf,[44] Zr[44]
e) $K_3Ag_2M_4F_{23}$, M = Hf,[45] Zr.[45]

In addition, isolated $Ag^{II}$ centers occurs in $NaAgZr_2F_{11}$, the only known member of a $M^{I}Ag^{II}Zr_2F_{11}$ series.[46, 47] Properties and structural data for these solids are listed in Table 1.

Although $AgMF_6$, M = Zr, Hf, are claimed in refs. [39, 40], in fact they have not been synthesized so far. Prof. B. G. Müller writes about these compounds in a personal communication to us:

"Trying to synthesize $AgMF_6$ (M = Zr, Hf) similar to other compounds of the same formular type by reaction of a mixture of, for example, $Ag_2SO_4 + 2\,ZrOCl_2 \cdot 8\,H_2O + F_2/Ar$ at higher temperature one obtains deep blue–violet powder samples of $Ag_3Zr_2F_{14} + ZrF_4$ (*together* giving the analytical value of "$AgZrF_6$"). At that time all powder patterns were very complex, so it was not possible to identify for example $ZrF_4$ or other compounds. Later I found out by single-crystal structure determination that obviously $Ag_3Zr_2F_{14}$ was the only product." [*]

Those substances which contain nonmagnetic dopants (such as $Ti^{4+}$ or $Sb^{5+}$ ions) are typical dilute one-electron paramagnets (the $Ag^{II}$ centers are magnetically isolated) and obey the Curie–Weiss law with $\mu_{eff} = 1.8–2.1\ \mu_B$. The largest deviation from Curie-law behavior is observed for $AgTiF_6$ (Curie constant $\Theta = -70$ K).[48] The magnetic behavior of compounds with magnetic dopants (such as $Ru^{5+}$ or $Mn^{4+}$ ions) is more complex. The $Ag^{II}$ cation is found in these substances usually in the elongated octahedral (4+2) environment.[49, 50] A typical $Ag^{II}$–$F^-$ bond length is 2.00–2.15 Å. Two additional, more weakly bound, fluoride anions typically coordinate the $Ag^{II}$ centers at 2.35–2.44 Å. Such coordination of $Ag^{II}$ most often results in a deep blue color of these compounds.

$AgSb_2F_{12}$ is a very interesting substance. It occurs in both paramagnetic $\alpha$-$AgSb_2F_{12}$[36] and diamagnetic $\beta$-$AgSb_2F_{12}$ form.[37, 51] The structure of the $\alpha$ form is shown in Figure 1. The formula $Ag^{I}Ag^{III}[SbF_6^-]_2$ has been suggested[37] for the $\beta$ form. Mixed-valence (and not intermediate-valence) character of the $\beta$ form might be confirmed, for example, by the (2+4) and (4+2) local environments for the $Ag^{I}$ and $Ag^{III}$ centers, respectively.[52] Unfortunately, there is still no structural data for the $\beta$-$AgSb_2F_{12}$ form. Valence isomerism in $AgSb_2F_{12}$ is not improbable. A similar phenomenon has been observed for $AgF_2$ (see Sections 3.1.4 and 3.6.1)[15, 16] and for $Ag[Ag(CF_3)_4]$.[53] Existence of a mixed-valence $AgSb_2F_{12}$ form then would be the third interesting example of this subtle redox equilibrium in $Ag^{II}$–$F^-$ systems.

Compounds in the $Ag_3M^{IV}_2F_{14}$ family (M = Zr, Hf) contain two types of nonequivalent Ag atoms (Figure 2). The isolated Ag(1) atom has a typical elongated octahedral coordination. The Ag(2) atom occurs in distorted tetragonal (1+1+2) coordination, with two shorter (1.997–2.092 Å) and two longer (2.147 Å) Ag–F bonds (we neglect here four very long distances of 2.6–2.8 Å; their inclusion leads to an unusual hexagonal bipyramidal coordination of the Ag center by F atoms). Two Ag(2) atoms are linked together in a linear $[Ag_2F_3]^+$ ion (we neglect here all the Ag–F contacts of 2.147 Å). The formula of this compound might be tentatively written as $[Ag_2F_3]^+Ag^{II}[Hf_2F_{11}]^{3-}$. The presence of the $[Ag_2F_3]^+$ unit links the $Ag_3M^{IV}_2F_{14}$ family of compounds to those containing $[Ag^{II}–F^-]$ infinite chains (see next Section).[54]

Quaternary compounds $K_3Ag_2M_4F_{23}$, M = Zr, Hf (Figure 3) provide still another example of an "unusual" coordination at $Ag^{II}$ centers: a pentagonal bipyramid. Isolated bipyramids are strongly distorted, with equatorial distances of $2 \times 2.04$ Å, 2.29 Å, and $2 \times 2.64$–2.67 Å, and axial ones of 2.20–2.25 Å. Neglecting two very long contacts of 2.64–2.67 Å gives us an

[*] Here, and elsewhere in the paper, we show in boxes the comments of Neil Bartlett and Berndt G. Müller (private communication, August–September 2000) on the material presented. We feel that these remarks are extremely valuable, not just as historical commentary, but also in revealing much interesting and unpublished chemistry.

Table 1. Comparison of structural information and properties for solids which contain magnetically isolated $Ag^{2+}$ ions in an elongated octahedral environment.

| Compound | Crystal data[a] | $R(Ag^{II}–F^-)$ [Å] | $R(Ag^{II}\cdots F^-)$ [Å] | Color | Magnetic behavior (temperature range [K]) | $\mu_{eff}$ [$\mu_B$] | $\Theta$[b] [K] |
|---|---|---|---|---|---|---|---|
| $Ag^{II}[AuF_4]_2$ | monoclinic $P2_1/n$, $a=5.229$, $b=11.066$, $c=5.516$, $\beta=94.6$, $Z=2$ | 2.072 – 2.162 | 2.484 – 3.028 | light green | Curie-Weiss (6 – 280) | 1.82 | − 2 |
| $Ag^{II}[AgF_4]_2$ | monoclinic $P2_1/n$, $a=5.047$, $b=11.054$, $c=5.449$, $\beta=97.2$, $Z=2$ | 2.056 – 2.200 | 2.558 – 2.900 | red-brown | Curie-Weiss (4 – 280) | 1.92 | − 4 |
| $Ag^{II}[BiF_6]_2$ | triclinic $P\bar{1}$, $a=5.218$ $b=5.579$ $c=8.934$, $\alpha=76.1$, $\beta=88.9$, $\gamma=65.1$ | 2.096, 2.122 | 2.440 | turquoise | Curie-Weiss (35 – 280) | 2.1 | – |
| $Ag^{II}[BiF_6][RuF_6]$ | isostructural with $Ag^{II}[BiF_6]_2$ | – | – | olive green | Curie-Weiss (13 – 251), $T_C=37$ K | – | – |
| $Ag^{II}[SbF_6]_2$ | triclinic $P\bar{1}$, $a=5.224$ $b=5.467$ $c=8.779$, $\alpha=75.8$, $\beta=89.0$, $\gamma=65.3$ | 2.095, 2.132 | 2.431 | blue | param. | 1.95 | + 3 |
| $Ag^{II}[NbF_6]_2$ | triclinic $P\bar{1}$, $a=9.061$, $b=5.670$, $c=5.207$, $\alpha=118.7$, $\beta=91.6$, $\gamma=102.3$ | – | – | blue | – | – | – |
| $Ag^{II}[TaF_6]_2$ | triclinic $P\bar{1}$, $a=9.044$, $b=5.596$, $c=5.198$, $\alpha=118.8$, $\beta=91.5$, $\gamma=102.4$ | 2.030, 2.067 | 2.367 | blue | param. | 1.95 | – |
| $Ag_3Hf_2F_{14}$ | monoclinic $C2/m$, $a=9.249$, $b=6.686$, $c=9.073$, $\beta=90.30$ | 1) 2.066, 2) 1.997 – 2.147 | 1) 2.354, 2) 2.608 – 2.788 | blue violet | antiferrom. | 1.1 | – |
| $Ag_3Zr_2F_{14}$ | monoclinic $C2/m$, $a=9.225$, $b=6.676$, $c=9.063$, $\beta=91.30$ | – | – | blue violet | antiferrom. | 1.1 | – |
| $M^{II}Ag_2Zr_2F_{14}$, $M^{II}Ag_2Hf_2F_{14}$ (M = Mg, Ni, Zn, Cu) | M = Cu: monoclinic $C2/m$, $a=9.123$, $b=6.612$, $c=8.994$, $\beta=90.7$ | | | blue or red violet | | | |
| $AgM^{II}_2Zr_2F_{14}$, $AgM^{II}_2Hf_2F_{14}$ (M = Ca, Cd, Hg) | – | | | emerald or bright green | | | |
| $K_3Ag_2Zr_4F_{23}$ | monoclinic $P2_1/c$, $a=7.838$, $b=11.174$, $c=10.156$, $\beta=97.45$ | 2.041 – 2.042 | 2.197 – 2.294 | blue | param. | | |
| $K_3Ag_2Hf_4F_{23}$ | monoclinic $P2_1/c$, $a=7.821$, $b=11.154$, $c=10.131$, $\beta=97.51$ | – | – | blue | param. | 1.99 | + 2.8 |
| $NaAgZr_2F_{11}$ | triclinic $P\bar{1}$, $a=7.809$, $b=5.700$, $c=5.832$ $\alpha=106.1$, $\beta=111.5$, $\gamma=96.6$ | 2.048 | 2.181 – 2.339 | blue | param. | 1.87 | – |
| $Ag^{II}[GeF_6]$ | – | – | – | light blue | param. | – | – |
| $Ag^{II}[SnF_6]$ | triclinic $P\bar{1}$, $a=5.204$, $b=5.253$, $c=5.632$, $\alpha=115.7$, $\beta=89.3$, $\gamma=118.8$ | 2.100 – 2.102 | 2.411 | light blue | param. | 1.99 | − 6 |
| $Ag^{II}[PbF_6]$ | – | – | – | light blue | param. | 1.92 | − 24 |
| $Ag^{II}[TiF_6]$ | triclinic $P\bar{1}$, $a=5.160$, $b=5.161$, $c=5.675$, $\alpha=117.0$, $\beta=91.3$, $\gamma=118.5$ | 2.124 – 2.174 | 2.326 | light blue | param. | 2.21 | − 70 |
| $Ag^{II}[MnF_6]$ | – | – | – | black brown | param. | 4.43 | − 66 |
| $Ag^{II}[CrF_6]$ | – | – | – | brown | – | – | – |
| $Ag^{II}[RhF_6]$ | – | – | – | black | param. | – | – |
| $Ag^{II}[PdF_6]$ | triclinic $P\bar{1}$, $a=5.023$, $b=5.085$, $c=9.976$, $\alpha=89.6$, $\beta=103.1$, $\gamma=120.9$ | 1) 2.083 – 2.116, 2) 2.065 – 2.158 | 1) 2.421, 2) 2.404 | deep brown or dark green | param. | 1.97 or 1.80 | 4.4 |
| $Ag^{II}[PtF_6]$ | triclinic $a=5.04$, $b=5.10$, $c=10.04$, $\alpha=90.1$, $\beta=103.0$, $\gamma=120.5$ | – | – | brown violet, brown or dark violet | param. | – | – |

[a] Crystal symmetry, space group, cell dimensions [Å], angles [°], number of formula units per unit cell. [b] $\Theta$ is defined by equation: $\chi = C/(T-\Theta)$, where $\chi$ is magnetic susceptibility, $C$ is Curie constant, $T$ is temperature, and $\Theta$ a measure of deviation (positive or negative) from the Curie – Weiss law.

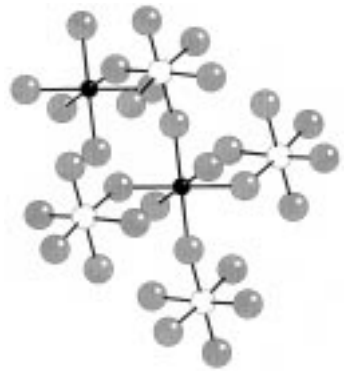

Figure 1. Crystal structure of $Ag^{II}[SbF_6]_2$; Ag: black spheres, Sb: white spheres, F: light gray spheres. The octahedral coordination of the $Ag^{II}$ center is elongated.

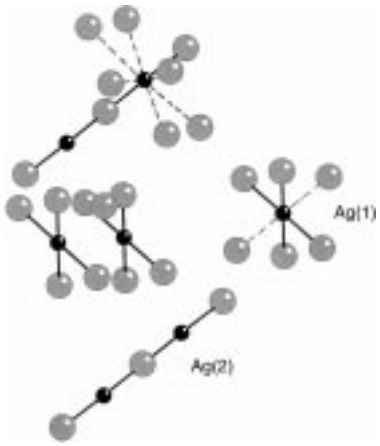


Figure 2. Crystal structure of $Ag_3Hf_2F_{14}$. Ag(1) in elongated octahedral coordination (longer axial bonds are indicated by broken lines) and Ag(2) with distorted hexagonal bipyramidal coordination (black spheres), F: light gray spheres, Hf atoms have been omitted. Notice the linear $[Ag(2)_2F_3]^+$ ions in the structure of this compound.

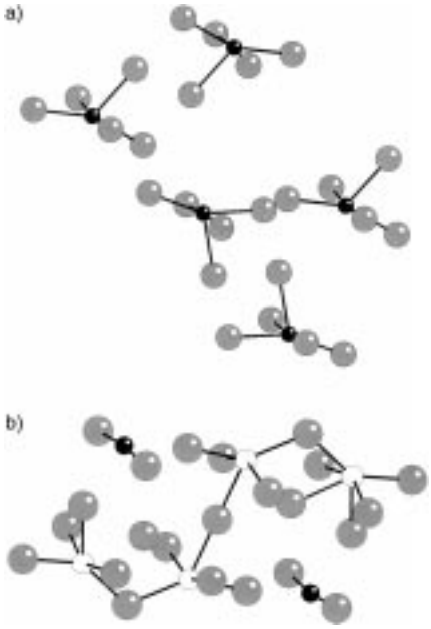


Figure 3. Two views of the crystal structure of $K_3Ag_2Zr_4F_{23}$; a) Zr and K atoms have been omitted. Note the pentagonal pyramid of F atoms around the Ag centers in this compound; Ag: black spheres, F: light gray spheres; b) K atoms have been omitted. Note the isolated $[AgF_2]^0$ units and the $[Zr_4F_{19}]^{3-}$ ions; Ag: black spheres, Zr: white spheres, F: light gray spheres.

alternative coordination of the Ag center: a distorted tetragonal pyramid (Figure 3a). Two very short Ag–F bonds of 2.04 Å (Ag–F(2) and Ag–F(6) in Müller's original notation) with an F-Ag-F angle of 173.9° point to the presence of isolated $[AgF_2^0]$ units in the structure (Figure 3b). The formula of this compound might be written as: $[K^+]_3[AgF_2]_2[Zr_4F_{19}]^{3-}$.

The Zr- and Hf-containing ternary and quaternary $Ag^{II}$ fluorides which contain isolated $[AgF_2^0]$ and $[Ag_2F_3]^+$ units thus provide insight into the first stages of infinite $[Ag^{II}-F^-]_\infty$ chain formation, according to the process in Equation (1). A hypothetical $[Ag_3F_4]^{2+}$ ion and higher members of this homologous series have not yet been made.[55]

$$[AgF_2^0] \xrightarrow{+[AgF^+]} [Ag_2F_3]^+ \xrightarrow{+[AgF^+]} [Ag_3F_4]^{2+} \xrightarrow{+[AgF^+]} \cdots \xrightarrow{+[AgF^+]} \{[AgF]^+\}_\infty \quad (1)$$

The structure of $NaAgZr_2F_{11}$ contains isolated $Ag^{II}$ centers with an interesting 2+2+2 distorted octahedral coordination ($2 \times 2.048$ Å, $2 \times 2.181$ Å, $2 \times 2.339$ Å). A similar distortion of the octahedron is also found in $CsAgF_3$ (see Section 3.1.3) and in $[AgF]^+[RuF_6]^-$ (Section 3.1.2).

### *3.1.2. Structures Containing $[Ag^{II}-F^-]^+$ Infinite Chains*

There are many ternary fluorides known containing infinite $[Ag^{II}-F^-]$ chains.[56, 57] They belong to three principal types:

a) $[AgF]^+[MF_4]^-$, M = Au,[29] B[29]

b) $[AgF]^+[MF_6]^-$, M = Bi,[28] Sb,[28] As,[29, 58, 59] Au,[29] Ir,[28] Ru[28]

c) $\{[AgF]^+\}_2[AgF_4]^-[MF_6]^-$, where M = Au,[14] Pt,[14] Ru,[14] As,[14] Sb.[14]

Infinite $[Ag^{II}-F^-]$ chains are also found in quaternary fluorides of the formula:

d) $[AgF]^+[M_3(M')_3^{IV}F_{19}]^-$, M = Cd, Ca, Hg; M′ = Zr, Hf[60]

e) $M^IAg^{II}(M')^{III}F_6$, M = Cs, Rb, K; M′ = Al, Ga, In, Tl, Sc, Fe, Co.[61, 62]

Properties and structural data for these solids are listed in Table 2. Most of these substances are temperature-independent paramagnets. This feature is anticipated for a partially filled band, obeying Fermi–Dirac statistics. Many of these compounds indeed exhibit high reflectance (bronze-luster), typical for metals. The magnetic interaction between paramagnetic $Ag^{II}$ centers might formally lead to antiferromagnetic properties, as for the isostructural pseudo-1D $[CuF]^+[AuF_4]^-$ below 85 K. However, this is not the case for most $Ag^{II}$ compounds. A Peierls distortion has been suggested for $[AgF]^+[AsF_6]^-$, $[AgF]^+[SbF_6]^-$, and $[AgF]^+[AuF_6]^-$.[63] Further investigations show, however, that a sudden drop in magnetic susceptibility (for all three of the above substances at 63 K) occurs on washing them with anhydrous HF and should be probably attributed to an impurity. Neil Bartlett writes:

"In our first paper on the $AgF^+$ salts [ref. [29] herein] we were not at the time aware that the "dips" in susceptibility that we were observing in the $[AgF]^+[MF_6]^-$ were a consequence of the washing of them with anhydrous HF. At the same time I was puzzled (and still am) by the absence of a Peierls distortion in the $[AgF][BF_4]$ structure—we even did that

Table 2. Comparison of structural information and properties for solids containing infinite $[Ag^{II}–F]^+$ chains.

| Copmound | Crystal data[a] | $R(Ag^{II}–F^-)$ [Å] | $R(Ag^{II}\cdots F^-)$ [Å] | ∢(F-Ag-F) [°] | ∢(Ag-F-Ag) [°] | Magnetic behavior (temperature range [K]) | Color |
|---|---|---|---|---|---|---|---|
| $[AgF][BF_4]$ | tetragonal, $P4/n$, $a=6.700$, $b=4.011$ | 2.002 – 2.010 | 2.327 – 2.330 | 180.0 | 180.0 | temp.-indep. param. (6 – 280) | violet or bronze |
| $[AgF][AuF_4]$ | triclinic, $P\bar{1}$, $a=5.906$, $b=4.769$, $c=3.933$, $\alpha=107.0$, $\beta=99.5$, $\gamma=90.8$ | 2.072 – 2.162 or 1.967[b] | 2.484 | 180.0[b] | 180.0[b] | | |
| $[AgF][AgF_4]$ | triclinic, $P\bar{1}$, $a=5.00$, $b=11.09$, $c=7.36$, $\alpha=90.1$, $\beta=106.5$, $\gamma=90.2$ | 2.008 – 2.036 | 2.370 – 2.619 | | | | chestnut brown |
| $[AgF][BiF_6]$ | – | | | | | temp.-indep. param. (50 – 280) | |
| $[AgF][SbF_6]$ | – | | | | | temp.-indep. param. (63 – 280) | |
| $[AgF][AsF_6]$ | orthorhombic, $Pnma$, $a=7.585$, $b=6.997$, $c=9.85$ | 1.995, 2.004 | 2.394 – 2.439 | 175.5 | 143.3 | temp.-indep. param.[c] (63 – 280) | |
| $[AgF][AuF_6]$ | orthorhombic, $Pnma$, $a=7.600$, $b=7.156$, $c=10.137$ | | | | | temp.-indep. param.[c] (63 – 280) | |
| $[AgF][IrF_6]$ | orthorhombic, $Pnma$, $a=7.628$, $b=7.067$, $c=10.253$ | 1.977, 2.014 | 2.311 – 2.467 | 176.1 | 146.0 | | |
| $[AgF][RuF_6]$ | monoclinic, $P2_1/n$, $a=8.343$, $b=5.493$, $c=11.929$, $\beta=108.4$ | 2.007 – 2.018, 2.140 – 2.158[d] | 2.548 – 2.659 | 155.9 | 176.2 | temp.-indep. param. (40 – 280) | |
| $[AgF]_2[AsF_6][AgF_4]$ | monoclinic, $P2/c$, $a=5.605$, $b=5.257$, $c=7.806$, $\beta=96.6$ | 2.003 | 2.32 – 2.34 | 180.0 | 153.9 | temp.-indep. param. (50 – 280), Curie-like dependence below 50 K | black |
| $[AgF]_2[SbF_6][AgF_4]$ | monoclinic, $P2/c$, $a=5.70$, $b=5.27$, $c=7.83$, $\beta=97.2$ | – | – | – | – | – | – |
| $[AgF]_2[AuF_6][AgF_4]$ | monoclinic, $P2/c$, $a=5.66$, $b=5.24$, $c=7.79$, $\beta=97.5$ | – | – | – | – | – | – |
| $[AgF]_2[PtF_6][AgF_4]$ | monoclinic, $P2/c$, $a=5.69$, $b=5.25$, $c=7.81$, $\beta=97.7$ | – | – | – | – | – | – |
| $[AgF]_2[RuF_6][AgF_4]$ | monoclinic, $P2/c$, $a=5.67$, $b=5.23$, $c=7.80$, $\beta=97.2$ | – | – | – | – | – | – |
| $AgM'_3M_3F_{20}$ ($M'=$ Cd, Ca, Hg; M = Zr, Hf) | hexagonal, $P6_3/m$, $a=10.48–10.59$, $c=8.286–8.330$ | 2.072 – 2.103 | 2.28 – 2.31 | 180.0 | 180.0 | param., $\Theta=0–20$ K, M = Zr: antiferrom., $T_N=3$ K | green |
| $CsAgAlF_6$ | orthorhombic, $Pnma$, $a=7.38$, $b=7.24$, $c=10.35$ | 2.06 – 2.08 | 2.29 | 177.1 | 125.9 | antiferrom., $\mu=1.30\,\mu_B$ | ultramarine blue |
| $CsAgFeF_6$ | orthorhombic, $Pnma$, $a=7.33$, $b=7.56$, $c=10.55$ | 2.047 – 2.054 | 2.27 – 2.30 | 175.5 | 126.9 | – | dark green |
| $CsAgM'F_6$ ($M'=$ Sc, In, Tl) | cubic, $a=10.79–10.88$ | $6\times 2.03–2.07$[e] | – | | | antiferrom., $\mu=1.16–1.30\,\mu_B$ | green, gray green |
| $RbAg(Al,Fe)F_6$ | orthorhombic, $Pnma$, $a=7.19$, $b=7.39$, $c=10.32$ | | | | | | dark green |

[a] Crystal symmetry, space group, cell dimensions [Å], angles [°]. [b] Computed with the assumption that the compound has the $[CuF]^+[AuF_4]^-$ structure. [c] On possible Peierls distortion at 63 K, see text. [d] Complex structure; see text. [e] In this structure ("$RbNiCrF_6$"-type) the $Ag^{II}$ and $M^{III}$ (Sc, In, Tl) centers are statistically distributed on the same position, so it is not possible (by powder data) to locate the $Ag^{II}$ center or describe its coordination (B. G. Müller).

structure twice (first on a blue crystal, second on a bronze one—the structures were the same). I conjectured (incorrectly) that the "dips" in susceptibility in the $[AgF]^+[MF_6]^-$ salts might be due to a Peierls distortion. They are a consequence of solvolysis of the $[AgF]^+[MF_6]^-$ salts by the anhydrous HF. X-ray powder patterns of the washed materials are indistinguishable from those of the salts, which do not show the "dips". Figure 6 of our later paper [ref. [28] herein] gives the susceptibility data for high purity $[AgF]^+[MF_6]^-$ (M = As, Bi) but the $[AgF][IrF_6]$ data, showing a "dip" near 63 K probably contains the mystery material. Incidentally, we made many attempts (but only at ~293 K) to detect metallic conductivity in $[AgF][BF_4]$ and the $[AgF]^+[MF_6]^-$ salts (even in single crystals) but without success."

The structure of $[AgF]^+[BF_4]^-$ is shown in Figure 4. Usually the $Ag^{II}$ cation is found in these substances in a compressed octahedral (2+4) environment. A typical $Ag^{II}$–$F^-$ bond length is 1.98 – 2.18 Å. Four additional more weakly bound fluoride anions coordinate the $Ag^{II}$ center at 2.31 – 2.47 Å.[64] The $Ag^{II}–F^-$ units are joined into $\{[AgF]^+\}_\infty$ chains, presumably responsible for the temperature-independent paramagnetism

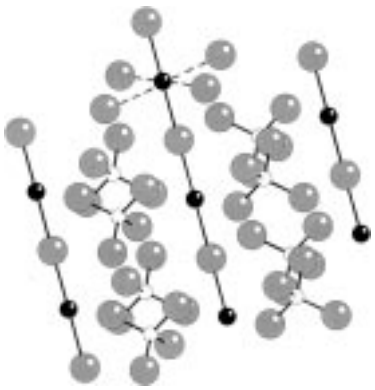

Figure 4. Crystal structure of $[AgF]^+[BF_4]^-$ showing the infinite linear $[AgF]^+$ chains. The octahedral coordination of the $Ag^{II}$ center is compressed. Longer bonds are indicated by broken lines; Ag: black spheres, B: small white spheres, F: light gray spheres.

of these substances. The $\{[AgF]^+\}_\infty$ chain may be linear ($\sphericalangle$(Ag-F-Ag) = 180°, $\sphericalangle$(F-Ag-F) = 180°), as in $[AgF]^+[BF_4]^-$, bent only at the F atoms ($\sphericalangle$(Ag-F-Ag) = 154°, $\sphericalangle$(F-Ag-F) = 180°), as in $\{[AgF]^+\}_2[AsF_6]^-[AgF_4]^-$, or bent at the Ag atoms ($\sphericalangle$(Ag-F-Ag) = 176°, $\sphericalangle$(F-Ag-F) = 143°), as in $[AgF]^+[AsF_6]^-$. $\{[AgF]^+\}_\infty$ zigzag chains occur also in the quaternary $CsAgAlF_6$ (Figure 5). Kinked $\{[AgF]^+\}_\infty$ chains run at right angles to the $\{[AlF_5]^{2-}\}_\infty$ chains in this interesting compound.

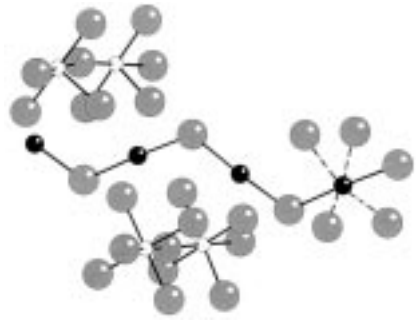

Figure 5. Crystal structure of $Cs^+[AgF]^+[AlF_5]^{2-}$ showing the infinite kinked $[AgF]^+$ chains. Note the $Ag^{II}$ centers in a compressed octahedral coordination, longer bonds indicated by broken lines; Ag: black spheres, Al: white spheres, F: light gray spheres (Cs atoms have been omitted).

There are also kinked $\{[AgF]^+\}_\infty$ chains in $Ag_2F_5$ (= $[AgF]^+[AgF_4]^-$; structure illustrated in Figure 17 and described in Section 3.1.6); the local coordination of the $Ag^{II}$ center is approximately of the 2+4 type. The structure of $[AgF]^+[AuF_4]^-$ is unknown. Most probably it has a structure similar to that of $[AgF]^+[AgF_4]^-$, with kinked $\{[AgF]^+\}_\infty$ chains. But if $[AgF]^+[AuF_4]^-$ is instead isostructural with $[CuF]^+[AuF_4]^-$, then it would have linear $\{[AgF]^+\}_\infty$ chains, and the $Ag^{II}$–$F^-$ bond length would be unusually short, 1.967 Å.

Surprisingly the structure of $[AgF]^+[RuF_6]^-$ (shown in ref. 28[65]) differs from the structures of the other members of the $[AgF]^+[MF_6]^-$ series. $[AgF]^+[RuF_6]^-$ contains a ribbonlike structure, similar to the polymeric puckered sheets in the structure of $AgF_2$ (see Section 3.1.4). The local environment of the $Ag^{II}$ center is of the (2+2+2) type, with two short $Ag^{II}$–$F^-$ bonds of 2.007 – 2.018 Å, two longer bonds of 2.140 – 2.158 Å, and two very long separations of 2.548 – 2.659 Å. The structure of the $[AgF_2]_\infty$ ribbon in $[AgF]^+[RuF_6]^-$ may be considered intermediate between the $\{[AgF]^+\}_\infty$ chain and the $[AgF_2]_\infty$ puckered sheet.

The recently discovered $[AgF]^+[M'_3M_3F_{19}]^-$ family (where M′ = Cd, Ca, Hg; M = Zr, Hf) is an interesting exception.[60] These compounds crystallize in a hexagonal system and the local coordination of F atoms around the Ag centers is regular trigonal bipyramidal (Figure 6). Such coordination is not found in any other silver fluoride, except for the $K_3Ag_2M_4F_{23}$ (M = Zr, Hf) series. It is remarkable that in spite of the significant dilution of the Ag centers in this material, $[AgF]^+$ infinite chains are formed.

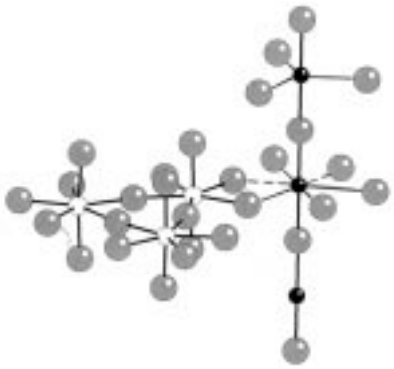

Figure 6. Crystal structure of $[AgF]^+[Cd^{2+}]_3[Zr_3F_{18}]^{6-}[F^-]$, showing the infinite linear $[AgF]^+$ chains and the isolated $[Zr_3F_{18}]^{6-}$ ions. Note the trigonal bipyramidal (or alternatively distorted hexagonal bipyramidal) coordination of the $Ag^{II}$ centers; Ag: black spheres, Zr: white spheres, F: light gray spheres (Cd atoms are omitted).

### *3.1.3. Structures Containing Infinite $[Ag^{II}(F^-)_2]$ Planes or Isolated $[Ag^{II}(F^-)_4]^{2-}$ Squares*

There are several ternary fluorides known containing infinite $[AgF_2]_\infty$ planes or isolated $[Ag^{II}(F^-)_4]^{2-}$ squares. They belong to four principal types:

a) $[MF][AgF_2]$, M = Cs,[66–68] Rb,[66, 68] K,[66–68] Na[68]
b) $[MF]_2[AgF_2]$, M = Cs,[69] Rb,[69] K,[66, 69] Na[68]
c) $M[AgF_4]$, M = Ba,[67, 70, 71] Sr,[67, 70, 71] Ca,[70, 71] Cd,[70, 71] Hg[70, 71]
d) $[MF_2]_2[AgF_2]$, M = Ba.[67]

In addition, a puckered $[AgF_2]_\infty$ sheet is found in $AgF_2$ (described in Section 3.1.4). Properties and structural data for ternary fluorides containing infinite $[AgF_2]_\infty$ planes or isolated $[Ag^{II}(F^-)_4]^{2-}$ squares are listed in Table 3.

Compounds in the $M[AgF_4]$ series are paramagnets and obey the Curie – Weiss law with $\mu_{eff} = 1.6 - 1.9\ \mu_B$. On the other hand, substances in the $[MF][AgF_2]$ and $[MF]_2[AgF_2]$ series exhibit strong collective magnetic behavior and metallic luster, as exemplified by the antiferromagnets $[RbF]_2[AgF_2]$, $[CsF]_2[AgF_2]$, and $[KF]_2[AgF_2]$.[72]

The structures of $[CsF][AgF_2]$ and $[CsF]_2[AgF_2]$ are shown in Figures 7 and 8, respectively. The $Ag^{II}$ cation is found in

Table 3. Comparison of structural information and magnetic properties for solids containing an $Ag^{2+}$ ion in square $AgF_2$ sheets and isolated $[AgF_4]^{2-}$ squares. Data for $AgF_2$ (puckered sheets) and $AgF_3$ (helical chains) are also included.

| Compoud | Structure data[a] | $R(Ag^{II}–F^-)$ [Å] | $R(Ag^{II}\cdots F^-)$ [Å] | Magnetic behavior (temperature range [K]) | $\mu_{eff}$ [$\mu_B$] | $\Theta$ [K] | Notes |
|---|---|---|---|---|---|---|---|
| $[CsF][AgF_2]$ | tetragonal, $a=6.48$, $c=8.52$ | 2.07, 2.13 | 2.51 | $T_N=50$ K, above temp.indep. param. | | | forms dimorphs |
| $[RbF][AgF_2]$ | tetragonal, $a=6.33$, $c=8.44$ | 2.06, 2.10 | 2.42 | antiferrom., over $T_N$ temp.indep. param. | | | $T_N$ = ? |
| $[KF][AgF_2]$ | orthorhombic, $a=6.18$, $b=6.27$, $c=8.30$ | 2.08 | 2.20 | $T_N=80$ K, above temp.indep. param. | | | |
| $[CsF]_2[AgF_2]$ | tetragonal, $a=4.58$, $c=14.19$ | 2.128 | 2.29 | antiferrom., $T_N=20$ K | | +45 | metallic luster |
| $[RbF]_2[AgF_2]$ | – | | | Curie-Weiss (60–300) antiferrom., $T_N=25$ K | 1.6 | +44 | metallic luster |
| $[KF]_2[AgF_2]$ | – | | | antiferrom., $T_N=60$ K | 1.9, 1.6 | +6 | metallic luster |
| $[BaF_2][AgF_2]$ | $a=6.03$, $c=11.46$ | ca. 2.05 | | Curie-Weiss (6–280) | 1.9 | −4 | $KBrF_4$-type |
| $[SrF_2][AgF_2]$ | $a=5.73$, $c=11.12$ | ca. 2.05 | | Curie-Weiss (6–280) | 1.9 | −6 | $KBrF_4$-type |
| $[HgF_2][AgF_2]$ | $a=5.52$, $c=10.92$ | ca. 2.05 | | Curie-Weiss (6–280) | 1.9 | −6 | $KBrF_4$-type |
| $[CaF_2][AgF_2]$ | $a=5.49$, $c=10.86$ | ca. 2.05 | | Curie-Weiss (6–280) | 1.9 | | $KBrF_4$-type |
| $[CdF_2][AgF_2]$ | $a=5.42$, $c=10.80$ | ca. 2.05 | | Curie-Weiss (6–280) | 1.9 | | $KBrF_4$-type |
| $[BaF_2]_2[AgF_2]$ | $a=4.32$, $c=17.6$, $Z=2$ | | | Curie-Weiss | 1.8 | +4 | $[BaF_2]_2[CuF_2]$-Typ? |
| $\alpha$-$AgF_2$ | orthorhombic, *Pbca*, $a=5.073$, $b=5.529$, $c=5.813$ | 2.068–2.074 | 2.584 | complex behavior (see text), $T_C=163$ K | | | cf. $T_C(CuF_2)=69$ K |
| $AgF_3$ | hexagonal, $a=5.078$,$c=15.452$, $V_0=345.1$ | 1.863–1.990 | 2.540 | diamagnetic | | | |

[a] Crystal symmetry, space group, cell dimensions [Å], angles [°], number of formula units per unit cell.

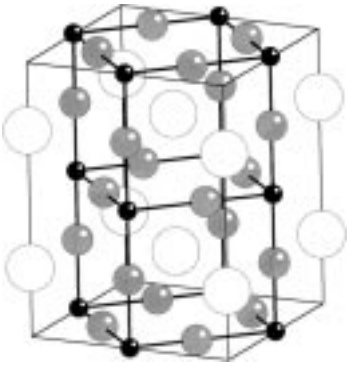

Figure 7. Unit cell of $[CsF][AgF_2]$. Note the elongated octahedral coordination of the $Ag^{II}$ centers; Ag: black spheres, Cs: white spheres, F: gray spheres.

Figure 8. Unit cell of $[CsF]_2[AgF_2]$. Note the elongated octahedral coordination of the $Ag^{II}$ centers; Ag: black spheres, Cs: white spheres, F: gray spheres.

these substances in an elongated (2+2+2; for $CsAgF_3$) or compressed (2+4; for $Cs_2AgF_4$) octahedral environment. In the first case, the $Ag^{II}$–$F^-$ bond length is in the range 2.06–2.13 Å and two additional fluoride anions coordinate to the $Ag^{II}$ center at 2.42–2.51 Å. In the latter case, a typical $Ag^{II}$–$F^-$ bond length is 2.13 Å and four additional fluoride anions coordinate the $Ag^{II}$ center at 2.29 Å. In both cases, $[AgF_2]_\infty$ planes are found.

The strongly elongated octahedral coordination of the Ag centers in $Cs_2AgF_4$ (and $Rb_2AgF_4$) deduced from ESR spectra[73] does not agree with structural data for $Cs_2AgF_4$.[69] Herein we have preferred the crystallographic structure of $Cs_2AgF_4$ over the ESR data. Prof. B. G. Müller writes:

"All structural data of compounds $M_2AgF_4$ (M = K, Rb, Cs) as well as $Ba_2AgF_6$ are based on powder data, spacegroup and especially *f*-parameters [i.e. parameters determining position of atoms in [MF] layers along the crystallographic *c* axis; note by W.G. and R.H.] therefore could not determined exactly at that time, but the violet color is typical for planar $[AgF_4]$ groups."

$[KF][AgF_2]$ is an interesting exception. It adopts the $CsAgF_3$ structure, but exhibits an orthorhombic distortion, the only one in its series. This distortion leads to slight deviations of the four F-Ag-F angles from 90°. Here the $[AgF_6]$ units appear as compressed octahedra, with two short $Ag^{II}$–$F^-$ bonds of 2.08 Å and four longer $Ag^{II}$–$F^-$ separations of 2.20 Å.[74]

Compounds in the series $M[AgF_4]$, where M = Ba, Sr, Ca, Cd, Hg, crystallize in a $KBrF_4$ structure, as do the $MAgF_4$ compounds (M = K, Rb, Cs—see Section 3.1.5). The coordi-

Figure 9. Hypothetical unit cell of $[BaF_2]_2$-$[AgF_2]$; Ag: black spheres, Ba: white spheres, F: gray spheres.

nation of the $Ag^{II}$ centers in these compounds is very different from that found in the $[MF][AgF_2]$ series: Ag is found here as isolated $AgF_4^{2-}$ ion squares.[75] The $M^{II}AgF_4$ compounds are typical dilute paramagnets.[76] Unfortunately, refinements of the structures of $M^{II}AgF_4$ compounds have not been published.

The only known compound in the $[MF_2]_2[AgF_2]$ series, $Ba_2AgF_6$, is paramagnetic, and probably crystallizes in a tetragonal system with the $Ba_2ZnF_6$ structure (Figure 9) or in the related $Ba_2CuF_6$ structure.[77] Although its structure has not been determined, we may assume that it contains $[AgF_2]$ planes with $Ag^{II}$ centers in a distorted octahedral or almost square-planar coordination (similar to the $[MF][AgF_2]$ and $[MF]_2[AgF_2]$ series) and an average in-plane Ag–F bond length of about 2.16 Å ($=a/2 = 4.32$ Å/2).

### 3.1.4. The Structures of α-$AgF_2$ and $AgF_3$

Because of the confusion in the literature regarding two simple binary silver fluorides, $AgF_2$ and $AgF_3$, with unique structures, they are treated separately here.

$AgF_2$ occurs in two forms: a disproportionated (high-temperature) $Ag^I[Ag^{III}F_4]$ and a nondisproportionated (low-temperature) $Ag^{II}F_2$ form. Hereafter we call these β- and α-$AgF_2$, respectively. α-$AgF_2$ is blue and changes color to brown on contact with air.[66] There has been a long debate on the crystal structure of α-$AgF_2$. Ruff and Giese[78] proposed in 1934 an orthorhombic $HgCl_2$-like structure for α-$AgF_2$ with lattice constants $a = 6.24$, $b = 5.48$, $c = 4.86$ Å and with four formula units per cell. In 1966, Charpin et al.[79] also found an orthorhombic unit cell with $a = 5.813$, $b = 5.529$, $c = 5.073$ Å. In the same year, however, Baturina et al.[80] proposed a distorted rutile structure for α-$AgF_2$ similar to the monoclinic $CuF_2$ structure. Then, in 1971 the measurements of Fischer et al.[15] confirmed the orthorhombic structure derived previously by Charpin et al., and the structure of α-$AgF_2$ was refined. Still, in 1988 a new structure (pseudohexagonal with unit cell dimensions of $a = 5.870$, $b = 5.572$, $c = 5.112$ Å) was proposed by Kiselev et al.[81] for a solid with formal composition $AgF_2$. The latest data by Jesih et al.[82] agreed again with the assignment made by Charpin et al.

The structural data for α-$AgF_2$ by Fischer et al. are included in Table 3. The structure of α-$AgF_2$ is presented in Figure 10. α-$AgF_2$ contains a puckered $AgF_2$ sheet with four short (2.068 – 2.074 Å) Ag–F bonds. Each Ag atom is coordinated by two additional F atoms at 2.584 Å, originating from neighboring $AgF_2$ sheets. The distance between two closest Ag atoms is only 3.78 Å. Indeed, α-$AgF_2$ is a weak ferromagnet with a Curie temperature $T_c$ of 163 K.[83] The magnetic structure of this compound is very complex:[84] "The spin configuration consists of ferromagnetic planes parallel to

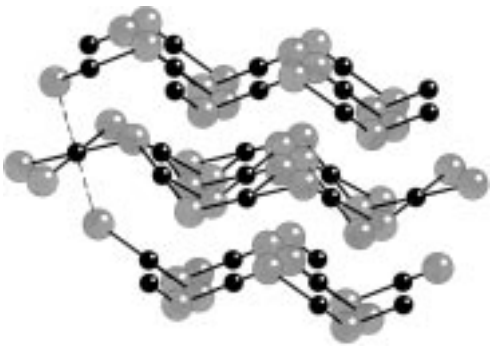

Figure 10. Crystal structure of $AgF_2$, view showing the puckered $AgF_2$ sheets. Note (at left) the elongated octahedral coordination of the $Ag^{II}$ centers; Ag: black spheres, F: gray spheres.

(100). The main components of the magnetic moments are parallel to *a* and form an antiferromagnetic structure where silver atoms occupying centers of $AgF_4$ squares with a common fluorine have opposite spin directions. In addition, small ferromagnetic components point along *c*, i.e. perpendicular to the puckered $AgF_2$ layers […]. The resultant magnetic structure is slightly canted with spins parallel to the pseudohexagonal close-packed nets formed by the fluorines perpendicular to *b*."[85]

The long-range antiferromagnetic order in α-$AgF_2$ below the Curie temperature is also emphasized by the largest deviation from Curie – Weiss law among compounds containing $Ag^{II}$ centers ($\Theta = -715$ K).

There has also been much controversy about $AgF_3$. $AgF_3$ was synthesized by Žemva et al.[16] as late as in 1991. It seems that previous claims of $AgF_3$ by Bougon et al.[86] and by Kiselev et al.[13] were not sufficiently documented. The structure of $AgF_3$ was finally refined in the hexagonal system. (Figure 11). The structure contains unique helical $[Ag(F_{2/2})(F_{2/1})]$ chains of $6_1$ (or $6_5$) symmetry, with four short (1.863 – 1.990 Å) and two long (2.540 Å) Ag–F bonds. The F-Ag-F angle between the two shortest Ag–F bonds is 140.2°, while the Ag-F-Ag angle between the two shortest Ag–F bonds is 176.6°. The distance from the Ag center to the

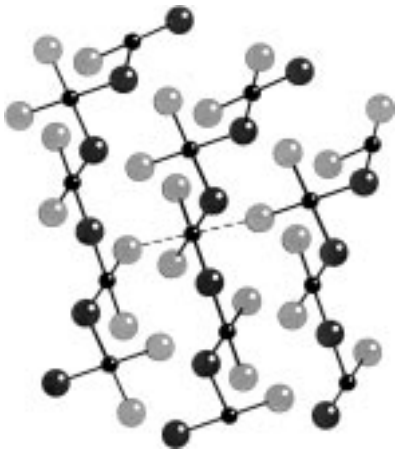

Figure 11. Crystal structure of $AgF_3$, view showing the helical $AgF_3$ chains. Note the elongated octahedral coordination of the $Ag^{III}$ centers; Ag: small black spheres, F: Large gray spheres and black spheres (two slightly different kinds of F atoms).

bridging F atom is untypically large for silver(III) fluorides (1.99 Å) close to the shortest $Ag^{II}$–$F^-$ bond seen in quasi-1D silver(II) fluorides (2.00 Å). The structure of $AgF_3$ has no counterpart in other solid $Ag^{II}$ or $Ag^{III}$ fluorides, and is analogous only to the structure of $AuF_3$.[16, 87, 88] $AgF_3$ is thermodynamically unstable and releases $F_2$ at $+25\,^\circ C$ on contact with anhydrous hydrogen fluoride.[89] It might be used for energy and fluorine storage.

We thought that adducts of $AgF_3$ and the strongest F-abstracting agents such as $SbF_5$ and $BiF_5$ might exist (at low temperatures) Prof. Bartlett confirms (private communication, 2000) that this was attempted in the 90's.

"We tried very hard to get $[Ag^{III}F_2]^+[AsF_6]^-$, by adding $AsF_5$ to anhydrous HF over $AgF_3$ at dry-ice temperatures. The anhydrous HF and $AsF_5$ were removed at low temperature, but […] the product was $[AgF]^+[AsF_6]^-$. George Lucier did, I believe, try $BiF_5$ with $AgF_3$. All of the efforts to make $[AgF_2]^+$ indicated that it must be a very fragile species. Because of these failures I suggested to George that we carry out experiments to detect the $[AgF_2]^+$ as a powerfully oxidizing transient. I guessed that the cation would be a strong enough one-electron oxidizer to take the electron from $[PtF_6]^-$ (we knew that $Ag^{II}$ would not oxidize it). George was able to obtain a better than 70% yield of $PtF_6$ with $BiF_5$ as the F-acceptor. This certainly implies a long life for the $[AgF_2]^+$ at room temperatures (at which the $MF_6$, M = Pt, Ru, Rh, are generated). My guess is that an appropriate stoichiometric quantity of $SbF_5$ in anhydrous HF, at $-80\,^\circ C$, added (slowly) to a similarly cooled suspension of $AgF_3$ in anhydrous HF, could give $[AgF_2]^+[Sb_2F_{11}]^-$. Certainly one must avoid excess acid at any point in the synthesis, and the $AgF_3$ be given adequate time to react and dissolve as the $[AgF_2]^+$ salt."

### 3.1.5. Structures Containing Isolated $[Ag^{III}(F^-)_4]^-$ Squares or Isolated $[Ag^{III}(F^-)_6]^{3-}$ Octahedra

$Ag^{III}$ is "isoelectronic" with $Au^{III}$ and $Pd^{II}$ ($d^8$ configuration). Square-planar coordination for $[AgF_4]^-$ is expected,[90] and indeed is typical both for $Ag^{III}$ (and for $Au^{III}$ and $Pd^{II}$) containing species. It is found in many ternary $Ag^{III}$ fluorides in the series $M^I[AgF_4]^-$ (M = Cs,[68, 91, 92] Rb,[68, 91, 92] K,[68, 91–93] Na,[68, 92] Li,[94] $O_2$,[13] $XeF_5$.[95, 96]). Compounds isostructural to the $Ln[AuF_4]_3$, $LnF[AuF_4]_2$, $Ln_2F[AuF_4]_5$, or $Ln_2F_7[AuF_4]$ series (Ln = lanthanide)[97] have not yet been synthesized.

The structures of $MAgF_5$ (M = Ba[91]) and $M_2AgF_5$ (M = Rb[68]) are unknown.

Table 4 presents structural data for solids containing square $[AgF_4]^-$ units. Figure 12 shows the structure of $KAgF_4$.

The crystal structures of ternary fluorides containing the $Ag^{III}$ cation are similar to structures containing the $Au^{III}$ cation[98, 99] (crystallized in the $KBrF_4$ structural type). These

Table 4. Comparison of structural information and magnetic properties for solids containing an $Ag^{3+}$ ion in isolated $[AgF_4]^-$ squares and in isolated $[AgF_6]^{3-}$ octahedra.

| Compound | Crystal data[a] | $R(Ag^{III}–F^-)$ [Å] | $R(Ag^{III}\cdots F^-)$ [Å] | Magnetic behavior (temperature range [K]) | Notes |
|---|---|---|---|---|---|
| $Cs[AgF_4]$ | tetragonal, $a = 4.308$, $c = 7.048$ | | | diamagnetic | $NaAlF_4$-Structure? |
| $Rb[AgF_4]$ | tetragonal, $a = 6.043$, $c = 12.318$ | | | diamagnetic | |
| $K[AgF_4]$ | tetragonal, $a = 5.902$, $c = 11.806$ oder $a = 5.847$, $c = 11.553$ | $4 \times 1.889$ | $8 \times 3.086$ | diamagnetic | |
| $Na[AgF_4]$ | tetragonal, $a = 5.551$, $c = 10.649$ | | | diamagnetic | |
| $Li[AgF_4]$ | monoclinic, probably $C2/c$, $a = 4.87$, $b = 5.93$, $c = 10.08$, $\beta = 93.0$, $Z = 4$ | | | diamagnetic | |
| $[XeF_5]^+[AgF_4]^-$ | tetragonal, $I4/m$, $a = 5.593$, $c = 20.379$ | 1.902 | | diamagnetic | |
| $[O_2]^+[AgF_4]$ | hexagonal, $a = 8.186$, $c = 9.904$ | | | | |
| $Ba[AgF_4]_2$ | $KAgF_4$ defect structure? | | | | |
| $Ag[AgF_4]_2$ | monoclinic, $P2_1/n$, $a = 5.047$, $b = 11.054$, $c = 5.449$, $\beta = 97.2$, $Z = 2$ | 1.846 – 1.909 | 2.786 – 3.313 | Curie-Weiss (4 – 280) | red brown |
| $Rb_2AgF_5$ | tetragonal, $a = 6.094$, $c = 12.414$ | | | | |
| $[BaF_2][AgF_3]$ | | | | diamagnetic | yellow, decompostion |
| $Rb_3AgF_6$ | tetragonal, $a = 6.190$, $c = 12.034$ | | | ? | high-spin? |
| $Cs_2KAgF_6$ | cubic, $a = 9.175$ | $6 \times 2.13$ | (octahedral coordination) | param. | high-spin? |

[a] Crystal symmetry, space group, cell dimensions [Å], angles [°], number of formula units per unit cell.

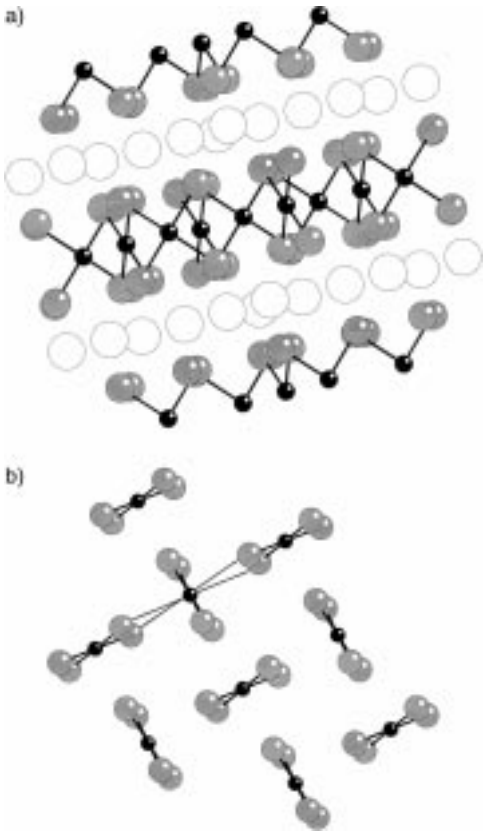


Figure 12. Crystal structure of $KAgF_4$; a) view showing the layers of isolated square $[AgF_4]^-$ ions; Ag: black spheres, K: white spheres, F: gray spheres; b) view showing the relative orientation of the square $[AgF_4]^-$ ions. Note the 4+4 coordination of the $Ag^{III}$ centers; Ag: black spheres, F: gray spheres (K atoms have been omitted).

contains the isolated square-planar $[AgF_4]^-$ unit, with four equivalent short (1.89–1.91 Å) Ag–F bonds. There are also four additional secondary Ag···F interactions at 2.9–3.0 Å. The $d^8$ metal configuration is expected to be diamagnetic in this conformation. Interestingly, another high-symmetry structure of composition $ABX_4$ (in which $AgF_2$ planes might occur, Figure 13), the $NaAlF_4$ structure, is not preferred by the majority of compounds containing $[AgF_4]^-$ or $[AgF_4]^{2-}$ ions.

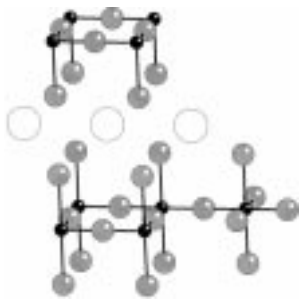

Figure 13. Hypothetical crystal structure of $CsAgF_4$ in the $NaAlF_4$ structure, view showing $AgF_2$ and $CsF_2$ layers. Note the elongated octahedral coordination of the $Ag^{III}$ centers; Ag: black spheres, Cs: white spheres, F: gray spheres.

The structure of $CsAgF_4$, ($Z = 1$) is claimed to be simpler than that of $KAgF_4$ ($Z = 4$); a reduction of unit-cell dimensions by $\sqrt{2}$ ($a$, $b$) and by 2 ($c$) has been discussed.[68, 92] Under these conditions, $CsAgF_4$ might be the only $MAgF_4$ compound which adopts the $NaAlF_4$ structure. The $NaAlF_4$ structure indeed might be preferred over the $KBrF_4$ structure because of the large dimensions of the $Cs^+$ ion (ca. 167 pm) which stabilizes puckered $CsF_2$ sheets.[100]

It is worth mentioning that the presence of high spin (HS) $Ag^{III}$ centers in the deep purple red $Cs_2KAgF_6$[68, 101] and in $Rb_3AgF_6$,[68] in which the $Ag^{III}$ centers are in an undistorted octahedral environment (Figure 14) has been discussed. It was initially uncertain whether the paramagnetism of the samples might be attributed to the products of reactor corrosion. The synthesis of $Cs_2KAgF_6$ has been repeated in an $Al_2O_3$ reactor, to exclude paramagnetic pollutants.[102]

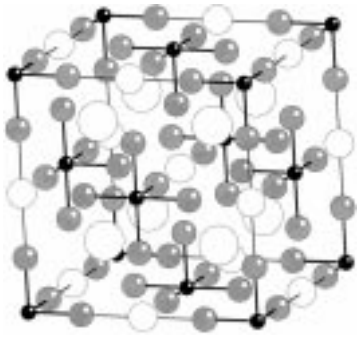

Figure 14. Unit cell of $Cs_2KAgF_6$. The structure contains isolated $[AgF_6]^{3-}$ octahedra; Ag: black spheres, F: light gray spheres, Cs: large white spheres, K: medium white spheres.

Could it be that the fluoride crystal field is so low that the typical square-planar environment low spin (LS) $d^8$ configuration might not necessarily be preferred for $Ag^{III}$ centers (similar to paramagnetic $Cu^{III}$ centers in $M^I_3CuF_6$ compounds)? The crystal structure of $Cs_2KAgF_6$ seems to confirm the presence of HS $Ag^{III}$ centers. There are six equivalent long (2.13 Å) Ag–F bonds; dramatic elongation of the Ag–F bonds in $Cs_2KAgF_6$ compared to compounds containing LS $Ag^{III}$ (1.90 Å) might be attributed to the occupation of both strongly antibonding Ag(d) orbitals ($x^2 - y^2$ and $z^2$) by one electron each. Bonding in HS $Ag^{III}$ fluorides is thus probably more ionic than in LS $Ag^{III}$ compounds.

### 3.1.6. *Mixed-Valence $Ag^{II}/Ag^{I}$ and $Ag^{II}/Ag^{III}$ Systems*

Several formally mixed-valence $Ag^{II}/Ag^{III}$ systems have been introduced in previous sections. These are: $Ag_2F_5$, $Ag_3F_8$ (that is, $Ag^{II}\{[AgF_4]^-\}_2$), and $Ag_3MF_{12}$, (that is, $\{[AgF]^+\}_2[AgF_4]^-[MF_6]^-$ where M = Au, Pt, Ru, As, Sb). These compounds are typical disproportionated (mixed-valence) compounds. For example, $\{[AgF]^+\}_2[AgF_4]^-[AsF_6]^-$ contains kinked $[Ag^{II}F]^+$ chains and isolated $[Ag^{III}F_4]^-$ squares (Figure 15). The local coordinations of the $Ag^{II}$ and $Ag^{III}$ centers also differ greatly in $Ag_3F_8$ and $Ag_2F_5$ (see Figure 16 and 17, and Tables 1 and 2, respectively).

$Ag_3F_8$ has a very interesting structure (Figure 16). One may distinguish in it ribbons of the formula $Ag^{II}[Ag^{III}F_4]_2$. Local 2+2+2+2 coordination of the $Ag^{II}$ center is not found in any other silver fluoride (there are four short 2.06–2.20 Å and four long 2.59–2.90 Å Ag-F distances), and may be considered as a distorted square-planar coordination. The $Ag^{III}$ cation also occurs in a square-planar environment with four

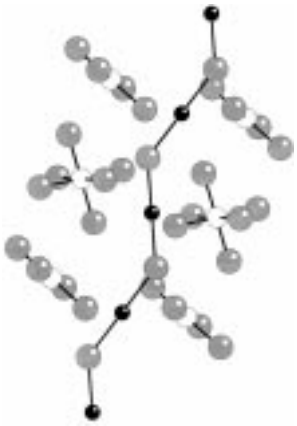

Figure 15. Crystal structure of $[AgF]_2[AgF_4][AsF_6]$. The structure contains an infinite kinked $[AgF]^+$ chain, isolated $[AgF_4]^-$ square planes, and isolated $[AsF_6]^-$ octahedra; $Ag^{II}$: black spheres, $Ag^{III}$ and $As^{VI}$: white spheres, F: light gray spheres.

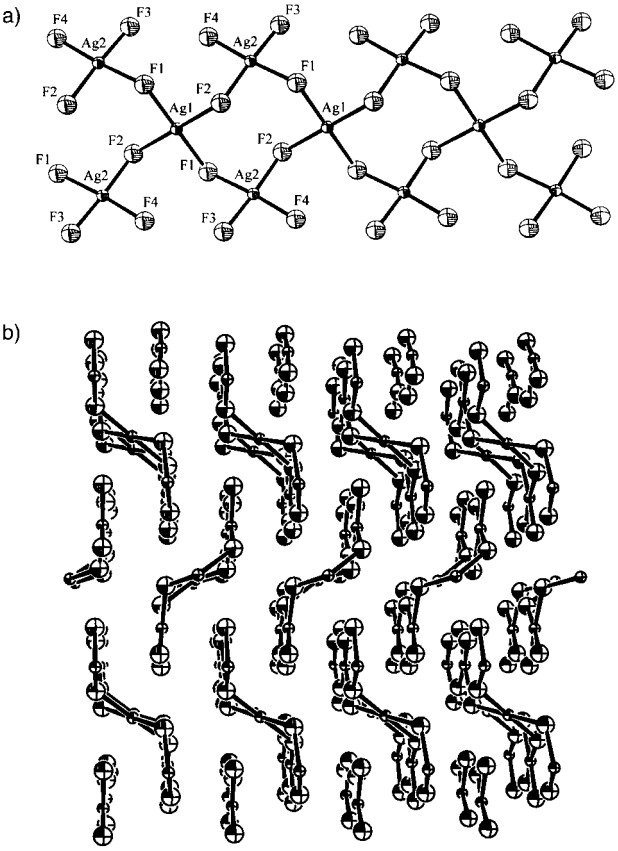


Figure 16. Crystal structure of $Ag[AgF_4]_2$. There are infinite "ribbons" in the structure, stacked in the *c* direction. Local coordination of the $Ag^{II}$ and $Ag^{III}$ centers is elongated octahedral; a) view of a ribbon; b) stacking of the $Ag[AgF_4]_2$ ribbons. Illustration courtesy of N. Bartlett.

Ag–F bonds of 1.85 – 1.91 Å and four secondary interactions at 2.79 – 3.31 Å. The unique $Ag[AgF_4]_2$ ribbons are stacked along one of the crystallographic axes.

The structure of $Ag_2F_5$, another binary mixed-valence silver fluoride, is very complex (Figure 17). There are three different kinds of $Ag^{II}$ and three different kinds of $Ag^{III}$ atoms. All the $Ag^{II}$ cations have a similar coordination sphere, a compressed octahedron with two short Ag–F bonds (2.006 – 2.033 Å) and four long Ag–F bonds (2.14 – 2.58 Å). The $Ag^{II}$ cations are joined in a kinked $[AgF]^+$ infinite chain ($\measuredangle$(Ag-F-Ag) = 144 – 145°, $\measuredangle$(F-Ag-F) = 176 – 180°). An approximate formula of this compound may be written as $[AgF][AgF_4]$. On the other hand, all the $Ag^{III}$ cations are in a typical square-planar coordination with four F atoms at 1.89 – 1.92 Å and two F atoms much further away. It would be interesting to trace the magnetic interaction of the paramagnetic $Ag^{II}$ centers; unfortunately, no magnetic measurements have been carried out for $Ag_2F_5$.

Figure 17. Crystal structure of $[AgF][AgF_4]$, view showing an infinite $[AgF]^+$ zigzag chain surrounded by $[AgF_4]^-$ ions. The local coordination of the $Ag^{II}$ and $Ag^{III}$ centers is elongated octahedral and square planar, respectively; $Ag^{II}$ and $Ag^{III}$: black spheres, F: gray spheres.

We will now introduce two more mixed-valence compounds: a nonstoichiometric $AgF_{2+\delta}$ and $CsAgF_{3+\delta}$ ($0 < \delta < 1$). In this Section we will not include the genuine intermediate-valence fluoride of $Ag^{III}$ and $Ag^{V}$, paramagnetic $Cs_2Ag^{IV}F_6$, crystallizing in the $K_2PtCl_6$ structure.[103]

Phases with formula $CsAgF_{3+\delta}$ are created upon thermal decomposition of $CsAgF_4$ at about 370 – 500 °C.[68, 92] $CsAgF_{3.53}$, obtained at 500 °C, crystallizes in a body-centered tetragonal system with $a = 6.339$ Å and $c = 9.150$ Å. It is a red-brown, formally mixed-valence compound, possibly a solid solution of $CsAgF_3$ and $CsAgF_4$, or—more probably—a compound with a defect $CsAgF_3$ structure (having CsF/$AgF_2$/$CsF_2$/$AgF_2$ layer order?). Strikingly, no similar $MAgF_{3+\delta}$ phases are obtained with this method for M = Rb, K, Na. Structural, spectroscopic, magnetic, and electric conductivity data is missing for the $CsAgF_{3+\delta}$ phases, these phases have not been investigated so far by other groups; most probably it is a disproportionated compound, as suggested by infrared (IR) spectra (the IR spectrum of $CsAgF_{3.53}$ may be obtained by overlapping the spectra for $CsAgF_3$ and $CsAgF_4$). It would be of interest to examine closer the coexistence of the $Ag^{II}$ and $Ag^{III}$ centers in this compound by varying the external pressure.

The same group claims $AgF_{2+\delta}$ is another nonstoichiometric compound containing silver in an oxidation state close to II.[81, 104] However, they find that the $AgF_{2+\delta}$ which they investigate is a single phase only in the range $-0.09 < \delta < 0.01$. No further data are given for this compound. The presence of $AgF_{1.91}$ does not seem improbable to us. For example, it is known that $AgF_{2.00}$ crystals are usually nonstoichiometric on the surface, and they are evidently F deficient.[105] $AgF_{2.00}$ might decompose slowly, releasing $F_2$. Neil

Bartlett (private communication) comments on this subject are as follows:

"Your comments on off-stoichiometry $AgF_2$ reminded me of work done in my lab in Vancouver in the mid-60's. My postdoctoral associate D. Stewart found that the action of $F_2$ on $Ag^+$ in anhydrous HF precipitated material of composition $Ag_9F_{16}$ (i.e. $AgF_{1.78}$), whereas fluorination of silver nitrate in a bomb gave stoichiometric $AgF_2$. Both materials gave the same powder pattern, as far as line position was concerned, but some relative line intensities were different. I do still have X-ray photographs in my immediate possession. These show the orthorhombic cell of $Ag_9F_{16}$ to be indistinguishable in size from that of $AgF_2$! I should add that the magnetic properties of $Ag_9F_{16}$ are very similar to those of $AgF_2$ and the molar susceptibilities of $Ag_9F_{16}$ and $Ag_8F_{16}$ are essentially the same! I spoke on these findings at a "Fluorine Meeting" sometime in the later 60's (2nd European Symposium on Fluorine Chemistry, Göttingen 1968). From time to time over the past 35 years I have had various people look at this problem. My co-worker R. Hagiwara, in the early 90's, repeated D. Stewart's preparations and confirmed them, but we did not solve the structural problem posed by $Ag_9F_{16}$. That $Ag^+$ could be incorporated into the $AgF_2$ stucture and not change the unit cell size defies common sense. Clearly this merits careful re-examination, and should not be given serious weight in one's thinking until the findings are beyond all doubt."

To the best of our knowledge, $AgF_{1.91}$ would be the only example of a formally mixed-valence[106] $Ag^{II}/Ag^{I}$ compound to date.

It is difficult to predict whether hypothetical quaternary $Ag^{II}/Ag^{III}$ and $Ag^{II}/Ag^{I}$ fluorides might have a decisively comproportionated (intermediate-valence) or rather a disproportionated (mixed-valence) character. We will examine this prospect closer in Section 3.6.2.

As we conclude our tour through known $Ag^{II}$ and $Ag^{III}$ compounds, we want to pay tribute to the groups who did this incredibly difficult work. In Germany, the pioneering effort was that of R. Hoppe and B. G. Müller, who synthesized the first $Ag^{II}$ fluorides and determined their structures. More than half of the known compounds originate from this group. We have already mentioned the important contributions of N. Bartlett;[107] we also want to cite specifically the work of B. Žemva, the first to apply successfully acid–base reactions in anhydrous HF for synthesis of binary metal fluorides in high oxidation states.

## 3.2. Summary Analysis of Structural and Magnetic Data for Binary and Ternary $Ag^{II}$ and $Ag^{III}$ Fluorides

### 3.2.1. Coordination Preferences of $Ag^{I}$, $Ag^{II}$, and $Ag^{III}$ in a Fluoride Environment

Let us summarize the coordination preferences of $Ag^{II}$ and $Ag^{III}$ in a fluoride environment, based on the extensive experimental data presented in Sections 3.1.1–3.1.6. The diverse ways of coordination of Ag atoms by $F^-$ ions may be understood by thinking of them as distortions from octahedral coordination. Such a unified view provides a comparative, qualitative background for linear, compressed octahedral, elongated octahedral, and finally, the square-planar geometry (rare trigonal bipyramid, pentagonal bipyramid, and tetragonal pyramid coordinations are not included here). A quantitative comparison may be obtained through the dimensionless distortion parameter $D$ which is defined as the ratio of the axial bond length $R_{ax}$ to the equatorial bond length $R_{eq}$ in a distorted octahedron [Eq. (2)].

$$D = R_{ax}/R_{eq} \quad (2)$$

In Table 5 we give several structural parameters, for selected $Ag^{II}$ and $Ag^{III}$ fluorides, such as the axial and equatorial bond lengths, $R_{ax}$ and $R_{eq}$,[108] the distortion

Table 5. List of axial $R_{ax}$ and equatorial $R_{eq}$ bond lengths in distorted octahedral $Ag^{II}$ and $Ag^{III}$ fluoride complexes, together with distortion parameter $D = R_{ax}/R_{eq}$ and the shortest Ag–Ag distance $R$(Ag–Ag). The structures optimized in the DFT computations are also included.

| Verbindung | $R_{ax}$ [Å] | $R_{eq}$ [Å] | $D$ | $R$(Ag–Ag) [Å] |
|---|---|---|---|---|
| *$Ag^{II}$ compounds:* | | | | |
| ***experimental*** | | | | |
| $[AgF]AgF_4$ | 2.006–2.033 | 2.14–2.58 | 0.78–0.94 | 3.825 |
| $[AgF]AsF_6$ | 1.995–2.004 | 2.394–2.439 | 0.83 | 3.795 |
| $[AgF]IrF_6$ | 1.977–2.014 | 2.311–2.467 | 0.84 | 3.817 |
| $[AgF]AuF_6$ | 2.072–2.162 | 2.484 | 0.85 | 3.800 |
| $[AgF]AuF_4$ | 1.967[a] | | | 3.933[a] |
| $[AgF]_2[AgF_4][AsF_6]$ | 2.003 | 2.32–2.34 | 0.86 | 3.903 |
| $[AgF]BF_4$ | 2.002–2.009 | 2.327–2.330 | 0.86 | 4.011 |
| $CsAgFeF_6$ | 2.04–2.05 | 2.27–2.30 | 0.89 | 3.67 |
| $CsAgAlF_6$ | 2.06–2.08 | 2.29 | 0.90 | 3.69 |
| $Ag(M')^{II}_3M^{IV}_3F_{20}$ | 2.072–2.103 | 2.28–2.31 | 0.91 | 4.175 |
| $Cs_2AgF_4$ | 2.128 | 2.29 | 0.93 | 4.580 |
| $KAgF_3$ | 2.075 | 2.201 | 0.94 | 4.402 |
| *ideal octahedra* | | | *1.00* | |
| $NaAgZr_2F_{11}$ | 2.048–2.182 | 2.339 | 1.07–1.14 | 5.701 |
| $Ag_3Zr_2F_{14}$ | 1.981–2.076 | | | 3.963 |
| $Ag_3Hf_2F_{14}$ | 1) 2.354, 2) 1.997–2.147 | 1) 2.066, 2) 2.608–2.788 | 1) 1.14, 2) 0.74–0.79 | 3.972 |
| $\alpha$-$Ag^{II}[SbF_6]_2$ | 2.431 | 2.095–2.132 | 1.15 | 5.224 |
| $Ag^{II}[BiF_6]_2$ | 2.440 | 2.096–2.122 | 1.16 | 5.218 |
| $Ag^{II}[NbF_6]_2$ | | | | 5.207 |
| $Ag^{II}[TaF_6]_2$ | 2.367 | 2.030–2.067 | 1.16 | 5.198 |
| $RbAgF_3$ | 2.42 | 2.06–2.10 | 1.16 | 4.220 |
| $CsAgF_3$ | 2.51 | 2.07–2.13 | 1.20 | 4.260 |
| $[AgF]RuF_6$ | 2.548–2.659 | 2.007–2.018, 2.140–2.158 | 1.21–1.29 | 3.940 |
| $AgF_2$ | 2.584 | 2.068–2.074 | 1.25 | 3.776 |
| $CdAgF_4$ ($KBrF_4$-type) | | ca. 2.05 | | 3.833 |
| $BaAgF_4$ ($KBrF_4$-type) | | ca. 2.05 | | 4.264 |
| *$Ag^{III}$ compounds:* | | | | |
| ***experimental*** | | | | |
| $AgF_3$ | 2.540 | 1.863–1.990 | 1.28–1.36 | 3.500 |
| $[AgF]AgF_4$ | 1.890–1.927 | 2.635–3.320 | 1.38–1.74 | 3.726 |
| $[AgF]_2[AgF_4][AsF_6]$ | 2.61 | 1.80–1.81 | 1.45 | 7.806 |
| $XeF_5AgF_4$ | 2.921 | 1.902 | 1.54 | 3.955 |
| $KAgF_4$ | ca.3.08 | 1.889 | 1.63 | 4.134 |
| ***calculated*** | | | | |
| $KAgF_4$ ($NaAlF_4$-type) | 1.989 | 2.012 | 0.99 | 4.024 |
| $RbAgF_4$ ($NaAlF_4$-type) | 1.983 | 2.024 | 0.98 | 4.048 |
| $CsAgF_4$ ($NaAlF_4$-type) | 1.972 | 2.047 | 0.96 | 4.098 |

[a] Computed with the assumption of the $[CuF][AuF_4]$ structural type.

parameter $D$, and the closest distance between two $Ag^{II}$ centers or between two $Ag^{III}$ centers $R$(Ag–Ag). Data for structures optimized in the DFT computations (see Section 3.3) is also included.

Clearly, the $Ag^{II}$ center exhibits a fascinating flexibility toward Jahn–Teller distortion from the ideal octahedral geometry in different fluoride-dopant environments. The distortion parameter $D$ ranges from 0.78 (linear coordination), through 0.94 (compressed octahedron), and 1.07 (elongated octahedron), to 1.25 (square planar). The transition between the compressed and elongated octahedron is thus rather smooth (Figure 18). For $Ag^{III}$ compounds with typical square-planar coordination, $D$ usually takes on very large values (1.45–1.63).

The affinity of Ag centers towards $F^-$ ions apparently increases with the increasing formal oxidation state of Ag. $Ag^{III}$ is a very strong Lewis acid, which is found practically only in anionic form, as $[AgF_4]^-$ or $[AgF_6]^{3-}$. On the other hand, $Ag^I$ is a very weak Lewis acid, found typically as an isolated cation.

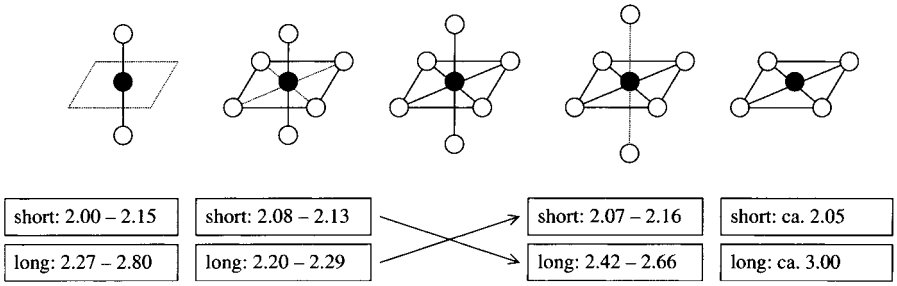


Figure 18. The $Ag^{II}$–$F^-$ bond lengths [Å] in different geometric environments.

The diversity of crystal structures of binary and ternary $Ag^{II}$ fluorides is very interesting. $Ag^{II}$ may act as a cation, as a neutral species, and as an anion, as exemplified by:

1) isolated $Ag^{II}$ cations, as in $Ag[BiF_6]_2$
2) $[AgF]^+$ ions in linear chains (two strong Ag–F bonds)
3) isolated $[Ag_2F_3]^+$ ions
4) $[AgF_2]^0$ in $AgF_2$ planes with elongated octahedral coordination (four strong bonds, but the F atoms are shared with other Ag atoms) or in isolated $[AgF_2]^0$ units
5) $[AgF_4]^{2-}$ ions in the form of isolated squares (four strong bonds) or in $AgF_2$ planes with compressed octahedral coordination (two strong bonds and four weak bonds, but F atoms are shared with other Ag atoms).

It is very important to understand this chameleonlike, amphoteric behavior of $Ag^{II}$ centers in different fluoride complexes, so as to be able to manipulate it in a desired manner. We hope to reach this goal by analyzing the electronic structure of several structurally well-characterized compounds of $Ag^{II}$ and $Ag^{III}$ (Section 3.3).

### 3.2.2. Summary of Magnetic Behavior of Silver Fluorides

The magnetic behavior of the $Ag^{II}$ fluorides is very diverse. Undoubtedly, exchange and superexchange are strongly dependent on the distance between the $Ag^{II}$ centers, and the way in which they are joined by $F^-$ ions. Figure 19 shows a graph of the Ag–Ag separation in different $Ag^I$, $Ag^{II}$, and $Ag^{III}$ fluorides.

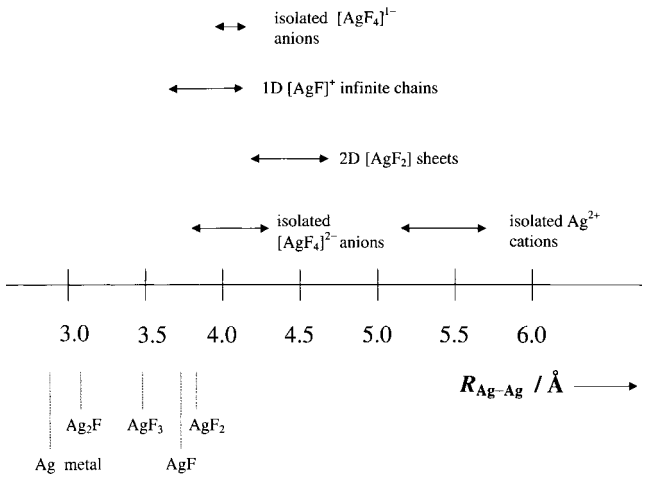


Figure 19. The shortest Ag–Ag distances in different Ag fluorides.

The closest Ag–Ag separation in magnetically dilute $Ag^{II}(d^9)$ fluorides is in the range 5.1–5.5 Å. These compounds are paramagnets. The Ag–Ag separation drops to 4.2–4.6 Å in compounds containing $[AgF_2]_\infty$ sheets. Most of these are weak antiferromagnets; Neél temperatures $T_N$ do not exceed 80 K. $AgF_2$ is an exception; it is a weak ferromagnet with an Ag–Ag separation of 3.78 Å and Ag-F-Ag angles of 118–130°. But there is also antiferromagnetic order in this compound below the Curie temperature $T_c$ (note that both the Curie temperature for ferromagnetic $AgF_2$ and the Neél temperatures for antiferromagnetic fluorides correlate with the closest Ag–Ag separation; see Figure 29 and Section 3.6.1.). Compounds containing isolated $[AgF_4]^{2-}$ ions have Ag–Ag separations in the range 3.8–4.3 Å. Still they are paramagnetic, probably a result of the mutually perpendicular orientation of half-filled $x^2-y^2$ orbitals on different Ag centers. Solids with $\{[AgF]^+\}_\infty$ chains have Ag–Ag separations of 3.7–4.2 Å. Most of them (with both linear or kinked $\{[AgF]^+\}_\infty$ chains and "short" Ag–Ag separations of 4.0–4.2 Å) are temperature-independent paramagnets. There might be a tendency to undergo Peierls distortion (resulting in a diamagnetic phase) in some of them at low temperatures. Compounds of $Ag^{III}(d^8)$ containing isolated $[AgF_4]^-$ ions have the closest Ag–Ag approach of about 4.0 Å (still too far for any significant overlap) and they are diamagnetic. AgF and ternary $Ag^I(d^{10})$ fluorides have the closest Ag–Ag separation of around 2.9–3.5 Å, and are diamagnetic.

## 3.3. DFT Band-Structure Calculations for Selected Binary and Ternary $Ag^{II}$, $Ag^{III}$, and $Ag^I$ Fluorides

To determine the electronic structure of binary and ternary $Ag^{II}$, $Ag^{III}$, and $Ag^I$ fluorides in geometrically different environments, we performed DFT band-structure calculations

for a selection of structurally well-characterized binary and ternary fluorides. Our main interest is in extended 1D and 2D structures containing $Ag^{II}$ centers. Such compounds might in principle have a half-filled band, and possibly be metallic. Hence, for the DFT calculations we have chosen: 1) [AgF][$BF_4$], representative of compounds with a linear $[AgF]^+$ chain, 2) $CsAgF_3$, as an example of compounds with $AgF_2$ planes and elongated octahedral coordination of the Ag center, 3) $Cs_2AgF_4$, with an undistorted $K_2NiF_4$ structure, and 4) $AgF_2$, with a puckered-sheet structure. Since we would like also to look at $Ag^{II}$ compounds from a broader perspective, we have added computations for $Ag^{III}$ and $Ag^{I}$ compounds: 5) $KAgF_4$, an example of isolated $Ag^{III}$ centers as $[AgF_4]^-$ ions, and 6) AgF, an $Ag^{I}$ fluoride. We also include computational data for 7) a hypothetical form of $KAgF_4$, as optimized in the $NaAlF_4$ structure ($Z=1$).

In the literature we could not find any electronic-structure calculations for $Ag^{II}$ and $Ag^{III}$ fluorides in the solid state.

### 3.3.1. Methods of Calculations

The density-functional theory (DFT) computations have been performed with the Vienna Ab Initio Simulation Package (VASP)[109, 110] version 4.4. This code performs ionic and electronic optimizations using soft and ultrasoft Vanderbilt potentials to describe the electron–ion interactions. VASP uses very effective matrix diagonalization schemes and Pulay mixing to evaluate the electronic ground state. This allows reduction in the number of plane waves in the basis set and saves much computational time.

The electronic wavefunctions were expanded into plane-waves with a typical cutoff of $500 \pm 100$ eV for electronic minimizations (density of states, DOS calculations). The energy difference of $1 \times 10^{-3}$ eV per unit cell between two cycles has been used as a termination criterion for both electronic and ionic minimizations. We have used a conjugate gradient algorithm for ionic minimizations. Final DOS computations have been done with the highest precision (cutoff is set to 130 % of the typical value) and largest number of k-points. We have used automatic Monkhorst-Pack k-points generation schemes. Standard pseudopotentials included in VASP 4.0 have been used for all atoms without further modifications. Our computations are not spin polarized.

In our analysis, we need to see the contribution of various atomic orbitals to the total DOS, so as to gauge the extent of ionicity or covalence of the Ag–F bond.[111] All the atomic contributions to the DOS are shown *per one atom* of given type, if not otherwise indicated. The total DOS is always given per one formula unit ($Z=1$).

The results of our calculations are presented in Figure 21–27. In each Figure we show the DOS, and various contributions to them. There is a vast amount of information in our calculations; we have attempted to summarize the salient features in numerical form in Table 6. To support the interpretation of the results, we show first in Figure 20 the well-known diagram of the way the metal orbitals split in the various distorted octahedral ligand fields. We have assumed a weakly π-electron-donating ligand, such as $F^-$ ions, involved in *both* σ and π bonding with the metal. The axial ($z$) distance *increases*, and the equatorial distances ($x$, $y$) *decrease* from left to right in Figure 20. In the $O_h$ symmetry octahedron the distances are, of course, equal. Clearly, the $e_{2g}$ level splits along such a distortion coordinate, its important $z^2$ component moves systematically down (from left to right), and $x^2-y^2$ moves up in energy. The $t_{2g}$ set in $O_h$ transforms as e + a in $D_{4h}$. It is the extent of π bonding which controls the magnitude of the splitting of the e and a sets. The diagram is only schematic, deviations from this general picture may occur. For example (depending on the relative strength of the σ and π bonding), the $xy$ level might lie above the $z^2$ level in a square-planar coordination, and the $xz$, $yz$ levels might lie above the $x^2-y^2$ level in a linear coordination.

Table 6. Comparison of important parameters for several binary and ternary $Ag^{I}$, $Ag^{II}$, and $Ag^{III}$ fluorides in the solid state (results of DFT plane-wave pseudopotential computations). Chemical formula, formal oxidation state of Ag (OS), number of formula units in the elementary cell $Z$, total energy per formula unit ($E$ [eV FU$^{-1}$]), energy of the Fermi level ($E_F$ [eV]), total density of states at the Fermi level ($DOS_F$ [states (eV FU)$^{-1}$], density of states corresponding to $d^9$ occupation ($DOS_{1/2}$), composition (%) of $DOS_{1/2}$ ($Ag_{1/2}$, $F_{1/2}$, $Dop_{1/2}$; Dop = dopant), the $Ag_{1/2}$:$F_{1/2}$ ratio, maximum splitting of the F(p) and Ag(d) levels ($\Delta E_{split}$ [eV]), and dispersion of $d^9$-$d^{10}$ band ($\Delta E_{disp}$ [eV]). For compounds with two kinds of F atoms (F(1), F(2)) the contributions (%) of F(1) and F(2) to $DOS_{1/2}$ have been separated.

| Chemical formula | AgF | $AgF_2$ | $CsAgF_3$ | $Cs_2AgF_4$ | [AgF]$BF_4$ | $KAgF_4$ | $KAgF_4$[a] |
|---|---|---|---|---|---|---|---|
| OS | +1 | +2 | +2 | +2 | +2 | +3 | +3 |
| $Z$ | 4 | 4 | 4 | 2 | 2 | 4 | 1 |
| $E$ [eV FE$^{-1}$] | −7.73 | −11.60 | −21.29 | −30.20 | −37.56 | −24.40 | −23.89 |
| $E_F$ [eV] | −0.28 | −0.72 | −2.63 | −2.96 | −2.21 | −2.02[b] | −1.23 |
| $DOS_F$ [states (eV FE)$^{-1}$] | 0.000 | 1.114 | 0.997 | 2.596 | 1.070 | 0.000 | n.d.[c] |
| $DOS_{1/2}$ [states (eV FE)$^{-1}$] | 3.210[d] | 1.114 | 0.997 | 2.596 | 1.070 | 5.710[e] | n.d. |
| $Ag_{1/2}$ [%] | 81 | 65 | 71 | 61 | 71 | 34 | n.d. |
| F(1) [%] | – | – | 15 | 19 | 16 | – | n.d. |
| F(2) [%] | – | – | 8 | 10 | 13 | – | n.d. |
| $F_{1/2}$ [%] | 19 | 35 | 23 | 29 | 29 | 64 | n.d. |
| $Dop_{1/2}$ [%] | – | – | 6 (Cs) | 10 (Cs) | 0 (B) | – | n.d. |
| $Ag_{1/2}$:$F_{1/2}$ | 4.26 | 1.86 | 3.09 | 2.10 | 2.45 | 0.53 | n.d. |
| $\Delta E_{split}$ [eV] | 5.6 | 7.5 | 6.2 | 5.4 | 8.4 | 8.0 | n.d. |
| $\Delta E_{disp}$ [eV] | 0.7 | 1.5 | 1.5 | 1.0 | 1.4 | 0.3 | n.d. |

[a] Optimized in the $NaAlF_4$ structure. [b] Midway between highest filled (−2.94) and lowest unfilled (−1.09) band. [c] n.d. = not determined. [d] At −0.607 eV. [e] At −3.157 eV.

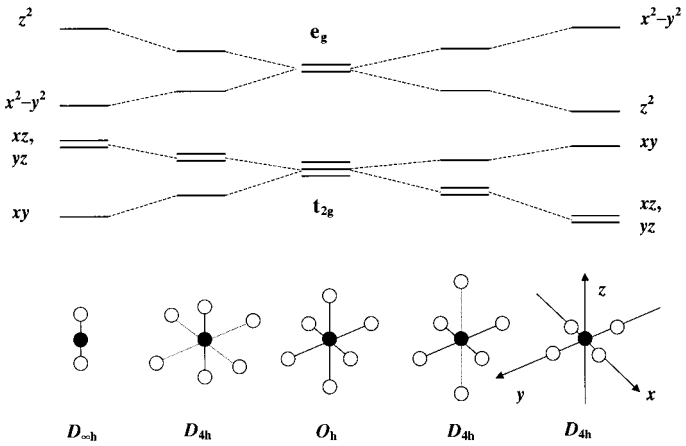


Figure 20. Energy diagram of the d-block levels of a transition metal in an undistorted and a distorted octahedral ligand field, a weakly electron-donating ligand creating both σ and π bonds with the metal center has been assumed. The apical ($z$) distance increases and the equatorial distances ($x$, $y$) decrease from left to right.

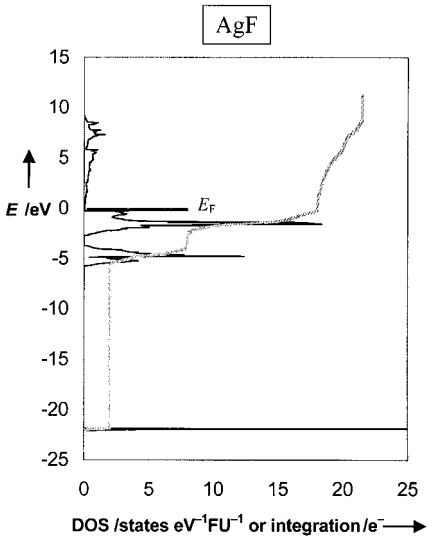


Figure 21. Total DOS of AgF (black curve) and its integration (gray curve).

What is important is that the $z^2$ levels will form the uppermost band (empty for $Ag^{III}$ ($d^8$), half filled for $Ag^{II}$ ($d^9$)) for compounds with a compressed octahedral (or almost linear) coordination of the Ag centers, while for compounds with elongated octahedral (or even square-planar) coordination of the Ag centers, the uppermost band will be built of $x^2$-$y^2$ levels.

### 3.3.2. *Electronic Structure of AgF: An $Ag^I$ Compound*

We begin with a simple cubic $Ag^I$ halide, as a calibration. AgF crystallizes in the NaCl structure ($Z = 4$). Each $Ag^+$ ion is surrounded by six $F^-$ ions at a distance of 2.467 Å. The electronic structure of AgF has been subject of several previous theoretical studies.[11, 112–115]

Our results (Figure 21) resemble in their essential features the literature results.[11] In AgF one sees several sets of states centered approximately at 1) −22, 2) −5, 3) −2 (valence band), 4) +5 (conduction band), and 5) +7.5 eV. Analysis of the different atomic contributions to DOS and the DOS integration allows us to classify the very narrow (in energy) group of states at −22 eV (1) as mainly F(2s), and the rather broad bands at +5 to +7.5 eV (4 and 5) as mainly being Ag(5s) and Ag(5p).[116] Two remaining sets of states extend over the energy range −5.8 to −0.2 eV. The first set (2) is at −3.7 to −5.8 eV and is dominated by F(p); the second set (3) at −0.2 to −2.6 eV (valence band), is mainly Ag(d).

Our computational results, similar to those of Onwuagba,[11] do not give a significant gap between the valence and conduction bands. This is because of the large width of the Ag(s) band, which almost penetrates the uppermost Ag(d) bands. This is actually a problem (perhaps a deficiency of the DFT calculations), for AgF is clearly a semiconductor with a substantial indirect band gap of 2.7–2.8 eV.[117] The DOS near the top of the valence band (0.1 eV below the Fermi level) is composed of 76% Ag(d) and 23% F(p) states.

Figures 22a–c show a smaller energy window, omitting the low lying F(s) levels and the conduction band, the total DOS of AgF, but now in a smaller −10 eV to +1 eV energy range, and its breakdown into the most important contributions: Ag(d) and F(p). To facilitate comparison with other silver fluorides, we will consequently show in the following Figures the total DOS and Ag(d) and F(p) contributions within exactly the same energy window.

We imagine that AgF is ionic; what evidence is there in the calculations for or against such an assignment? There is a gap between the uppermost F(p) and the lowermost Ag(d) states of about 1.1 eV (Figure 22a). Only 10% of the all Ag(s,p,d) states enter the F(p) band, while 76% of the all Ag(s,p,d) states are in the Ag(d) band. The remaining Ag(s,p,d) states are found in the conduction band (14%); their contribution to the F(s) bands is negligible. Overall, mixing of F and Ag states is relatively weak: the contribution of the Ag(d) states to the

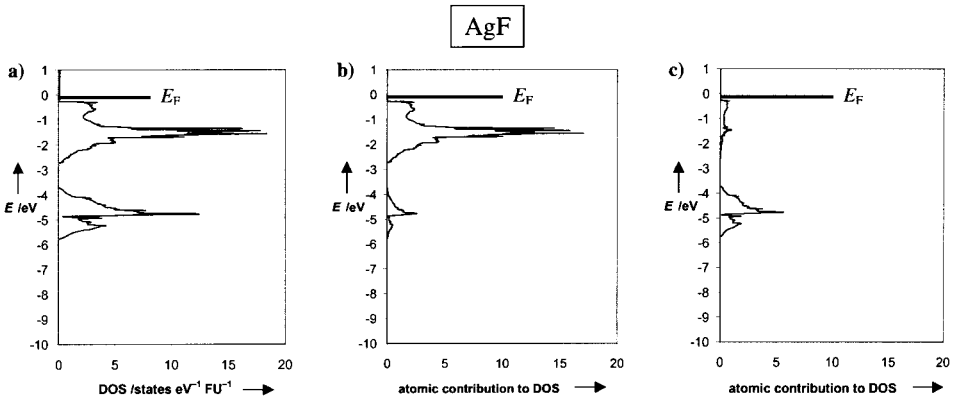


Figure 22. a) Total DOS of AgF in the −10 to +1 eV range and the contributions to it by b) Ag(d) and c) F(p) states.

F(p) band is rather small, as is the contribution of the F(p) states to the Ag(d) band. Based on these observations, we would argue that bonding in AgF indeed has predominantly ionic character, and the formulation of this compound is close to $[Ag^+F^-]$.

But even AgF shows some covalency; recall the composition 76% Ag(d) and 23% F(p) (cited above) of the states at the top of the valence band. We note here that, as much as the simplistic human mind would like to have it, there is no absolute division of ionic and covalent bonding, a situation we know from $H_2$. There are just extremes, more or less ionic or covalent—AgF is closer to the ionic limit.

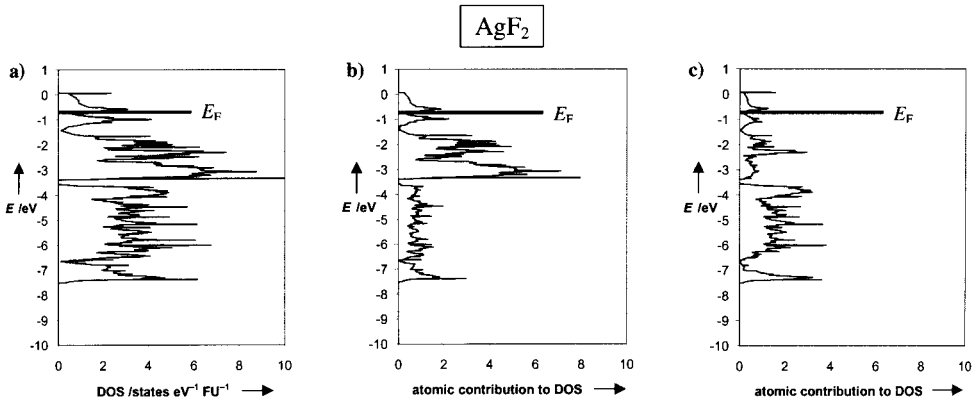


Figure 23. a) Total DOS of $AgF_2$ in the $-10$ to $+1$ eV range and its partitioning to b) Ag(d) and c) F(p) states.

### 3.3.3. Electronic Structure of $AgF_2$: An $Ag^{II}$ Compound

The crystal structure of $AgF_2$ is composed of puckered sheets of $AgF_2$ stoichiometry (see Figure 10). The DOS of this interesting compound (shown in Figure 23a–c) in the -7.5 to $+0.1$ eV range is composed of states with mixed Ag(d)/F(p) character. In the region from $-7.5$ to $-3.5$ eV one finds states that are thoroughly mixed Ag(d)/F(p) but are dominated by F(p). The reverse is true in the upper band, from $-3.4$ to $+0.1$ eV, mainly Ag(d) with strong F(p) mixture. In a normal picture of metal–ligand bonding the Ag(d)/F(p) wavefunctions in the lowermost states of the former band are Ag–F bonding,[118] and the corresponding orbitals in the uppermost states of the latter band are Ag–F antibonding. Much experience and the workings of perturbation theory would argue for such a characterization.[119] In the discussion that follows, we will make a corresponding assignment of bonding character to various groups of states.

There is an indication of a substantial covalent contribution to the bonding in $AgF_2$. The overall contribution of the Ag(s,p,d) states to the "F(p)" band is larger than in AgF, as is the contribution of the F states to the "Ag(d)" band. For example, 30% of the total Ag(s,p,d) states are in the "F(p)" band, and 57% of the Ag(s,p,d) states are in the "Ag(d)" band. The remaining Ag(s,p,d) states are to be found in the conduction band (12%) and in the "F(s)" band (1%). Clearly, there is increased mixing of the F(p) and Ag(d) states in $AgF_2$, as compared to AgF.

The uppermost $\sigma^*$ $(x^2-y^2)$ band is nicely split off from the rest of the Ag(d) block, half-filled and split in two, which gives DOS peaks at $-1.0$ and $-0.6$ eV. Certainly, this is not a consequence of the two slightly different Ag–F bond lengths (2.068 and 2.074 Å); the puckering of the $[AgF_2]$ sheets is likely to be the reason for the $x^2-y^2$ band split. The Fermi level $E_F$ is in a region of a substantial DOS, pointing to metallic character. A spin-polarized computation would be needed to confirm this.[120] Experimentally, $AgF_2$ is a spin-canted ferromagnet.

### 3.3.4. Electronic Structure of $KAgF_4$: An $Ag^{III}$ Compound

$KAgF_4$ and $BaAgF_4$ are isotypic examples of $KBrF_4$-type structures (see Figure 12) containing isolated $Ag^{III}/Ag^{II}$ centers in the form of square planar $[AgF_4]^-$ and $[AgF_4]^{2-}$ ions, respectively. $BaAgF_4$ contains magnetically isolated $Ag^{II}$ centers, and is paramagnetic. $KAgF_4$ is diamagnetic. Unfortunately, the structure of $BaAgF_4$ has not been refined; we have computed only the DOS of $KAgF_4$. The DOS of $KAgF_4$ (Figure 24a–c) is composed of sharp peaks in the $-9.0$ to $-0.7$ eV range (in the energy range shown; there are other F states below). The sharp band profile is, of course, characteristic of a molecular compound—it shows bands at specific (molecular) levels, with little dispersion. There is also a set of unfilled Ag(s) and Ag(p) states of at $+3.0$ to $+7.5$ eV (above the energy window shown). As for the $Ag^{II}$-containing compounds, the Ag(d) and F(p) states are strongly mixed with each other, within many of the sharp molecular bands.

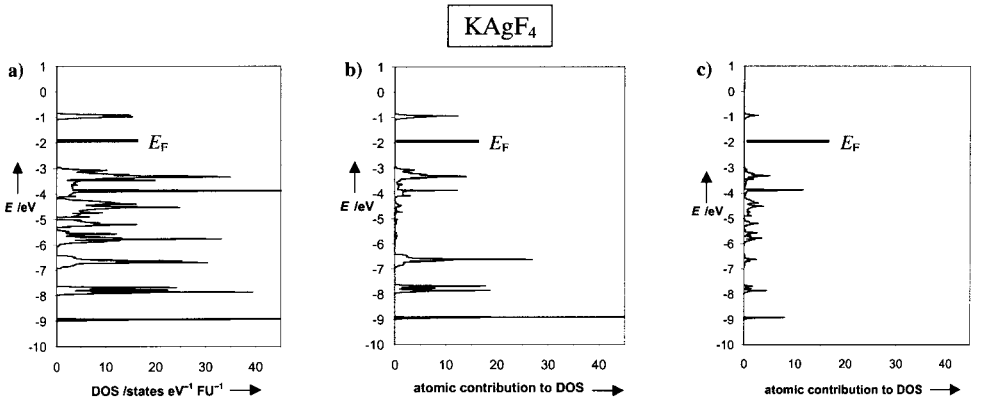


Figure 24. a) Total DOS of $KAgF_4$ in the $-10$ to $+1$ eV range and its partitioning to b) Ag(d) and c) F(p) states. The contribution of F(p) states is per *one* F atom.

Probably the most interesting feature of $KAgF_4$ is that the "quite molecular" DOS in the region of the Ag–F bonding states ($-6.5$ to $-9.0$ eV) is dominated by Ag(d) states, while in the uppermost Ag–F antibonding states (sharp DOS peak at $-0.7$ eV, unfilled) there is a slight excess of F(2p) orbitals (a contribution per *one* F atom is shown in Figure 24c, there are four F atoms). The classical picture used for ionic inorganic compounds (states originating from main group ligand orbitals below the d-block metal), that is, an ionic formulation of $KAgF_4$ as $K^{I}Ag^{III}(F^{-})_4$, must be modified in this case.

The Ag–F bonding is substantially covalent in $KAgF_4$. $AgF_3$ (at $+20\,^{\circ}C$) and $KAgF_4$ (at about $+370\,^{\circ}C$) both evolve molecular $F_2$. We see theoretically (as we did in a survey of the chemistry) that $Ag^{III}$ is able to generate holes in the F(p) band.[121] This is rather rare in transition metal chemistry, to put it mildly.[122]

The uppermost $\sigma^*$ $x^2-y^2$ group of states (the sharp DOS peak at about $-0.9$ eV) is not filled, as expected for a square-planar molecular compound. The computed band gap between the occupied $z^2$ and the unoccupied $x^2-y^2$ levels is about 2.0 eV. It is thus smaller than the experimental optical band gap of about 3 eV (the compound is yellow, it absorbs in the violet). According to our computations, $KAgF_4$ should be an insulating material, in agreement with experimental results.

The energy penalty to be paid upon transformation of $KAgF_4$ from the $KBrF_4$ to the $NaAlF_4$ structure was of interest to us. $KAgF_4$ in the $NaAlF_4$ structure would be a 2D compound, containing $AgF_2$ and $KF_2$ layers (Figure 13).[123] We have optimized $KAgF_4$ in the $NaAlF_4$ structure to evaluate the energy of transformation. The computed value is quite large, about 0.5 eV per formula unit. Clearly, $[AgF_4]^-$ is an exceptionally weak $F^-$ donor, unable to donate $F^-$ ions to a weak $F^-$ acceptor ($K^+$). This means that attempts to obtain quasi-2D structures containing $Ag^{III}$ units may be unsuccessful.

### 3.3.5. Electronic Structure of [AgF][BF$_4$]: An Ag$^{II}$ Compound with Linear [AgF]$^+$ Chains

The electronic structure of $[AgF][BF_4]$ is shown in Figure 25a–d. This phase contains linear $[AgF]^+$ chains (from here on the AgF fluorine atom will be called F(1)) and isolated $[BF_4]^-$ ions (the $BF_4^-$ fluorine is F(2)). The $\sigma$ states of the closed-shell molecular tetrahedral $[BF_4]^-$ unit are at about $-9.8$ to $-8.0$ eV, forming quite narrow bands.[124] They have mixed B/F(2) character with a dominant F(2) component. There are also broad, bonding[118] bands of $\sigma$ levels of the $[AgF]^+$ chain, lying in the $-6.8$ to $-8.0$ eV range. These bands are presumably composed of Ag($z^2$) and F(p) orbitals, since the coordination of the Ag center is compressed octahedral (see Figures 5 and 24). Our analysis here depends in part on a partitioning of the total DOS into $[BF_4]^-$ and $[AgF]^+$ sublattice contributions, which we have studied, but do not present here.

There is another set of bands in the $-6.5$ to $-1.4$ eV region. These bands originate mainly from the nonbonding[125] F(p) and antibonding[118] Ag(d)/F(p) levels (the nonbonding levels of the F(2) atoms contribute mainly in the lower energy range

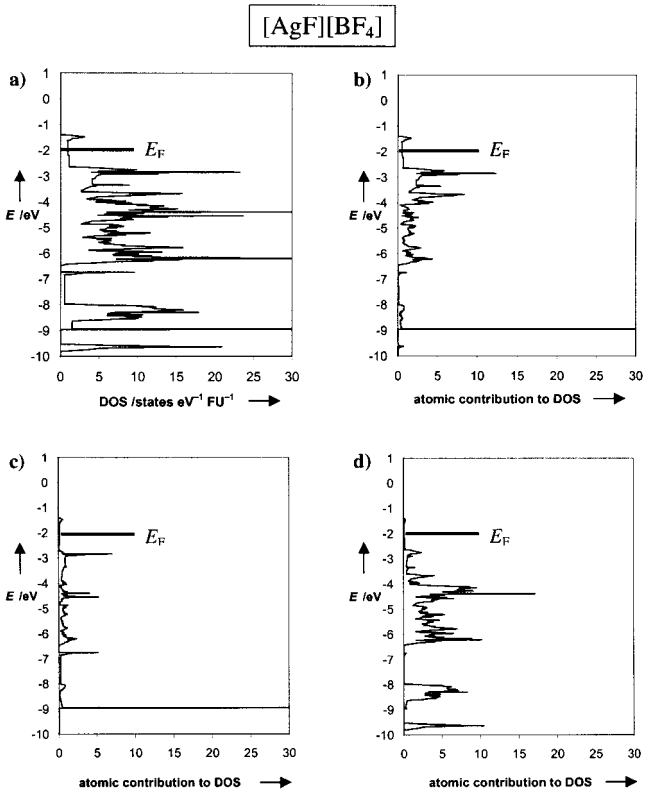


Figure 25. a) Total DOS of $[AgF(1)][BF(2)_4]$ ($\equiv [AgF][BF_4]$) in the $-10$ to $+1$ eV range and the contributions to it by b) Ag(d), c) F(1)(p) and d) F(2)(p) states.

from $-6.5$ to $-4.0$ eV). There is no gap between the nonbonding (F) and antibonding (Ag/F) levels, but the integration of the DOS (not shown here) allows us divide this region between the "$\pi$-type lone pairs of F atoms" ($-6.5$ to $-4.0$ eV, 20p electrons from 5F atoms) and "Ag(d) levels" ($-4.0$ to $-1.4$ eV, room for 10 Ag(d) electrons). The latter bands, however, have in fact mixed F/Ag character; the DOS at the Fermi level has contributions from both Ag (71%) and F states (29%).

The interaction between the $[AgF]^+$ and $[BF_4]^-$ sublattices is weak, but noticeable. In the important Fermi level region, the contribution from four F(2) atoms is roughly as large as the contribution from one F(1) atom. According to our computations, $[AgF][BF_4]$ is a quasi-1D metal, the unpaired electrons being delocalized in the uppermost $\sigma^*$ $z^2$ band. This is in agreement with its experimentally derived Pauli temperature-independent paramagnetism, and the metallic luster of the compound.

### 3.3.6. Electronic Structure of CsAgF$_3$

The complete DOS of perovskite $[CsF][AgF_2]$ and its decomposition into different atomic contributions are shown in Figure 26a–d. The structure (see Figure 7) contains $AgF_2$ planes (the F atoms in these planes will be called F(1)) and CsF planes (the CsF fluorine is F(2)); the coordination of the Ag unit is elongated octahedral. The DOS in the $-9.0$ to

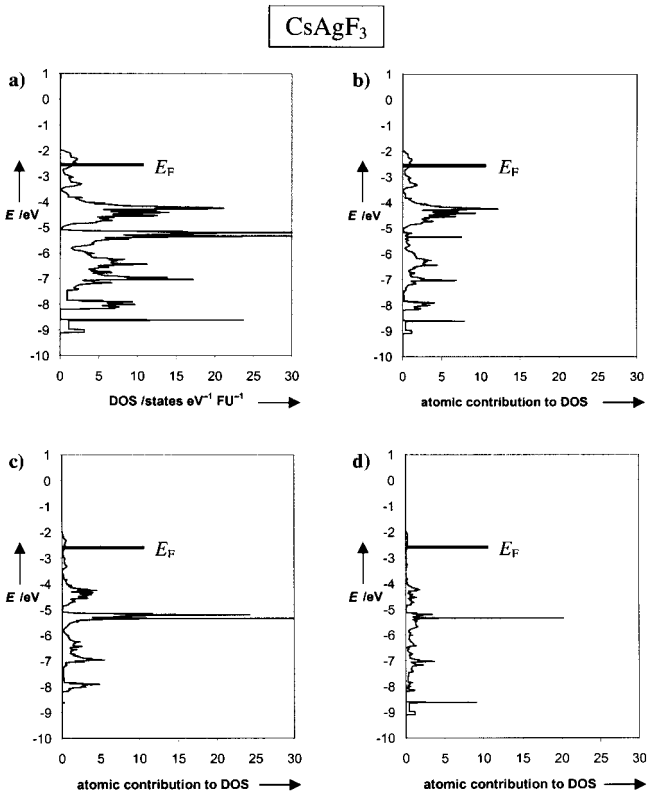


Figure 26. a) Total DOS of $[AgF(1)_2][CsF(2)]$ ($\equiv CsAgF_3$) in the $-10$ to $+1$ eV range and its partitioning into b) Ag(d), c) F(1)(p) and d) F(2)(p) states.

$-2.0$ eV region is composed of mixed Ag(d) and F(p) states (Cs does not contribute significantly in this energy window). Integration of DOS and analysis of atomic contributions allow us to divide these states into ones with dominant F character ($-9.0$ to $-5.0$ eV) and those with dominant Ag contribution ($-5.0$ to $-2.0$ eV). The uppermost σ* Ag–F antibonding ($x^2-y^2$) band is split into two bands, centered around $-2.7$ eV. The reason for this split may be in the geometric structure of the $AgF(1)_2$ planes: there are two different AgF(1) bond lengths of 2.06 Å and 2.13 Å in this sheet.

There is an indication of a covalent contribution to the bonding in $CsAgF_3$. As much as 43% of the Ag(s,p,d) states goes to the "F(p)" band, and 49% of the Ag(s,p,d) states remains in the $10e^-$ "Ag(d)" band. The rest of the Ag(s,p,d) states may be found in the conduction band (7%) and the "F(s)" band (1%). Compare these numbers to the respective ones for $AgF_2$. Apparently, about 14% of the Ag states are transferred from the "Ag(d)" and "Ag(s,p)" bands to the "F(p)" and "F(s)" bands in $[CsF][AgF_2]$. Making the puckered $[AgF_2]$ sheets present in $AgF_2$ planar, and sandwiching them between the [CsF] layers, probably introduces some positive charge into the $[AgF_2]$ planes, and increases the covalency of Ag–F bonding.

$[CsF][AgF_2]$, which exhibits metallic luster and is a Pauli paramagnet above $T_N$, should indeed be metallic, according to our computations; the unpaired electrons are delocalized in the uppermost σ* $x^2-y^2$ band of the $[AgF_2]$ sheets.

### 3.3.7. Electronic Structure of $Cs_2AgF_4$

$Cs_2AgF_4$ is an example of a compound with alternating $AgF_2$ planes (the F atoms here will be called F(1)) and two CsF planes (with F(2) atoms; see Figure 8). This compound has a structure similar to perovskite-related $K_2NiF_4$; the only difference is in the compressed (and not elongated) octahedral environment around the metal center.[73] There are two equal Ag–F(1) bonds in the structure of $Cs_2AgF_4$ (compare to $CsAgF_3$ with two different Ag–F(1) bonds). The DOS of this compound (shown in Figure 27a–d) in the $-8.1$ to $-2.8$ eV range is composed of states having mixed Ag(d) and F(p) character, as in $CsAgF_3$. Analyzing the integration curve and contributions of different sites, we may divide these states roughly into Ag–F bonding ones ($-8.1$ to $-6.3$ eV, with dominant F(p) contribution), Ag–F nonbonding ones ($-6.3$ to $-5.3$ eV), and Ag–F antibonding ones ($-5.3$ to $-2.8$ eV, with dominant metal contribution; "Ag(d)" bands).

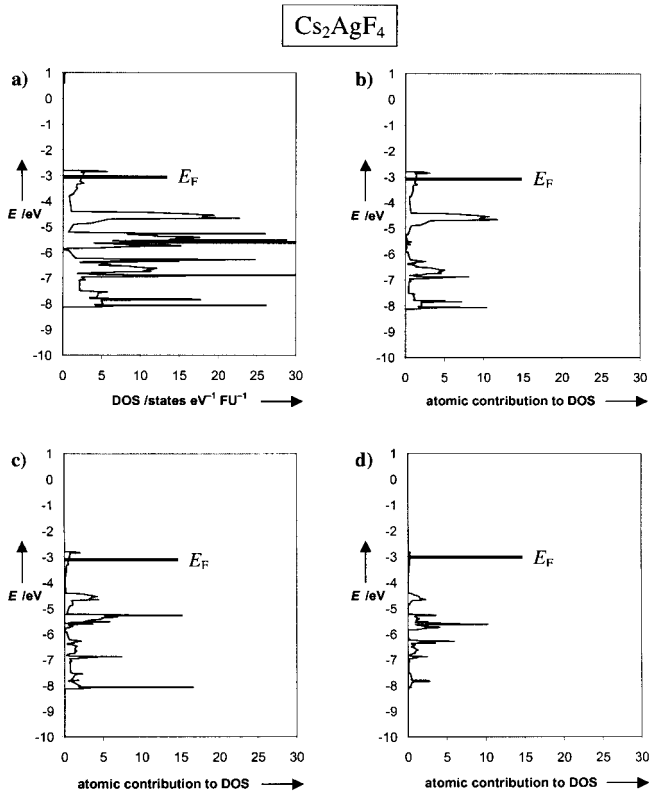


Figure 27. a) Total DOS of $[AgF(1)_2][CsF(2)]_2$ ($\equiv Cs_2AgF_4$) in the $-10$ to $+1$ eV range and its partitioning to b) Ag(d), c) F(1)(p) and d) F(2)(p) states.

The covalency of the Ag–F bonding in $Cs_2AgF_4$ is quite similar to that in $CsAgF_3$. For example 43% of the all Ag(s,p,d) states are in the "F(p)" band, and 50% of the Ag(s,p,d) states are in the $10e^-$ "Ag(d)" band. The remaining Ag(s,p,d) states are in the conduction band (6%) and in the "F(s)" band (1%).

The uppermost group of states is half-filled and is not split. States at the Fermi level are composed of Ag orbitals (61%), F(1) orbitals (19%), and F(2) orbitals (10%). The atomic contributions of F(1) and F(2) (per *one* F atom) to the states at

the Fermi level are very similar, 9.5 % and 10 %, respectively. It is interesting that the substantial difference in the Ag–F(1) and Ag–F(2) bond lengths (2.29 Å and 2.19 Å, respectively) is not reflected in different contributions from F(1) and F(2) to the states at the Fermi level, as one might expect from Figure 20. Most probably the states at the Fermi level originate from both σ* $z^2$ and σ* $x^2-y^2$ bands. There is substantial DOS at the Fermi level; $Cs_2AgF_4$ is metallic, according to our computations.

### 3.3.8. *Summary of Electronic Structure Computations for $Ag^{II}$, $Ag^{III}$, and $Ag^{I}$ Fluorides*

Analysis of the data from Table 6 allows a semi-quantitative comparison of the bonding situation in $[AgF]^+$ infinite chains, $[AgF_2]^0$ planes, and in systems containing isolated $Ag^I$ and $Ag^{III}$ species.

In the $Ag^{II}$-containing compounds, the states at the Fermi level are composed of mixed F(p) and Ag(d) levels (the states at the Fermi level are presumably Ag–F antibonding). It is very instructive to compare contributions from the Ag and F orbitals to the DOS for different compounds of $Ag^I$, $Ag^{II}$, and $Ag^{III}$. For this purpose we have computed the composition of the total DOS corresponding to the $d^9$ configuration ($DOS_{1/2}$ in Table 6, the index ½ refers to the half-filling of this band for the $d^9$ configuration; $DOS_{1/2} = DOS_F$ for compounds of $Ag^{II}$) in all compounds of $Ag^I$, $Ag^{II}$, and $Ag^{III}$ investigated. The position of $DOS_{1/2}$ shifts predictably to lower energy with the oxidation state of silver: about −0.6 eV for $Ag^I$, about −2.0 to −3.0 eV for $Ag^{II}$, and −3.2 eV for $Ag^{III}$. These levels are composed predominantly of Ag orbitals (80 % Ag) for $Ag^I$, show slight domination of silver (60–70 % Ag) for $Ag^{II}$, and are dominated by F orbitals (35 % Ag) for $Ag^{III}$. The relative contribution of Ag and F orbitals to the bands corresponding to the $d^9$ occupation in $KAgF_4$ is such that the Ag atom contributes roughly the same to these states as one F atom. Clearly, an increase in the Ag oxidation state (introducing holes into the band structure of the $Ag^I$ and $Ag^{II}$ compounds) leads to increased covalency of the Ag–F bond.

The $Ag^{II}$–$F^-$ bonding is substantially covalent in character.[126] The Ag–F bonding in $KAgF_4$ ($Ag^{III}$) is more, and in AgF ($Ag^I$) is less covalent than that in $Ag^{II}$ fluorides. The lowest occupied Ag(d)/F(p) bonding states are dominated by F(s,p) contributions in AgF and by Ag(s,p,d) contributions in $KAgF_4$. Apparently, Ag(d) states "sink" into the F(p) ones, as we move from $Ag^I$ through $Ag^{II}$ to $Ag^{III}$ compounds.

The most pronounced covalent character of the $Ag^{II}$–$F^-$ bond is obtained for $[AgF][BF_4]$ (the ratio of the total Ag:F contributions is 2.45:2[127] = 1.23). This is in agreement with our intuition on quasi-1D and quasi-2D structures. The affinity of $Ag^{II}$ towards $F^-$ ions is such that it creates either two very strong, short ("more covalent") bonds (as in $[AgF][BF_4]$) or four longer ("more ionic"), but still appreciably strong bonds (as in $BaAgF_4$). The coordination found in compounds with $AgF_2$ planes appears to be intermediate between the two limiting cases described above.

The energies of the Fermi level ($E_F$) of course vary in a wide range (−3.0 to −0.7 eV) for the $Ag^{II}$ compounds, for example, $E_F = -0.3$ eV for AgF, and $E_F = -2.0$ eV for $KAgF_4$. $Cs_2AgF_4$ and $CsAgF_3$ are predicted[128] to be the strongest oxidizing agents among the systems studied, stronger even than $KAgF_4$ ($Ag^{III}$-containing compound). This is also revealed in the contribution of Ag(s,p,d) states to the occupied Ag–F bonding states, which increases in the direction: $AgF_2$ (31 %) < $CsAgF_3 \approx Cs_2AgF_4$ (44 %). This effect might be connected with introducing a partial positive charge into the $[AgF_2]$ sheets when they are gradually separated upon intercalation of the [CsF] layers. A choice between Na, K, Rb, and Cs, and between $MAgF_3$ and $M_2AgF_4$ structures should leave some space for manipulation of this charge.

The magnitude of the $DOS_F$ found in $Ag^{II}$–$F^-$ compounds ranges from about 1 to about 2.6 states (eV FU)$^{-1}$, where FU = formula unit. The largest value, of 2.6 states (eV FU)$^{-1}$, is computed for $Cs_2AgF_4$. Very large local DOS (sharp peaks in DOS) are found, as expected, for $KAgF_4$ ($DOS_{1/2} \approx$ 10 states (eV FU)$^{-1}$, a compound containing molecular $[AgF_4]^-$ centers.

The difference in energy between the F(p) (bottom of the Ag–F bonding levels) and the Ag(d) bands (top of the Ag–F antibonding levels) is 5.4–8.4 eV in all silver fluorides investigated. The $d^8$-$d^{10}$ uppermost two-electron band is spread over 1.0–1.5 eV in $Ag^{II}$ fluorides, and over only 0.3–0.7 eV in compounds of $Ag^I$ and $Ag^{III}$ containing fairly well separated Ag centers.

$KAgF_4$ crystallizes in a $KBrF_4$ structure (with isolated $[AgF_4]^-$ units; Figure 12). We wanted to see how much this structure is favored over the simple $NaAlF_4$ structure (having $[AgF_2]^+$ planes; Figure 13). The calculated preference is 0.5 eV FU$^{-1}$. This value suggests that introducing $Ag^{III}$ centers into the $AgF_2^0$ sheets in $KAgF_3$ should be very difficult, if it is to happen without decomposition of this structure into isolated $[AgF_4]^-$ ions. $Ag^{III}$ usually needs four "unshared" $F^-$ ligands, while $Ag^{II}$ (a weaker Lewis acid) is typically saturated having between two and four "shared" $F^-$ ions. $CsAgF_4$ is probably the only $MAgF_4$ compound which crystallizes in the $NaAlF_4$ structure. The $NaAlF_4$ structure might be preferred for this compound, because of the large dimensions of the $Cs^+$ ion.[100]

Why did we not pursue the theoretical analysis in this paper with the extended Hückel method but instead used the VASP density-functional code? With the extended Hückel procedure we would have been able to apply a host of interpretational tools analyzing orbital contributions in detail, and looking at bonding through overlap or Hamilton populations. The reason we did not do so is that the problem at hand (a comparison of bonding in $Ag^I$, $Ag^{II}$, and $Ag^{III}$ fluorides) is singularly unsuited to the extended Hückel method, despite our substantial experience with it. The extended Hückel method, in its usual implementation, does not allow the energies of Ag orbitals (or their extent in space) to vary as the oxidation state of silver varies. And yet that variation is at the heart of what we wish to understand—the real and important differences among $Ag^I$, $Ag^{II}$, and $Ag^{III}$ centers. For this reason we were willing to give up interpretability for greater accuracy.

### 3.4. Analogies and Differences among the $Ag^{II}$-, $Cu^{II}$-, and $Au^{II}$-Containing Systems

$Ag^{II}$ is isoelectronic with $Cu^{II}$ and with ephemeral $Au^{II}$. Hence, it is instructive to analyze the behavior of $Ag^{II}$-containing systems from the perspective of analogous $Cu^{II}$ and $Au^{II}$ compounds.

#### *3.4.1. General Comparison of the Properties of Ag, Cu, and Au in Different Oxidation States*

"Like copper, silver and gold have a single s electron outside a completed d shell, but in spite of the similarity in electronic structures and ionization potentials there are few resemblances between Ag, Au, and Cu. And there are no simple explanations for many of the differences although some of the differences between Ag and Au may be traced to relativistic effects on the 6s electrons of the latter." [129]

We begin a discussion of this topic with several arguments of a chemical nature, based on electronegativities, oxidation states, and some structural aspects. Numerical data relevant to the discussion are collected in Table 7. An analogous comparison for F and O is shown in Table 11 in the Appendix.

Table 7. Comparison of several important properties of Cu, Ag, and Au and their compounds.[a]

| | Cu | Ag | Au |
|---|---|---|---|
| 1st $E_i$ [kJ mol$^{-1}$] | 745.5 | 731.0 | 890.1 |
| 2nd $E_i$ [kJ mol$^{-1}$] | 1957.9 | 2070 | 1980 |
| 3rd $E_i$ [kJ mol$^{-1}$] | 3555 | 3361 | no data |
| 1st $E_{ea}$ [kJ mol$^{-1}$] | 118.4 | 125.6 | 222.8 |
| Pauling EN | 1.90 | 1.93 | 2.54 |
| Mulliken-Jaffe EN | 1.49 (4s) | 1.47 (5s) | 1.87 (6s) |
| redox potential $E^0$ [V] (acidic solution): | | | |
| | ? ($Cu^{III}/Cu^{II}$) | 1.980 ($Ag^{II}/Ag^{I}$) | 1.83 ($Au^{I}/Au^{0}$) |
| | 0.520 ($Cu^{I}/Cu^{0}$) | 1.67 ($Ag_2O_3/Ag^{I}$) | 1.52 ($Au^{III}/Au^{0}$) |
| | 0.159 ($Cu^{II}/Cu^{I}$) | 1.36 ($Ag_2O_3/Ag^{II}$) | 1.36 ($Au^{III}/Au^{I}$) |
| | | 0.799 ($Ag^{I}/Ag^{0}$) | |
| redox potential $E^0$ [V] (basic solution): | | | |
| | – | 1.757 ($Ag_2O_3/Ag^{I}$) | – |
| | | 1.711 ($Ag_2O_3/Ag_2O_2$) | |
| | | 0.604 ($AgO/Ag_2O$) | |
| | | 0.342 ($Ag_2O/Ag$) | |
| $R(M^{I})$ [Å] | 0.91 (cn = 6, $O_h$) | 1.42 (cn = 8, cubic) | 1.51 (cn = 6, $O_h$) |
| | 0.74 (cn = 4, $T_d$) | 1.29 (cn = 6, $O_h$) | |
| | | 1.14 (cn = 4, $T_d$) | |
| $R(M^{II})$ [Å] | 0.87 (cn = 6, $O_h$) | 1.08 (cn = 6, $O_h$) | 1.09 (cn = 6, $O_h$) |
| | 0.71 (cn = 4, $T_d$) | 0.93 (cn = 4, $D_{4h}$) | |
| | 0.71 (cn = 4, $D_{4h}$) | | |
| $R(M^{III})$ [Å] | 0.68 (cn = 6, $O_h$) | 0.89 cn = 6, $O_h$) | 0.99 (cn = 6, $O_h$) |
| | | 0.81 cn = 4, $D_{4h}$) | 0.82 (cn = 4, $D_{4h}$) |
| $R(M^{V})$ [Å] (calcd) | 0.38 (cn = 6, $O_h$) | 0.53 cn = 6, $O_h$) | 0.56 (cn = 6, $O_h$) |
| $R$(vdW) [Å] | 1.40 | 1.72 | 1.66 |
| bond enthalpy [kJ mol$^{-1}$] of diatomic molecules MX: | | | |
| X = O | 269.0 ± 20.9 | 220.1 ± 20.9 | 221.8 ± 20.9 |
| X = Cl | 382.8 ± 4.6 | 341.4 | 343 ± 9.6 |
| X = F | 413.4 ± 13 | 354.4 ± 16.3 | – |
| melting ($T_m$), boiling ($T_b$) sublimation ($T_s$) and/or decomposition ($T_d$) [°C]: | | | |
| $M^{I}$ oxide | $T_m$ = 1235, $T_d$ = 1800 | $T_d$ = 230 | – |
| $M^{I}$ chloride | $T_m$ = 430 | $T_m$ = 455, $T_b$ = 1550 | $T_d$ = 170 (→Au+$AuCl_3$) |
| $M^{I}$ fluoride | $T_d$ = 908 | $T_m$ = 435, $T_b$ = 1159 | – |
| $M^{II}$ oxide | $T_m$ = 1326 | – | – |
| $M^{II}$ chloride | $T_m$ = 620, $T_d$ = 993 | – | – |
| $M^{II}$ fluoride | $T_d$ = 950 | $T_m$ = 690, $T_d$ = 700 | – |
| $M^{III}$ oxide | – | – | $T_d$ = 160 (−O), $T_d$ = 250 (−3O) |
| $M^{III}$ chloride | – | – | $T_d$ = 256 |
| $M^{III}$ fluoride | $T_d$ = −40 | $T_d$ = 20 | $T_s$ = 300 |

[a] $E_i$ = ionization energy; $E_{ea}$ = electron affinity; EN = electronegativity (in Pauling units); cn = coordination number; vdW = van der Waals.

The Pauling electronegativities (PENs) for Cu, Ag, and Au are 1.90, 1.93, and 2.54, respectively.[130] Such diversity of PENs within a given transition metal group is otherwise observed only in Group 6. Absolute values of PEN allow one to classify Cu and Ag midway between the most electropositive ("most metallic"[131]) element in the d-block, Hf (PEN(Hf) = 1.30), and the most electronegative ("most nonmetallic") one, Au itself. The PEN(Au) = 2.54 is appreciable; chemists call Au a noble metal. The PEN(Au) compares with PEN of several nonmetallic or semimetallic elements, such as C (2.55), Se (2.55), and I (2.66). However, the Mulliken – Jaffe electronegativity of Au is 1.87, much below values for I (2.74, for 14.3 % s orbital[132]), Se (2.60, for 16.7 % s orbital[132]), and C (2.48, $sp^3$ orbital[132]), weakening our PEN-based classification of Au as a nonmetal.[133]

"Typical" oxidation states are II (and I) for Cu, I (and II) for Ag, and III (and I) for Au.[134] $Cu^{III}$ occurs less frequently than $Cu^{II}$.[135] $Au^{I}$ has a strong tendency towards disproportionation to metallic $Au^0$ and $Au^{III}$. $Au^{II}$ was first reported in solution,[136] is stable in the gas phase,[137] and immensely rare in the solid state.[138–140] Oxidation state V has been obtained for several Au compounds;[88, 95, 141–144] it has been claimed in one case for Ag,[145] and has never been reached for Cu.[146] Apparently, the relative availability of two $d(z^2)$ electrons for removal from the square planar $M^{III}(d^8)$ species is related to the contraction of the $d(z^2)$ lone pair, in the order: Cu (the most contracted, most difficult to oxidize) > Ag > Au (the least contracted).

A fluoride environment stabilizes the "untypical" oxidation state II of Au and Ag. A number of fluoride complexes of $Ag^{II}$ have been prepared and structurally characterized (see Section 3.1). Also, the first "purely inorganic" $Au^{II}$ complexes in the solid state have been obtained in fluoride systems.[19, 30, 147]

The relative stability of different oxidation states of Cu, Ag, and Au in different ligand environments is very interesting. It is known that $Cu^{II}$ exhibits strong "chemical affinity"[148] to $O^{2-}$; for $Cu^{I}$ and $Ag^{I}$ this is true for $S^{2-}$ and $Cl^{-}$; and for $Au^{III}$ and $Au^{I}$ to $Cl^{-}$ (compare, for example, melting, boiling, sublimation, and decomposition temperatures of different compounds of Group 11 metals, given in Table 1). Usually a

large chemical affinity is indicative of *covalent* bonding between the elements. In this context, the large affinity of $Ag^{II}$ to $F^-$ ions is of great interest.[149] It hints at efficient mixing of the Ag(d) and F(p,s) orbitals, which we have already noticed in the band calculations, and is provided by the energetic proximity and similar spatial extent of these orbitals. Surprisingly strong mixing of the fluorine and silver orbitals has been noted even for $Ag^I$ (a relatively weak Lewis acid) in an fcc phase of AgF.[150, 151]

$Ag^{II}$ is an incredible species. When solvated in anhydrous hydrogen fluoride, it is one of the best oxidizing agents known. It oxidizes Xe to $Xe^{II}$, generates $C_6F_6^+$ salts from $C_6F_6$, liberates $IrF_6$ from its anion and $S_2O_6F_2$ from $SO_3F^-$ ions, and oxidizes $CF_3CF{=}CF_2$ quantitatively to $CF_3CF_2CF_3$. It has been stated in the literature that the electronegativity (in context of orbital electronegativity or configuration energy) of $Ag^{II}$ (and even more likely of $Ag^{III}$) is close to that of the $F^-$ ion itself.[152] These experimental observations, together with the fact that many $Ag^{II}$ and $Ag^{III}$ compounds easily liberate $F_2$, indeed point to an energetic proximity of the Ag(d) and F(p,s) orbitals.

Valuable information about the character of the M–F (M = Cu, Ag, Au) bond is provided by theoretical studies for MF, $MF_2$, and $MF_3$ molecules in the gas phase, M = Cu,[153–158] Ag,[153, 156, 159, 160] Au.[153, 156, 161, 162] These studies clearly indicate, that:

a) The largest relativistic contraction of bond lengths occurs for $Au^I$ (0.36 Å), followed by $Ag^I$, $Au^{II}$, and $Au^{III}$ (ca. 0.16–0.18 Å)[163]
b) Relativistic effects are responsible for weakening of $Au^I$ bonding to electronegative ligands, as compared to a hypothetical nonrelativistic case[164]
c) The decomposition of $[MF_4]^-$ species according to equation: $[MF_4]^- + E_{dec} \rightarrow [MF_2]^- + F_2$, is least favored for M = Ag, thus indicating great stability of $Ag^{III}$–$F^-$ bonds
d) A very strong coupling of the neutral $Ag(4d^{10}5s^1)F(2s^22p^5)$ and ionic $Ag^+(4d^{10}5s^0)F^-(2s^22p^6)$ configurations ("valence tautomerism"[165]) is observed at relatively short interatomic separation in the $^{3,1}\Sigma^+$ states of the AgF molecule (for CuF only the ionic configuration contributes appreciably). Again, a leading motive is strong covalent Ag–F bonding.

Large covalency is seen also in relativistic computations for $Au^{III}$ and $Au^V$ molecular fluorides,[166] and is also deduced from electronic absorption[167] and ESR[168] spectra of the corresponding solids.

### 3.4.2. Comparison of Geometric Structures of Fluorides, Oxides, and Chlorides of Ag, Cu, and Au in the Solid State

The diversity of the chemistry of the three Group 11 members is impressive. Despite of it, interestingly, there is still much structural similarity between Ag-, Cu-, and Au-containing solids:

a) The very stable $M^I$ complexes often show a linear geometry with two ligands. This is exemplified by $Cu_2O$, $[AgCl_2]^-$, the $[AgO_2]$ unit,[169] and $[AuCl_2]^-$.
b) $M^{II}$ complexes typically have an elongated octahedral coordination geometry, as seen in $Cu^{II}(OH_2)_6$, $\alpha$-$CuZrF_6$, $CsAgF_3$, and $Au[SbF_6]_2$. This is consistent with a strong Jahn–Teller distortion in the $d^9$ configuration.
c) Sometimes $M^{II}$ complexes have a compressed octahedral geometry, as in $KCuF_3$[170, 171] and $K_2CuF_4$,[172] $KAgF_3$ and $Cs_2AgF_4$. This is the opposite phase of the Jahn–Teller deformation mentioned in (b).[173]
d) More seldom, the $M^{II}$ complexes are two-coordinate linear species (with four additional weak interactions), as seen for $[CuF][AuF_4]$[174] and $[AgF][BF_4]$. This could be seen as the limiting case of an compressed octahedron.
e) The $M^{III}$ complexes usually have a local square-planar geometry, as in the case of $[CuF_4]^-$,[175] $[AgF_4]^-$,[176] $[AuF_4]^-$, $[AuCl_4]^-$, and the $[AuO_4]$ unit.[177] This is of course what would be expected of a $d^8$ transition metal complex.
f) $Cu^{III}$ (and much more seldom high-spin $Ag^{III}$) complexes are also found as octahedral species (elongated in $K_3CuF_6$, undistorted in $Cs_2KAgF_6$).

Given the similarity of the covalent radii of Ag and Au (especially in oxidation states II and III), the occurrence of isotypic compounds for these two metals is not surprising. Also, as may be seen from the above comparison, compounds of Cu and Ag are often isotypic, although there are some deviations from this rule. An interesting example of similarity of Ag and Cu is provided by a fluoride complex, $Ag^{II}_3[ZrF_7]_2$.[178] Two kinds of $Ag^{II}$ center appear in this compound. It is known that one of these centers, Ag(1), may be easily substituted by $Cu^{II}$, thus giving $Cu^{II}Ag^{II}_2[ZrF_7]_2$, a mixed Ag/Cu compound. $Ag^I_2Cu^{II}_2O_3$, isotypic with $Cu^I_2Cu^{II}_2O_3$, is another example.[179]

Many structural features are shared between the $Ag^{II}$ fluorides and the famous cuprate superconductors.[180]

The $[AgF_2]_\infty$ planes occurring in some $MAgF_3$ and $M_2AgF_4$ compounds are typical of the analogous $MCuF_3$ and $M_2CuF_4$ compounds, and they also bring to mind $[CuO_2]_\infty$ planes, an essential structural element for superconductivity in cuprates.[181] For example, $CsAgF_3$ adopts a slightly distorted perovskite structure (Figure 7), typical for some oxobismuthate superconductors. $Cs_2AgF_4$ crystallizes in the perovskite-related $K_2NiF_4$ structure (Figure 8), which occurs in superconducting $La_{2-x}Sr_xCuO_4$ and $Sr_2RuO_4$. The Ag center has elongated octahedral hexa-coordination in $CsAgF_3$ and $Cs_2AgF_4$. On the other hand, $[MX]_\infty$ chains[182] are observed in both Ag and Cu fluorides (Figure 5, 8, 10) and in some cuprate superconductors for example YBCO. Also Ag centers in a distorted tetragonal pyramidal penta-coordination, similar to pentacoordinate Cu in some oxocuprates (Figure 3), are known. Strong $[CuO_2]_\infty$ interlayer coupling, which leads to record critical temperatures, is found in the oxocuprate superconductors with tetragonal tetra coordination of Cu. Analogous $AgF_2$ planes with Ag centers in a tetragonal tetra coordination are still not known.

### 3.4.3. Comparison of Ag–F Systems, Superconducting Cu–O Systems and Members of Other Superconducting Families

The computational results for the Ag–F systems presented in Section 3.3, together with computational and experimental

results for different Ag–O,[183–188] Ag–Cl,[189] Cu–F,[190, 191] Cu–O,[183, 191–195] Cu–Cl,[183, 196, 197] Au–F,[30, 1a] Au–O,[183, 198] and Au–Cl[199, 200] systems in the literature, allow us examine Ag–F compounds from a broader perspective.

In Figure 28 we show a schematic energy level or DOS diagram (similar to some extent to the Zaanen–Sawatzky–Allen diagram[201]) for sulphide, chloride, oxide, and fluoride systems of Cu, Ag, and Au and summarize the essential

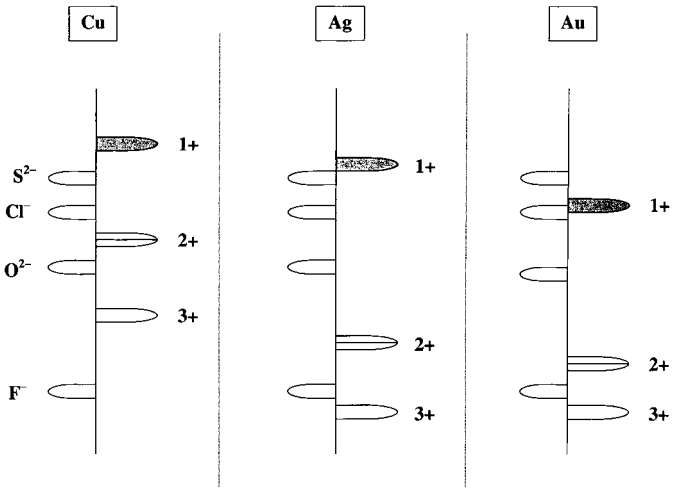


Figure 28. A schematic energy level diagram for sulphide, chloride, oxide, and fluoride systems of Cu, Ag, and Au in different oxidation states. The levels of the anion are on the left side, the levels of cations are on the right side.

features of the solid-state chemistry of different oxidation states of Cu, Ag and Au.[202] For example, Figure 28 shows that $Cu_2S_3$ (also $CuCl_3$, and $Cu_2O_3$) does not exist, because $Cu^{III}$ would oxidize sulfide anions to disulfide, or even to elementary sulfur. Analogous depopulation of the nonmetal states (holes in nonmetal levels) would be certainly observed for Cl and O, as well. Of course, the position of p nonmetal states and d metal states is flexible to some extent, and not rigidly set on the energy scale (this is especially true for larger, more polarizable anions and cations; the counter-ions also have some influence). This explains several known deviations from our simple picture, for example, why $AuCl_3$ or $Ag[W_6Br_{14}]$[203] exist.

A tendency of $M^{II}$ to disproportionate into $M^{I}$ and $M^{III}$ is more difficult to deduce, depending as it does on many factors. In a simplistic picture these are: 1) the degree to which the electrons of the $M^{III}$ cations are in orbitals that are more contracted than those of the $M^{II}$ centers (this decreases the energy of the M–L bonding orbitals), 2) the degree to which $M^{I}$ expands compared to $M^{II}$ (this increases the energy of the M–L antibonding orbitals), 3) the separation of hypothetical $M^{II}$ cations in a given solid, and 4) the spatial extent of the half-filled atomic orbital of the $M^{II}$ atoms. Criteria (3) and (4) are most important for "ionic" substances, where half-filled orbitals are localized on a metal center.

There are further analogies between Ag–F systems and superconducting oxocuprates. $Cu^{II}$ oxide complexes are very stable towards disproportionation, as are $Ag^{II}$ fluoride complexes. $Cu^{III}$ oxide complexes are relatively thermodynamically unstable, similar to $Ag^{III}$ fluoride complexes. The former complexes are obtained by prolonged oxidation in a stream of $O_2$; they spontaneously release oxygen. $Ag^{III}$ fluorides may be obtained only by fluorination with powerful oxidizers such as $O_2F$,[204] $F_2$,[13] $O_2F_2$, $XeF_2$, and $KrF_2$, and they easily evolve $F_2$.[205]

### 3.5. Hypothetical Intermediate-Valence Quaternary Fluoride $Ag^{II}/Ag^{III}$ and $Ag^{II}/Ag^{I}$ Systems as Potential Superconductors?

#### *3.5.1. BCS Contribution to Superconductivity*

We proceed to compare quantitatively the Ag–F systems with several well-known families of superconductors. In the spirit of the theory developed by Bardeen, Cooper, and Schrieffer (BCS theory)[206] one needs to consider three important parameters: a density of states at the Fermi level ($DOS_F$), an electron–phonon coupling constant, and a cut-off frequency of the phonon spectrum.[207]

Frequencies of the stretching vibrations in $Ag^{III}$–$F^-$ compounds reach 600 $cm^{-1}$, (similar to those of oxocuprate superconductors), thus providing reasonably large Debye temperatures; the corresponding values for $Ag^{II}$–$F^-$ compounds are lower by around 20–30 %.[208]

Here we concentrate on the $DOS_F$ and the degree to which states near the Fermi level in 1D and 2D nets originate from metal and ligand; covalency of the M–L bond directly influences the strength of the electron–phonon coupling.[209] Numerical data supporting the following discussion are listed in Table 8.[210]

We must preface our remarks with a caveat. It is a daunting task, beyond our (or anyone's) powers, to compare critically computational results for Ag–F and Cu–O compounds. These results are obtained by several researchers using very different computational methods. We go ahead, but *the* reader is cautioned that the comparison that follows is somewhat shaky.

Consider first the $DOS_F$. It may be seen that the $Ag^{II}$–$F^-$ compounds have $DOS_F$ ($\approx$1.0 to 2.6 states (eV FU)$^{-1}$) smaller by a factor of about 2–4 than those for metallic $YNi_2B_2C$ or $HfN_2$ systems, similar to oxocuprates and $Sr_2RuO_4$, and larger by a factor of 4–8 than oxobismuthates, oxoantimonates, and fullerides. In addition, there are attractive DOS peaks close to $E_F$ for $AgF_2$ (Figure 23a), with DOS values exceeding $DOS_F$ by about three times.[211] They might be accessible by hole- or electron-doping in the $AgF_2$ planes.

In silver fluorides the states at the Fermi level are usually dominated by the contribution of metal states (60–70 %), which exceed that of the nonmetal (anion) states (30–40 %). This agrees roughly with the charge distributions in the $3b_{1g}$ half-filled orbital of the $[AgF_6]^{4-}$ ion (73–77 % Ag, 27–23 % F, multiple scattering X$\alpha$ (MS-X$\alpha$), and self consistent charge extended Hückel (SCCEH) results.[212] A more rigorous approach should, of course, take into account the ratio of Ag and F atoms participating in the bonding in a given compound.

Oxocuprates are definitely the most widely investigated superconducting family. Much attention has been paid to bismuthates and ruthenates as well. Let us compare the

Table 8. Comparison of important features of Ag–F compounds (obtained from our DFT computations) and several cuprate and non-cuprate superconductors (literature data).

| Compound | $T_c$ [K] | $DOS_F$[a] [states (eV FE)$^{-1}$] | $M_{tot}$ [%] | $X_{tot}$ [%] | $Dop_{tot}$ [%] | $M_{tot}$:$X_{tot}$ | $R$(M–X) [Å] | Ref. |
|---|---|---|---|---|---|---|---|---|
| *silverfluorides:* | | | | | | | | |
| $AgF_2$ | – | 1.114 | 65 | 35 | – | 1.71 | $4\times2.07$, $2\times2.58$ (Ag-F) | |
| $[AgF][BF_4]$ | – | 1.070 | 71 | 29 | 0 (B) | 1.15[b] | $4\times2.33$, $2\times2.01$ (Ag-F) | |
| $CsAgF_3$ | – | 0.997 | 71 | 23 | 7 (Cs) | 1.68 | $4\times2.07-2.13$, $2\times2.51$ (Ag-F) | |
| $Cs_2AgF_4$ | – | 2.596 | 61 | 29 | 10 (Cs) | 2.63 | $4\times2.29$, $2\times2.13$ (Ag-F) | |
| *oxocuprates:* | | | | | | | | |
| $HgBa_2Ca_2Cu_3O_{8+x}$ | 134 | | | | | | | [213, 214] |
| $Tl_2Ba_2Ca_2Cu_3O_{10}$ | 128–125 | 1.268 | 55 | 39 | 5 (Tl), 0.5 (Ba), 0.5 (Ca) | 1.41 | $4\times1.925$, $1\times2.66$ (Cu-O) | [215] |
| $(Sr_{1-x}Ca_x)_{1-y}CuO_{2+x}$[c] | 110 | 0.50[r] | 30[r] | 45[r] | 25[r] (Sr) | 0.67[r] | $4\times1.93$, $2\times2.50$ (Cu-O) | [216] |
| $HgBa_2CuO_{4+x}$ | 96 | 1.5[r] | | | | | $4\times1.94$, $2\times2.81$ (Cu-O) | [217] |
| $Tl_2Ba_2CuO_{6+x}$ | 90 | 4.23 | 12 | 65 | 20 (Tl), 3 (Ba) | 0.19 | | [218] |
| $YBa_2Cu_3O_7$ (YBCO) | 93 | 1.10 | 33 | 66 | 1 (Y, Ba) | 0.50 | $4\times1.93$, $1\times2.26$ (Cu-O) | [219] |
| $YBa_2Cu_2PbO_x$ | 80 | | | | | | | [220] |
| $CaCuO_{2+x}$ | 80 | 0.42[r] | 29[r] | 48[r] | 24[r] (Ca) | 0.60[r] | | [221] |
| $Sr_2CuO_{3+x}$ | 70 | | | | | | $4\times1.882$, $2\times1.932$ (Cu-O) | [222] |
| $PbCdSr_3BaCaYCu_4O_{14}$ | 47 | | | | | | | [223] |
| $La_{2-x}Sr_xCuO_4$ | 35[d] | 1.935 | 49 | 47 | 4 (La) | 1.05 | $4\times1.90$, $2\times2.40$ (Cu-O) | [224] |
| $Pb_2La_{2-x}Sr_xCu_2O_{6+\delta}$ | 33[e] | 1.762 | 55 | 41 | 4 (Pb) | 1.34 | | [225] |
| $Ba_2YRu_{0.85}Cu_{0.15}O_{6-x}$ | 30 | | | | | | | [210] |
| $Nd_{2-x}Ce_xSr_2Cu_2NbO_{10}$ | 28 | 3.75[r] | 38[r] | 60[r] | | | | [226, 227] |
| $Nd_{2-x}Ce_xCuO_4$ | 21 | | | | | | | [228] |
| $Bi_2Sr_2CuO_6$ | 12 | 1.06 | 36 | 43 | 19 (Bi), 3 (Sr) | 0.84 | | [218] |
| *other oxides:* | | | | | | | | |
| $Ba_{1-x}K_xBiO_3$ | 30–26[f] | 0.26[r] | 54[r] | 46[r] | 0 (Ba) | | $6\times2.128$ (Bi-O) | [229] |
| $Li_{1+x}Ti_{2-x}O_3$ | 13.7 | | | | | | | [210] |
| $Ba(Pb,Bi)O_3$ | 12 | | | | | | $6\times2.128$ (Bi-O) | [230] |
| $M'_xKCa_2Nb_3O_{10}$ ($M'$ = Li, Na) | 6–3 | | | | | | | [231] |
| $Li_{0.8}NbO_2$ | 5.5 | | | | | | | [210] |
| $M'_xWO_3$ ($M'$ = Li–Cs) | 5.4–1.1 | | | | | | | [210] |
| $Ba(Pb,Sb)O_3$[g] | 3.5–2.8 | 0.378 | 34 | 66 | 0 (Ba) | 0.52 | | [232] |
| $Li_{0.9}Mo_6O_{17}$ | 2 | | | | | | | [210] |
| $(Ag_7O_8)(NO_3)$ | 1.4 | | | | | | | [233] |
| $Sr_2RuO_4$ | 1.35[234] | 1.8[r] | 53[r] | 47[r] | 0 (Sr) | | $4\times1.930$, $2\times2.061$ (Ru-O) | [235] |
| NbO, TiO[h] | 1.0–0.8 | | | | | | | [210] |
| $SrTiO_3$ | 0.2–0.3 | | | | | | | [210] |
| *non-oxide materials:* | | | | | | | | |
| $Rb_2CsC_{60}$ | 35 | | | | | | | [236, 237] |
| $Li_{0.16}Hf(NCl)$ | 25.5 | 2.3[238] | | | | | 2.108 (Hf-N)[i] | [239] |
| $Nb_3Ge$[j] | 23.2 | 1.83 | | | | | | [240] |
| $V_3Si$[j] | 23 | 1.84 | | | | | | [241] |
| $K_3C_{60}$ | 18.5 | 0.28,[242] 0.16[243] | | | | | | [236] |
| S | 17.0[k] | | | | | | | [244, 245] |
| $LuNi_2B_2C$ | 16.6 | 2.4 | | | | | | [246] |
| $YNi_2B_2C$ | 15.6 | 4.03 | 54 (Ni) | 30 (Y) | 9 (B), 7 (C) | | | [247] |
| $PbMo_6S_8$[l] | 15.2 | | | | | | | [210] |
| $Li_{0.16}Zr(NCl)$ | 12.5 | 0.92[238] | | | | | 2.099, 2.339 (Zr-N) | [248] |
| [κ-(BEDT-TTF)Cu{N(CN)$_2$}]Br[s] | 12[249] | | | | | | | [210] |
| $Na_2CsC_{60}$ | 11.7 | 0.665 | | | | | | [250] |
| $CaTaN_2$ | 10 | 0.7 | | | | | | [251] |
| Nb | 9.3 | 1.43 | | | | | | [252] |
| $HfV_2$[m] | 8.9 | 2.95 | | | | | | [253] |
| $Ba_8Si_{46}$ | 8.0 | | | | | | | [254] |
| $BaHfN_2$ | 8 | | | | | | 2.186, 2.05 (Hf-N) | [255] |
| $La_2C_2Br_2$ | 7 | | | | | | | [256] |
| $SrSn_3$ | 5.4 | | | | | | | [257] |
| Hg[n] | 4.2 | | | | | | | [258] |
| anthracene[o] | 4 | | | | | | | [259] |
| SmS | 3 | 2.2[r] | | | | | | [260] |
| $UPd_2Al_2$[p] | 2.0 | | | | | | | [210] |
| CsI | 2[q] | | | | | | | [261] |
| $UPt_3$[p] | 0.43 | | | | | | | [210] |
| $KC_8$ | 0.4–0.1 | 0.3 | | | | | | [262] |

[a] DOS is presented per one metal atom for oxocuprates and oxobismuthates, per one carbon atom for fullerides, and per one nickel atom for nickel borocarbides. [b] Original value for this 1D compound has been multiplied by 2, to provide comparison with 2D structures. [c] DOS data for $x = 0$ and $y = 0$, $T_c$ for $x = 0.3$ and $y = 0.1$. [d] For $x = 0.15$. [e] For $x = 1$ and $\delta = 0.1$. [f] For $x = 0.4$. [g] Computational data are for $BaSbO_3$. [h] Both are nonstoichiometric, defect compounds. [i] For undoped HfNCl. [j] A15 phase. [k] Under high pressure. It is the highest $T_c$ value among elements. [l] Chevrel phase. [m] C15 Laves phases. [n] The first superconductor known. [o] It is the highest $T_c$ value in charge-injected molecular crystals. [p] A heavy fermion superconductor. [q] Above 180 GPa. [r] Data estimated from figures presented in a given references. [s] BEDT-TTF = bis(ethylenedithio)tetrathiafulvalen.

constitution of the states at the Fermi level for these families of compounds and for silver fluorides. First, the contribution of the metal to $DOS_F$ never surpasses 55% in oxide superconductors. If we compare the partitioning of the $DOS_F$ into metal and nonmetal contributions for compounds with similar metal-to-anion atom ratios, we find for $CsAgF_3$ 71:23, the 2223 compound $Tl_2Ba_2Ca_2Cu_3O_{10}$ 55:39, and $(Ba,K)BiO_3$ 54:46, $Cs_2AgF_4$ 61:29 and $La_2CuO_4$ 49:47, or $AgBF_5$ 71:29 and $(Nd,Ce)_2Sr_2NbCu_2O_{10}$ 38:60. Apparently, the Ag–F systems are slightly more ionic than the Cu, Bi, and Ru oxides. Since large vibronic coupling is likely to be associated with strongly bonding or strongly antibonding orbitals (the latter is the case for $d^9$ systems), the lower covalency for Ag–F systems in comparison with the CuO ones would result in some decrease in the electron–phonon coupling constant.

We retreat a little from the calculations to an ionicity index, the useful concept of optical electronegativity (OEN) introduced by Jørgensen in late '50s.[263] Some experimental data suggest that OEN $(F^-) = 3.9$ and OEN $(O^{2-}) = 3.5$,[264] others that OEN $(F^-) = 3.6-3.7$ and OEN $(O^{2-}) = 3.2-3.5$.[265] Values of OEN for $Cu^{II}$ and $Ag^{II}$ are 2.4 and 2.8, respectively.[212] Given that the differences of OEN between $Cu^{II}$ and $O^{2-}$ and between $Ag^{II}$ and $F^-$ ions are similar (0.8–1.1), the ionicity/covalency of the $Cu^{II}$–$O^{2-}$ and $Ag^{II}$–$F^-$ bonds should then be comparable.[266] The same conclusion may be obtained for the $Cu^{III}$–$O^{2-}$ and $Ag^{III}$–$F^-$ bonds.

The contribution of dopant levels to the states at the Fermi level, which increases the $DOS_F$ and thus potentially increases the superconductivity critical temperature $T_C$, is the last topic of this section. It has to be admitted that compared to Tl, Bi, or Ca in oxocuprates dopants contribute relatively weakly to $DOS_F$ in Ag–F systems. This situation might change if Sb, As, Ge, Si, Ti, Al, Be (and other elements forming strong bonds with F) were used as cationic or anionic dopants in the Ag–F systems.

There is much geometric instability of the $CuO_2$ nets in cuprate superconductors, most importantly a tetragonal-to-orthorhombic distortion. This distortion has a dramatic influence on the superconducting properties of these substances. Similarly, a tetragonal-to-orthorhombic distortion is observed when the Rb center in $RbAgF_3$ is substituted for K. Phase separation is often observed in oxocuprates,[267] and it occurs also for $BaAgF_5$, which easily separates into $BaF_2$ and $Ba[AgF_4]_2$. The frequencies of the Ag–F stretching vibrations in $Ag^{III}$–F compounds reach 600 $cm^{-1}$, similar to the frequencies of the Cu–O stretching modes of the oxocuprates, which are most important for superconductivity. Finally, many of the $Ag^{II}$–F compounds are often ground-state antiferromagnets, as are some $Cu^{II}$–$O^{2-}$ systems that are parent compounds for electron- or hole-doped $Cu^{II}/Cu^{III}$ and $Cu^{II}/Cu^{I}$ superconductors.

Note that silver is one of very few elements, which—in such a low oxidation state (+II)—creates substantially covalent extended nets in combination with the most electronegative element, fluorine. It also introduces holes into the F(p) band, at oxidation state +III.[268]

Interesting superconducting solids containing $[Ag_7O_8]^+$ clusters, for example, $[Ag_7O_8]^+[HF_2]^-$,[269] $[Ag_7O_8]^+[NO_3]^-$,[233] $[Ag_7O_8]^+[F]^-$,[270, 271] $[Ag_7O_8]^+[ClO_4]^-$,[271] $[Ag_7O_8]^+[BF_4]^-$,[272] $[Ag_7O_8]^+[HSO_4]^-$,[271, 273] and $[Ag_7O_8]^+[HCO_3]^-$[274] are known. The highest superconducting critical temperature ($T_c$) reported for these compounds is only 1.4 K ($[Ag_7O_8]^+[NO_3]^-$).[272] These are II/III mixed-valence (probably class II) compounds, with an average +2.43 oxidation state of silver.[275] The proximity of Ag(d) and F(p) levels, appreciably Ag/F-mixed character of the strongly Ag–F antibonding levels in proximity of the Fermi level, and relatively large values of $DOS_F$ in $Ag^{II}$ fluoride systems temptingly suggest that $Ag^{II}$ fluoride systems might be much better "BCS superconductors" than the known $Ag^{II}$ oxide clusters.[276]

### 3.5.2. *Non-BCS Contribution to Superconductivity: A "Magic Electronic State"*

Burdett has suggested that a "magic electronic state" occurs in superconducting oxocuprates.[277] This concept is very simple. Burdett argues that high-temperature superconductivity is likely to occur when there are enormously large variations in the wavefunction, which changes its character from one dominated by copper to another dominated by oxygen contributions [Eq. (3a), (3b)].

$$Cu^{III} + O^{2-} \longrightarrow Cu^{II\bullet} + O^{-\bullet} \quad (3a)$$

$$Cu^{II\bullet} + O^{2-} \longrightarrow Cu^{I} + O^{-\bullet} \quad (3b)$$

The equations [Eq. (3a), (3b)] describe the introduction of holes into the "oxygen band" by $Cu^{III}$ and even $Cu^{II}$ centers. If there is a precarious balance of this type small changes in the Cu–O distance might lead to effective transfer of charge (electrons) between copper centers through the oxygen p orbitals, thus inducing free flow of electric current.

Burdett draws an analogy between this phenomenon and another one, that of ionic and covalent curves crossing in alkali halides ("harpooning", Mulliken's sudden electron transfer[278]) [for example: Eq (4)]

$$Na^{I} + Cl^- \longrightarrow Na^{0\bullet} + Cl^{\bullet} \quad (4)$$

The major difference is that harpooning happens at large distances of several Å's in alkali halides, but electron transfer at relatively short distances of about 1.9 Å in cuprates. The covalent/ionic curve crossing in cuprates is avoided and leads to "repulsion" of the diabatic potential energy surfaces. This results in adiabatic curves, separated by an energy gap. It has been proposed independently that the position of the LUMOs of the bridging anion with respect to the metal levels plays a crucial role for disproportionation of mixed-valence *molecular* compounds.[279]

According to Burdett's concept, the magic electronic state might occur the Robin and Day class III [33] mixed-valence solids (fully comproportionated, intermediate-valence ones). We think, however, that Burdett's idea might also be extended to class II [33] mixed-valence compounds (systems with partial comproportionation), if higher frequency vibrational modes are considered ("dynamical comproportionation", "fluctuating valence").[280]

Indeed, computations of layered oxocuprates with $CuO_2$ planes (Table 8) suggest that the Fermi level has strongly mixed Cu/O character. For example, the computed ratio of atomic Cu to O contributions to the $DOS_F$ is 1.41 for $Tl_2Ba_2Ca_2Cu_3O_{10}$, 1.34 for $Pb_2La_{2-x}Sr_xCu_2O_{6+\delta}$, 1.05 for $La_{2-x}Cu_xO_4$, 0.84 for $Bi_2Sr_2CuO_6$, 0.67 for $(Sr_{1-x}Ca_x)_{1-y}CuO_{2+x}$, 0.50 for $YBa_2Cu_3O_7$, and 0.19 for $TlBa_2CuO_6$. A similar situation also occurs in non-cuprate superconducting oxides (0.52 for $Ba(Pb,Bi)O_3$). These numbers suggest that the ground state of different $Cu^{II}$ or $Bi^{IV}$ oxides might be dominated by O or Cu/Bi contributions, and that proper hole- or electron-doping in the system might shift this situation towards the desired one in which crossing of the ionic and covalent curves is avoided.

Introduction of holes into the fluorine band by $Ag^{III}$ or $Ag^{II}$ centers [Eq (5a), (5b)] is probably more difficult than introducing holes into the oxygen band by $Cu^{III}$ [see Equation (3a)].[281]

$$Ag^{III} + F^- \longrightarrow Ag^{II\bullet} + F^{0\bullet}, \quad (5a)$$

$$Ag^{II\bullet} + F^- \longrightarrow Ag^{I} + F^{0\bullet}, \quad (5b)$$

$Ag^{III}$ and even $Ag^{II}$ centers easily generate holes in the oxygen band (these two species decompose water, and are relatively unstable in oxides; AgO is in fact $Ag^IAg^{III}O_2$). But would they manage to generate holes in the fluorine band? Are the processes described by Equations (5a) and (5b) realistic?

There is some experimental and theoretical evidence that process (5a) and even (5b) might occur. As we have pointed out in Section 3.5.1 our computations (Table 2) document that the contributions of Ag and F to the $DOS_F$ in several $Ag^{II}$ fluorides are quite similar to the respective Cu and O contributions in oxocuprates with similar metal:anion ratios in the chemical formula. Since $Ag^{II}$ fluorides seem, however, a little more ionic than oxides of $Cu^{II}$, Burdett's "magic electronic state" might be reached only in some hole-doped $Ag^{II}$ fluorides. This seems less probable in the electron-doped systems, [Equation (5b)], and such a conclusion is supported by experimental observations. After hypothetical recombination of fluorine radicals according to the Equation (6a) gaseous fluorine is released upon heating from many $Ag^{III}$ fluorides (usually at 300–400 °C) and even from $Ag^{II}$ fluorides (usually at 500–700 °C). An analogous reaction in copper oxides might involve $O^{-\bullet}$ (isoelectronic to $F^{0\bullet}$) [Eq. (6b)], as has been discussed by many workers in the field.[281]

$$2F^{0\bullet} \longrightarrow F_2 \quad (6a)$$

$$2O^{-\bullet} \longrightarrow O_2^{2-} \quad (6b)$$

In our analysis of potential superconductivity in silver fluorides we have used one "physical" model (BCS) and one "chemical" one (Burdett's ideas). There are other models, intuitively attractive—Goddard's exchange coupling, Simon's flat-band scenario, etc. We cannot do everything, especially in the current situation of lack of consensus on the way to explain high-$T_C$ materials—the reader we hope will forgive us for moving ahead with these two models.

In the next Section we will analyze approaches which are commonly used to generate superconductivity in oxocuprates, and we will try to adapt them in theory for silver fluorides.

### 3.6. How to Obtain Superconductivity in Intermediate-Valence $Ag^{II}/Ag^{III}$ and $Ag^{II}/Ag^{I}$ Fluorides?

#### *3.6.1. Impediments to Superconductivity and Overcoming These*

In the previous Section we have pointed out many striking similarities between $Cu^{II}$–$O^{2-}$ and $Ag^{II}$–$F^-$ compounds. We will try now to explore for the Ag–F systems the same strategies that are used to generate superconductivity in doped $Cu^{II}$–$O^{2-}$ systems. Let us first give a brief description of the general approach used in oxocuprates.

At least five interesting phenomena may occur in mixed-valence systems, including three electron "*pairings*" (cases (a), (b), and (d) below). Some of them are connected with breaking the symmetry of the wavefunction (its spatial and/or spin part) describing a system.[282] Solid-state systems formally containing radicals $M^{n+\bullet}$ (for example $Ag^{2+\bullet}$), usually exhibit tendencies toward the following four processes:

a) covalent M–M bond creation [Eq. (7)]

$$M^{n+\bullet} + M^{n+\bullet} \longrightarrow (M{:}M)^{2n+} \quad (7)$$

b) disproportionation (taking on various guises, described as a "charge-density wave", "charge localization via Peierls distortion", "freezing of oxidation states", "lone pair creation") [Eq. (8)]

$$M^{n+\bullet} + M^{n+\bullet} \longrightarrow {:}M^{(n-1)+} + M^{(n+1)+} \quad (8)$$

c) ferromagnetism ($\uparrow\uparrow$) or antiferromagnetism ($\uparrow\downarrow$) (connected often to a "spin-density wave")

d) superconductivity ("creation of boson Cooper pairs", "resonating valence bond", "strong coupling of electrons at the Fermi level with optical phonon", "gap opening at the Fermi level")

e) one may get "normal" metallic behavior instead of superconductivity in such systems.

Process (d) is of greatest interest to us, so we have to learn how the first three effects might be avoided or quenched. We also try to avoid behavior (e) in silver fluorides by providing a sufficiently large value of the vibronic (electron–phonon) coupling constant. Let us think now of competing/coexisting[283] possibilities (a)–(d) in the context of $Ag^{II}$–F systems.

Covalent M–M bond creation (a) is empirically unlikely for Group 11 $M^{II}$ ($d^9$) systems. It occurs more often for isoelectronic Group 18 $M^I$ systems such as $Ni^I$,[284] $Pd^I$,[285] and $Pt^I$[286] and is quite common for Group 17 $M^0$ systems, that is, $Co^0$,[287] $Rh^0$,[288] and $Ir^0$.[289] In principle, the pairing of electrons into bonds and the low bond strength that would follow is prevented in $M^{II}$ ($d^9$) systems by the low bond strength that would follow and by coulombic repulsion of the metal centers. Nevertheless, spin pairing (some would call it "a very weak

Cu–Cu bond") occurs, for example, in some $Cu^{II}$ compounds, such as the acetates.[290, 291]

The disproportionation tendencies (b) of Cu, Ag, and Au[292] in different environments are collected in Table 9. Generally speaking, $Ag^{II}$ fluorides crystallizing in extended nets do *not* have a tendency toward disproportionation to $Ag^{I}$ and $Ag^{III}$. But several interesting exceptions exist. A binary fluoride, $AgF_2$, is one of them. It is known that $AgF_2$ occurs in two forms, a disproportionated one (high-temperature) and a nondisproportionated one (low-temperature). A formula $Ag[AgF_4]$ may be assigned to the first (diamagnetic) form. $Ag[SbF_6]_2$ is another example of "valence tautomerism" of Ag–F compounds. This compound contains isolated $Ag^{II}$ centers; it would be very interesting to examine whether indeed and why it exhibits a tendency to disproportionation. "Valence tautomerism" has been also suggested for $[AgF][AsF_6]$, $[AgF][SbF_6]$, and $[AgF][AuF_6]$, since Peierls transitions had been anticipated—probably erroneously—for these compounds.[293]

Table 9. Summary of the disproportionation tendency in $M^{II}/A$ systems ($M = Cu, Ag, Au$; $A = Cl^-, O^{2-}, F^-$).

| | $Cu^{II}$ | $Ag^{II}$ | $Au^{II}$ |
|---|---|---|---|
| $Cl^-$ | NO | YES | YES |
| $O^{2-}$ | NO | YES | YES |
| $F^-$ | NO | NO[a] | YES[b] |

[a] Three examples of disproportionated systems are known to date. [b] Five examples of comproportionated systems are known to date.

It is interesting that a more pronounced tendency towards charge separation may be obtained in $Ag^{II}$–F systems upon hole doping. Several examples of mixed-valence $Ag^{II}/Ag^{III}$ fluorides are known ($[AgF][AgF_4]$, $Ag[AgF_4]_2$, and $[AgF]_2[AgF_4][AsF_6]$). As far as we know, intermediate valence $Ag^{II}/Ag^{III}$ fluorides have not been obtained so far. There is evidence for an $Ag^{II}/Ag^{I}$ fluoride as a nonstoichiometric $AgF_{2-x}$ species. It is not known whether it is a mixed-valence or an intermediate valence compound.

Let us examine next possibility (c), the occurrence of collective magnetic phenomena in $Ag^{II}$ fluorides. Relevant numeric data are collected in Table 10 and illustrated in Figure 29.

The magnetic behavior of silver fluorides is very diverse (see Section 3.2.2). We find among these phases Curie-law obeying paramagnets, paramagnets with strong deviation from the Curie law (such as silver titanate), temperature-independent paramagnets, and antiferromagnets.[294] Also a weak ferromagnetic component has been suggested for $AgF_2$. The strength of the antiferromagnetic coupling of $Ag^{II}$ fluorides (measured by their Neél temperature $T_N$) proves its strong dependence on the distance between interacting paramagnetic centers (Figure 29). The data available are limited, so we can plot only five points in our $T_N$ versus $R$(Ag–Ag) dependence graph (including the Curie temperature for $AgF_2$, a weak ferromagnet with a strong antiferromagnetic component). The dependence is nearly linear for four quasi-2D fluorides with half-filled $x^2 - y^2$ bands.[295] The only point breaking linearity is that for a 1D antiferromagnet, with a half-filled $z^2$ band. Using Figure 29, we may predict that

Table 10. Magnetic behavior of the selected $Ag^{II}$–F systems; antiferromagnets are listed in the order of increasing Neél $T_N$ temperature.

| Compound | $R(Ag^{II}–F)$ [Å] | $R(Ag^{II}–Ag^{II})$ [Å] | Magnetic behavior (temperature range [K]) | $T_N$, $T_C$, or $\Theta$ [K] |
|---|---|---|---|---|
| $[BaF_2]_2[AgF_2]$ | ca. 2.16[a] | ca. 4.32[a] | param. | $\Theta = +4$ |
| $Ag^{II}[SbF_6]_2$ | 2.095 – 2.132 | 5.224 | temp.-indep. param. (50 – 280) | $\Theta = +3$ |
| $BaAgF_4$ | 2.05 | 4.264 | param., Curie-Weiss (6 – 280) | $\Theta = -4$ |
| $Ag^{II}[BiF_6]_2$ | 2.096 – 2.122 | 5.218 | temp.-indep. param. (35 – 280) | $\Theta \approx -40$ |
| $Ag^{II}[TiF_4]$ | 2.122 – 2.181 | – | param. with strong spin coupling | $\Theta = -70$[b] |
| $[AgF]^+[Cd^{2+}]_3[Zr_3F_{19}]^{7-}$ | 2.102 | 4.205 | antiferrom., above $T_N$ temp.-indep. param. | $T_N = 3$ |
| $[CsF]_2[AgF_2]$ | 2.29 | 4.580 | antiferrom. | $T_N = 20$ |
| $[RbF]_2[AgF_2]$ | – | – | Curie-Weiss (60 – 300), antiferrom. | $T_N = 25$ |
| $[AgF]_2[AsF_6][AgF_4]$ | 2.003 | 3.903 | temp.-indep. param. (50 – 280) below 50 K Curie-like behavior | |
| $[CsF][AgF_2]$ | 2.07 – 2.13 | 4.260 | above $T_N$ temp.-indep. param. | $T_N = 50$ |
| $[RbF][AgF_2]$ | 2.06 – 2.10 | 4.220 | antiferrom., above $T_N$ temp.-indep. param. | $T_N = ?$ |
| $[KF]_2[AgF_2]$ | – | – | antiferrom. | $T_N = 60$ |
| $[AgF]^+[AuF_6]^-$ | – | 3.800 | temp.-indep. param. (63 – 280) | |
| $[AgF]^+[AsF_6]^-$ | 1.995 – 2.004 | 3.795 | temp.-indep. param. (63 – 280) | |
| $[AgF]^+[BF_4]^-$ | 2.002 – 2.009 | 4.011 | temp.-indep. param. (6 – 280) | |
| $[KF][AgF_2]$ | 2.08 | 4.16 | antiferrom., above $T_N$ temp.-indep. param. | $T_N = 80$ |
| $\alpha$-$AgF_2$ | 2.068 – 2.074 | 3.776 | weak spin-canted ferromagnet, strong antiferrom. coupling | $T_C = 163$, $\Theta = -715$ |

[a] The $Ba_2ZnF_6$ structure was assumed. [b] $AgF_2$ impurity may be source of large negative $\Theta$ value.

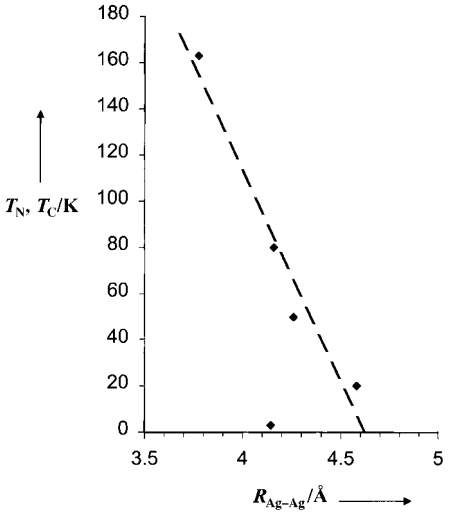


Figure 29. Correlation between the Neél temperature $T_N$ (in the antiferromagnetic $Ag^{II}$ fluorides) or the Curie temperature $T_c$ (in ferromagnetic $AgF_2$) and the closest Ag–Ag distance. The point off the linear dependence is from $[AgF]^+[Cd^{2+}]_3[Zr_3F_{19}]^{7-}$.

antiferromagnetic behavior would not be observed for quasi-2D $Ag^{II}$ fluorides with the closest Ag – Ag separation larger than 4.7 Å. It may be also seen from Table 10 that antiferromagnetism is usually weak or not observed in substances containing a kinked $[AgF]^+$ infinite chain. Antiferromagnetic superexchange occurs preferably in the 180° or 90° M-X-M conformation, and the above observation is in accordance with this rule (yet $AgFBF_4$ is an exception from it).

What about the possibility of decreasing the energy of a system by electron condensation into spin-less boson[296] pairs (possibility (d)?). In principle, people have elaborated numerous approaches to this unusual phenomenon. A brief summary of a vast literature is that we have a lot of clever people not reading each other's papers. There is little consensus. We tend to think of superconductivity in the spirit of a simple BCS theory, supported by Burdett's "magic state" approach. It is known that although the original BCS theory does not explain quantitatively high-temperature superconductivity, still a vibronic component is very important in ceramic materials.[297–299] Its importance is also apparent in Burdett's approach. In our view (we are voicing an opinion), superconductivity might be understood as a "dynamic" Peierls distortion,[300] to some degree similar to the "static" one which occurs in the "intermediate" class II of mixed-valence compounds. In other words, sometimes a large tendency to antisymmetrization might be hidden in geometrically symmetric or almost symmetric systems. Such a tendency may reveal itself only in a dynamic way, but does not lead to a definite, "static" band- gap opening, such as occurs during strong "frozen" Peierls distortion in a system with a half-filled band.[301]

In our recent studies of molecular systems, we have shown that large values of off-diagonal dynamic linear vibronic coupling constant may be obtained in triatomic molecules built of hard Lewis acids and bases of large electronegativity, with bonds as short and as strongly covalent as possible.[302–305] The same numerical and qualitative conclusions were reached for the diagonal vibronic coupling constant in $T_1$ states of diatomic AB molecules (A, B = halogen, alkali metal, or H). $Ag^{II}$ is a very hard Lewis acid, and the $F^-$ ion is a very hard Lewis base. We also showed how one could apply these conclusions to extended materials.[306] Our interest in covalent, strongly oxidizing ("very electronegative") Ag–F systems originates in large part from our theoretical findings for molecules.[307]

What approaches are used to generate superconductivity in different solids? Hole or electron doping in an antiferromagnetic insulator[308] (or semiconductor) is the most common one. It is illustrated schematically in Figure 30. The left part of the graph shows doping of the half-filled band with electrons.

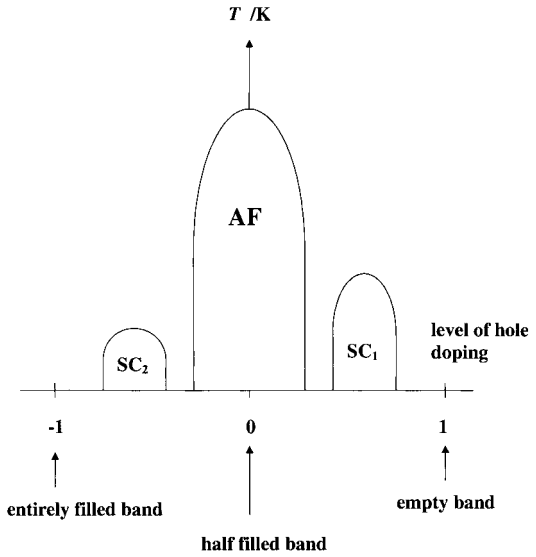


Figure 30. Scheme showing the appearance of two superconducting phases, $SC_1$ and $SC_2$, in the course of hole- (right side) or electron-doping (left side) of the antiferromagnetic (AF) parent compound with a half-filled band.

The right part illustrates doping with holes. The antiferromagnetism weakens and even disappears with increase of the doping level, both with electrons and holes. Diluting paramagnetic centers with electrons leads in case of the M–X antibonding band (as in cuprates) to elongation of the M–X bonds, and doping with holes leads to their compression. Quenching of antiferromagnetism should be thus a steeper function of doping level when electrons are doped into the half-filled band. Two superconducting phases ($SC_1$ and $SC_2$ in Figure 30) may appear on either side of the "antiferromagnetic" region, at certain levels of doping. Although critical superconducting temperatures obtained in electron-doped oxocuprates are an order of magnitude smaller than those for hole-doped systems, there is a belief that there are essential similarities in the appearance of superconductivity in both these families.[309]

The precise control of the distance between Cu centers proves to be one of the most important factors governing superconductivity in cuprate layered materials, this is because of the enormous sensitivity of $T_C$ to the Cu–O bond length.[310]

This control may be accomplished, for example, with use of a proper dopant. We think, a cationic dopant, which directly adjoins the formally negatively charged $[CuO_2]^{(2-\delta)-}$ planes[311] plays the role of a "clip", inducing "internal stress" in $CuO_2$ planes and preventing a "frozen" Peierls distortion (but allowing a dynamic one). We call such a dopant a "primary dopant", in contrast to other ("secondary") dopants present in the unit cell. An "improper" primary dopant may be sometimes successfully replaced by external pressure, according to a simple rule: the larger the dopant—the larger the external pressure necessary to prevent static Peierls distortion.[312] Following the same rule, systems with too small dopants will exhibit an "inverse" dependence of $T_C$ versus pressure, that is, their critical temperatures should *decrease* with external pressure.[313–316]

$Ca^{II}$ ($R_{ion} = 1.00$ Å), $Hg^{II}$ ($R_{ion} = 0.96$ Å), $Bi^{III}$ ($R_{ion} = 1.03$ Å), $La^{III}$ ($R_{ion} = 1.03$ Å), $Y^{III}$ ($R_{ion} = 0.90$ Å), $Sr^{II}$ ($R_{ion} = 1.18$ Å), and $Pb^{II}$ ($R_{ion} = 1.19$ Å), are the best dopants found so far for "clipping" $CuO_2$ planes (the average Cu–O distance is 1.88–1.95 Å, and the best dopants, the first three in the list, have $R_{ion} \approx 1.00$ Å[317]). A "primary" role for some of these dopants is exemplified by the large critical temperatures of 85 K reached in recently prepared $CaCuO_{3-\delta}$ monocrystals[318] (the oxygen content was not optimized), 96 K for $HgBa_2CuO_{4-\delta}$,[217] and 100 K for $Sr_3Cu_2O_{5+\delta}$.[319]

### 3.6.2. How to Obtain Intermediate-Valence $Ag^{II}/Ag^{III}$ and $Ag^{II}/Ag^{I}$ Fluoride Systems? Which Dopants Should One Use?

Neil Bartlett wrote in a description of his research:[152]

> "The aim of this work is the synthesis and characterization of new two and three dimensional solids that may be useful in electrical energy storage. Fluorides are emphasized because fluorine is small, lightweight, and highly electronegative. Thus high oxidation-state fluorides such as those of cobalt, nickel, copper or silver have high oxidizing potential and low formula weights. Emphasis is placed on the thermodynamically unstable fluorides, which have sufficient kinetic stability to be easily stored. Such fluorides are not only powerful oxidizers, but the metal center in each is comparable in electronegativity to fluorine. It is probable therefore, that some of the thermodynamically unstable fluorides will be metallic or even superconducting (like some copper oxide systems)."

In the gas phase, both $Ag^{II}$[320] and $Au^{II}$[321] are relatively stable. This situation may change dramatically in the solid state, where metal centers may communicate with one another; the first fluoride complexes of $Au^{II}$ in the solid state have been synthesized only in the last decade.

Importantly, strongly hole-doped binary and ternary $Ag^{II}$ fluorides, such as $Ag[AgF_4]_2$, $[AgF][AgF_4]$, and $[AgF]_2[AgF_4][AsF_6]$ (the formal oxidation state of Ag in these substances is +2.67, +2.5, and +2.33, respectively) are *not* stable toward disproportionation to $Ag^{II}$ and $Ag^{III}$ (see Figure 16, 17, and 15, respectively). Interesting attempts to melt the first two substances with alkali fluorides led to decomposition of the samples. On the other hand, very little is known about a nonstoichiometric $AgF_{2-x}$ ($x \approx 0.1$), formally a mixed-valence $Ag^{II}/Ag^{I}$ compound, an electron-doped silver fluoride of $Ag^{II}$. Given the dramatically different affinity of $Ag^{I}$, $Ag^{II}$, and $Ag^{III}$ towards F, strategies to obtain intermediate-valence $Ag^{II}/Ag^{I}$ and $Ag^{II}/Ag^{III}$ compounds will undoubtedly differ significantly. Let us remind ourselves of the preferences of $Ag^{I}$, $Ag^{II}$, and $Ag^{III}$ for bonding with $F^-$ ions:

a) $Ag^{I}$ interacts quite weakly with the $F^-$ ion, and its Lewis acidity is saturated already at one F atom per Ag atom.
b) $Ag^{II}$ exhibits stronger, but diverse affinity towards $F^-$. $Ag^{II}$ appears as the cation in $[AgF]^+$ infinite chains (creating two very strong bonds and four much weaker ones), as an isolated neutral $[AgF_2]$ species, and as an anion in isolated $[AgF_4]^{2-}$ units. The intermediate stages known (2+4, 2+2+2, and 4+2 coordination) emphasize the "amphoteric" behavior of $Ag^{II}$ in fluoride systems.
c) $Ag^{III}$ is the strongest $F^-$-abstracting agent known among these three oxidation states of silver. It occurs in isolated $[AgF_4]^-$ units (low-spin form) or even in isolated $[AgF_6]^{3-}$ units (high-spin form). Only in thermodynamically unstable $AgF_3$ do the $Ag^{III}$ assemble into quasi-1D helical chains.

Given the very different coordination preferences of $Ag^{I}$, $Ag^{II}$, and $Ag^{III}$ towards F, and very different $Ag^{n+}$–$F^-$ bond lengths (2.46 Å,[322], 2.00–2.07 Å, and 1.88 Å for $n = 1$, 2, 3, respectively), the comproportionation–disproportionation equilibrium in the hole- and electron-doped $Ag^{II}$ fluorides should be definitely shifted towards disproportionation. In other words, $Ag^{I}$ or $Ag^{III}$ will appear in $Ag^{II}$ compounds as local defects of the crystal structure. It also means that construction of intermediate valence hole- and electron-doped $Ag^{II}$ fluorides will be a difficult goal to reach in practice. How might one do it?

The broad spectrum of coordination environments seen in the $Ag^{I}$, $Ag^{II}$, and $Ag^{III}$ fluorides poses very specific requirements for construction of an intermediate-valence system. The tactics for constructing $Ag^{I}/Ag^{II}$ and $Ag^{II}/Ag^{III}$ systems will differ substantially. Our intuition is that the $Ag^{II}/Ag^{III}$ systems might be obtained only in fluorine-deficient systems, involving very "hard", strongly F-abstracting dopants. These dopants play a primary role in net-arrangement by covalent-bond creation, and prevent the affinity of $Ag^{III}$ to $F^-$ ions from being spontaneously fulfilled. On the other hand, the $Ag^{I}/Ag^{II}$ systems might be obtained in moderately fluorine-deficient systems, using moderately potent F-abstracting dopants. Such dopants will not liberate the $Ag^+$ ion[323] and thus will not destroy the 1D or 2D structure of the Ag–F net.

Covalent bonding between dopant and O centers in cuprates, as well as its interaction with $z^2$ lone pairs on Cu atoms also seems essential for 1) regulation of charge residing on $CuO_2$ planes, 2) for tuning the relative position of Cu(d) and O(p) levels, and 3) for introducing desired stress into the $CuO_2$ planes. Addition of dopant levels to the $DOS_F$ is another important role played by the dopant in different classes of superconducting materials.[324] This premise suggests that it makes sense to use Be, B, Al, C, Si, Ge, P, As, Sb, Bi, Se,

Te, I (as well as Ti, Zr, Hf, V, Nb, Ta, W, Mo, Ru, Os, Rh, Ir, Ni, Pd, Pt), as potential dopants for Ag–F systems. thus creating strong bonds with F centers at certain—usually the highest accessible—oxidation states.

When we showed him a draft of this paper, Prof. Bartlett described further his experimental search for superconductivity in Ag/F compounds in a private communication to us (August 2000):

"You may be surprised to learn that I have been looking for a superconductor in the Ag/F system for the past 8 years because of observations that we made in 1992. Briefly, we noted that whenever we prepared a $[AgF]^+[MF_6]^-$ salt and washed it with anhydrous HF, the magnetic susceptibility exhibited a sharp drop at 63 K, suggestive of a superconducting transition caused by an impurity. Since this anomaly (it looks like a Meissner effect) was independent of M = Sb, As, Au (ref. [29] herein), I assumed that the impurity was a mixed oxidation-state $Ag^{II}/Ag^{III}$ fluoride. The material that exhibits the 63 K anomally, does not produce identifying lines in the X-ray diffraction pattern (the parent materials give sharp strong patterns). My surmise has therefore been that the quantity present is small (< 5%). This surmise is obviously not valid if the material is non-crystalline. This set in train a set of investigations […]. My first and still favoured guess was that the 63 K diamagnetic phenomenon was caused by an electron-oxidized $AgF_2$ sheet-structure [i.e. $[AgF_2]^{n+}$, $n < 1$] intercalated (perhaps non-stoichiometrically) by $[AgF_4]^-$ species. I also allowed that $[MF_6]^-$ could be an intercalating species. It is my belief that some disorder in the placement of the anionic charges is necessary, if hole localization is to be avoided. […] I do not believe that a one dimensional $\{[AgF]^+\}_\infty$ chain would give rise to superconduction! […] It was this set of thoughts that caused me to look at the oxidation of $AgF_2$ with $[O_2]^+$ salts, unfortunately we only obtained the linearly coordinated $[AgF]_2[MF_6][AgF_4]$ salts. The $[AgF]_2[MF_6][AgF_4]$ salts do not show the anomaly until they are washed with anhydrous HF (i.e. solvolysed). We never obtained an intercalated sheet structure, like that of $Au[AuF_4]_2Au[SbF_6]_2$. It could be that an off-stoichiometry silver relative of the latter is the desired material."

## 4. Summary and Outlook

In this paper we have gathered all experimental data known to us to date for binary and ternary $Ag^{II}$ and $Ag^{III}$ fluoride systems in the solid state, with an emphasis on structures and magnetic properties.

Although about 100 $Ag^{II}$ and $Ag^{III}$ fluorides are known, much experimental and theoretical data for these interesting materials is missing. Crystal structures are known for about 40% of these compounds, we estimate, and have been refined only for about 15% of them. On the other hand, magnetic measurements have been carried out for almost all of them. Spectroscopic (IR,[325] Raman, UV/Vis,[326] NMR,[327] ESR[326, 328]) and thermodynamic data is often lacking. Electric conductivity measurements have not been performed as a function of temperature, external pressure, and magnetic field for many of these substances.[329] There is also no basic experimental data on the electronic structure of $Ag^{II}$ fluorides (X-ray and UV photoelectron spectroscopy (XPS, UPS), EXAFS (extended X-ray absorpsion fine structure), XANES (X-ray absorption near edge structure) etc.). The majority of these compounds has been synthesized in only two groups: one previously led by Hoppe and now by Müller (Gießen), another one directed by Bartlett (Berkeley).

"Whatever causes superconductivity above 40 K, it seems to involve the layers containing copper and oxygen atoms, which are common to all compounds exhibiting a high critical temperature $T_C$."[330] Chemistry is a living science. For example, only 10 years ago the existence of nondisproportionated $Au^{II}$ in the solid state would be questioned. Today we know from experiment that fluoride complexes of $Au^{II}$ are relatively stable in solid state.[30]

It is our opinion that both 2D and 1D Ag–F structures may, under certain conditions, give rise to superconductivity (also when doped with electrons, and not only with holes). And a special design is required to provide similar environments for $Ag^{I}$ and $Ag^{II}$, or $Ag^{II}$ and $Ag^{III}$ species (some stress has to be introduced into the structures) in potential superconducting materials. This is very difficult to do for $Ag^{II}/Ag^{III}$ compounds (and also for $Au^{II}/Au^{III}$ ones; note that $Au[AuF_4]_2Au[SbF_6]_2$ is a *mixed-valence* species, with average $Au^{II}$–F and $Au^{III}$–F bond lengths of 2.12 Å and 1.92 Å, respectively, see Figure 5 in ref. [30]). We think that $Ag^{III}$ is most likely to enter $AgF_2$ planes as a local defect. Synthesis of intermediate-valence $Ag^{II}/Ag^{I}$ compounds seems easier to us. The stretching force constant for the approximately 2.46 Å long $Ag^{I}$–F bond is rather small, and one may compress it so that the $Ag^{I}$–F bond resembles an $Ag^{II}$–F bond. However, following the same line of reasoning, the prospect for superconductivity in the $Ag^{I}/Ag^{II}$ systems appears to be less than that for $Ag^{II}/Ag^{III}$ ones.

Led by the isoelectronic character of $Ag^{II}$ and $Cu^{II}$ ($d^9$), and $F^-$ and $O^{2-}$ ($s^2p^6$) species, by the similarity of the ligand-field of $F^-$ and $O^{2-}$ ions, a strong covalent contribution in both $Cu^{II}$–$O^{2-}$ and $Ag^{II}$–$F^-$ bonding, apparent crystal structure analogies, as well as by our previous theoretical considerations on molecular systems,[302–305] we have analyzed the hypothetical occurrence of superconductivity in hole- or electron-doped $Ag^{II}$ fluorides. In particular, we have studied 1D (infinite chains)[331] and 2D ($AgF_2$ sheets) Ag–F nets, having formally mixed-valence $Ag^{II}/Ag^{I}$ and $Ag^{II}/Ag^{III}$ character. For this purpose we have examined analogies between the well-known superconducting cuprates ($Cu^{II}/Cu^{III}$–$O^{2-}$ and $Cu^{II}/Cu^{I}$–$O^{2-}$ systems) and the $Ag^{II}/Cu^{III}$–$F^-$ and $Ag^{II}/Ag^{I}$–$F^-$ solids.

To explain the connection between geometrical features and the electronic properties of these systems, we performed density functional theory (DFT) electronic-structure computations for some selected compounds. The DOS of $Ag^{II}$ and $Ag^{III}$ compounds in the $-10.0$ eV to 0.0 eV energy range contains sets of Ag–F bonding, Ag–F nonbonding, and Ag–F antibonding states. The relative position of the predominantly Ag(d) orbitals shifts predictably down as one goes from $Ag^{I}$ to $Ag^{II}$ to $Ag^{III}$, crossing the F(p) band near $Ag^{III}$.

In the calculations the $Ag^{II}$–$F^-$ bonds appear to be substantially covalent (similar to $Cu^{II}$–$O^{2-}$ bonds). States in the vicinity of the Fermi level in $Ag^{II}$ fluorides usually have strongly mixed Ag(d)/F(p) character and are Ag–F antibonding, thus providing the potential for efficient vibronic coupling. The values of $DOS_F$ and metal–ligand stretching frequencies for Ag–F materials are also close to those for oxocuprates. In addition, an "ionic/covalent" curve crossing is expected in some hole-doped $Ag^{II}$ fluorides, which might lead to the "magic electronic state" suggested by Burdett for oxocuprates.

In a separate paper we will show how to apply in practice the idea of using a dopant which "clips" the Ag-F-Ag fragments in 1D and 2D structures. We will analyze the possible structural and electronic changes in $Ag^{II}$–F systems upon hole- and electron-doping, and we will discuss strategies for preserving an intermediate-valence character of these systems, while repressing a tendency toward their disproportionation through dynamic band-gap opening. We intend to propose a concrete crystal-engineering based experimental strategy to 1) increase the density of states at the Fermi level, 2) augment the electron–phonon coupling constant, 3) dilute paramagnetic $Ag^{II}$ centers (quenching antiferromagnetism), 4) prevent Peierls distortion (preserving the intermediate-valence character of a system), and 5) generate the "ionic/covalent" curve crossing. We expect that under such conditions superconductivity might be induced in the Ag–F nets.

Intermediate-valence quaternary Ag–F compounds are not going to be easy to make, and possibly might be supported by applying external pressure. This factor may shift the comproportionation equilibrium and allow metallization of the mixed-valence compound.[332]

## 5. Acknowledgements

*This research was conducted using the resources of the Cornell Theory Center, which receives funding from Cornell University, New York State, the National Center for Research Resources at the National Institute of Health, the National Science Foundation, the Defense Department Modernization Program, the United States Department of Agriculture, and corporate partners. This work was also supported by the Cornell Center for Materials Research (CCMR), a Materials Research Science and Engineering Center of the National Science Foundation (DMR-9632275) and by NSF Research Grant (CHE 99-70089). The authors gratefully acknowledge Neil Bartlett, Bernd G. Müller, and Miguel Moreno for their valuable comments, and Prof. Bartlett's permission for reproducing here Figure 16 as well as for allowing us to quote him. Bernd G. Müller also allowed us to quote him and kindly sent us unpublished crystal structure data for $Ag_2F_5$ and $AgMF_6$ ($M = Sn, Ti, Pd$). We also thank Stephen Lee for making the VASP code available to us, to Robert Konecny and Peter Kroll for technical help, and to Gion Calzaferri for his comments on AgF. Stimulating discussions with Bill Wedemeyer are greatly appreciated.*

Received: September 25, 2000 [A 431]

## 6. Appendix

Table 11. Comparison of several important properties of oxygen and fluorine and their compounds.

| | O | F |
|---|---|---|
| 1st $E_i$ [kJ mol$^{-1}$] | 1313.9 | 6050.4 |
| 1st $E_{ea}$ [kJ mol$^{-1}$] | 141 | 328 |
| Pauling EN | 3.44 | 3.98 |
| Mulliken-Jaffe EN | 3.41 (16.7 % s) | 3.91 (14.3 % s) |
| redox potential $E^0$ [V] (acidic solution): | | |
| | 1.76 ($H_2O_2/H_2O$) | 3.05 ($F_2$/HF) |
| | 1.23 ($O_2/H_2O$) | 2.98 ($F_2/HF_2^-$) |
| | 0.695 ($O_2/H_2O_2$) | |
| | −0.13 ($O_2/HO_2$) | |
| Redox potential $E^0$ [V] (basic solution): | | |
| | 0.87 ($HO_2^-/OH^-$) | 2.87 ($F_2/F^-$) |
| | 0.40 ($O_2/OH^-$) | |
| | 0.20 ($O_2^-/HO_2^-$) | |
| | −0.06 ($O_2/HO_2^-$) | |
| $R(X^0)$ [Å] | 1.21 | 1.42 |
| $R(X^{-1})$ [Å] | 1.76 (Pauling) | 1.36 (Pauling), 1.19 (cn = 6, $O_h$), 1.17 (cn = 4, $T_d$) |
| $R(X^{-2})$ [Å] | 1.40 (Pauling), 1.28 (cn = 8), 1.24 (cn = 4, $T_d$) | – |
| $R$(vdW) [Å] | 1.52 | 1.47 |
| bond enthalpy [kJ mol$^{-1}$] of diatomic BX molecules: | | |
| B = F | 222 ± 17 | 158.8 |
| B = O | 498.4 ± 0.2 | 222 ± 17 |
| B = H | 427.6 | 570 ± 0.1 |
| B = Li | 333.5 ± 8.4 | 577 ± 21 |
| B = Cs | 295.8 ± 62.8 | 519 ± 8 |

[a] $E_i$ = ionisation energy; $E_{ea}$ = electron affinity; EN = electronegativity (in Pauling units); cn = coordination number; vdW = van der Waals.

[1] a) There is an important review paper on the $Ag^{II}$ and $Ag^{III}$ fluorides known up to 1987: B. G. Müller, *Angew. Chem.* **1987**, *99*, 120; *Angew. Chem. Int. Ed. Engl.* **1987**, *26*, 1081. The author has concentrated on the comparison of Ag, Cu, Au, and Pd, fluorides and on synthetic and structural aspects. Another review on transition metal derivatives of strong protonic acids and superacids mentions selected $Ag^{II}$ compounds b) F. Aubke, M. S. R. Cader, F. Mistry in *Synthetic Fluorine Chemistry* (Eds.: G. A. Olah, R. D. Chambers, G. K. S. Prakash), Wiley, New York, **1992**, chap. 3, p. 43). See also two other excellent reviews c) on crystal structure and bonding in transition metal fluoro compounds: W. Massa, D. Babel, *Chem. Rev.* **1988**, *88*, 275; and d) on classification of heavy metal fluorides with a body-centered cubic cationic sublattice: S. V. Borisov, N. A. Bliznyuk, E. S. Kuklina, *J. Struct. Chem.* **1994**, *35*, 279. However, silver fluorides are not covered by these last two reviews.

[2] S. Ido, S. Uchida, K. Kitazawa, S. Tanaka, *J. Phys. Soc. Jpn.* **1988**, *57*, 997.

[3] H. Kawamura, I. Shirotani, T. Hirooka, M. Fujihira, Y. Maruyama, H. Inokuchi, *Chem. Phys. Lett.* **1972**, *15*, 594.

[4] $Ag_2F$, which adopts the $Cd[OH]_2$ structure, is superconducting at 0.06 K: a) M. B. Robin, K. Andres, T. H. Geballe, N. A. Kuebler, D. B. McWhan, *Phys. Rev. Lett.* **1966**, *17*, 917; b) K. Andres, N. A. Kuebler, M. B. Robin, *J. Phys. Chem. Solids* **1966**, *27*, 1747.

[5] A. M. Raaen, I. Svare, T. A. Fjeldly, *Phys. Rev. B* **1980**, *21*, 4895.

[6] S. Hull, P. Berastegui, *J. Phys. Condens. Matter* **1998**, *10*, 7945.

[7] P. M. Halleck, J. C. Jamieson, C. W. T. T. Pistorius, *J. Phys. Chem. Solids* **1972**, *33*, 769.

[8] J. C. Jamieson, P. M. Halleck, R. B. Roof, C. W. T. T. Pistorius, *J. Phys. Chem. Solids* **1975**, *36*, 939.

[9] E. V. Gevorkyan, *Izv. Vyssh. Uchebn. Zaved. Fiz.* **1976**, *9*, 119.

[10] a) J. C. Jamieson, P. M. Halleck, R. B. Roof, C. W. Pistorius, *J. Phys. Chem. Solids* **1975**, *36*, 939; b) P. M. Halleck, J. C. Jamieson, C. W. Pistorius, *J. Phys. Chem. Solids* **1972**, *33*, 769.

[11] B. N. Onwuagba, *Solid State Commun*. **1996**, *97*, 267.

[12] N. Bartlett, G. M. Lucier, C. Shen, W. J. Casteel, Jr., L. Chacon, J. Münzenberg, B. Žemva, *J. Fluorine Chem*. **1995**, *71*, 163.

[13] Yu. M. Kiselev, A. I. Popov, K. V. Bukharin, A. A. Timakov, M. V. Korobov, *Russ. J. Inorg. Chem.* (*Engl. Transl.*) **1988**, *33*, 1852.

[14] C. Shen, B. Žemva, G. M. Lucier, O. Graudejus, J. A. Allman, N. Bartlett, *Inorg. Chem*. **1999**, *38*, 4570.

[15] a) P. Fisher, D. Schwarzenbach, H. M. Rietveld, *J. Phys. Chem. Solids* **1971**, *32*, 543; b) P. Fisher, G. Roult, D. Schwarzenbach, *J. Phys. Chem. Solids* **1971**, *32*, 1641.

[16] B. Žemva, K. Lutar, A. Jesih, W. J. Casteel, Jr., A. P. Wilkinson, D. E. Cox, R. B. Von Dreele, H. Borrmann, N. Bartlett, *J. Am. Chem. Soc*. **1991**, *113*, 4192.

[17] It seems that previous claims of obtaining $AgF_3$ (a) R. Bougon, M. Lance, *C. R. Acad. Sci. Ser. 2* **1983**, *297*, 117; b) R. Bougon, T. Bui Huy, M. Lance, H. Abazli, *Inorg. Chem*. **1984**, 23, 3667; c) ref. [13]) were premature.

[18] M. Kraus, M. Müller, R. Fischer, R. Schmidt, D. Koller, B. G. Müller, *J. Fluorine Chem.* **2000**, *101*, 165.

[19] O. Graudejus, A. P. Wilkinson, N. Bartlett, *Inorg. Chem.* **2000**, *39*, 1545.

[20] Very few examples of the $Ag^{2+}$ ion in $Cl^-$ and $Br^-$ systems are known. For $[Pd(dddt)_2]Ag_{1.5}Br_{3.5}$ (dddt = 5,6-dihydro-1,4-dithiin-2,3-dithiolate) see: a) E. B. Yagubskii, L. A. Kushch, V. V. Gritsenko, O. A. Dyachenko, L. I. Buravov, A. G. Khomenko, *Synth. Met.* **1995**, *70*, 1039; b) L. A. Kushch, S. V. Konovalikhin, L. I. Buravov, A. G. Khomenko, G. V. Shilov, K. Van, O. A. Dyachenko, E. B. Yagubskii, C. Rovira, E. Canadell, *J. Phys. I* **1996**, *6*, 1555; c) S. V. Kapelnitskii, L. A. Kushch, *Phys. Solid State Engl. Transl.* **2000**, *42*, 350. For $Ag^{II}$ in $Cl^-$ and $Br^-$ host lattices see: d) T. Miyanaga, *J. Phys. Soc. Jpn.* **1979**, *46*, 167; e) M. Moreno, *J. Phys. Soc. Jpn.* **1975**, *53*, 1545; f) J. A. Aramburu, M. Moreno, *Solid State Commun.* **1986**, *58*, 305; g) J. A. Aramburu, M. Moreno, *Solid State Commun.* **1987**, *62*, 513.

[21] M. Jansen, P. Fischer, *J. Less-Common Met.* **1988**, *137*, 123.

[22] B. Standke, M. Jansen, *Z. Anorg. Allg. Chem*. **1986**, *535*, 39.

[23] However, $Ag^{II}$ centers may be stabilized as an impurity in some oxide hosts, see for example: a) J. L. Pascual, L. Seijo, Z. Barandiaran, *J. Chem. Phys.* **1993**, *98*, 9715. $Ag^{II}$ also oxidizes water, but an $[Ag(OH)_4]^-$ ion has been observed in highly basic solutions b) R. J. Lancashire in *Comprehensive Coordination Chemistry*, *Vol. 5* (Eds.: G. Wilkinson, R. D. Gillard, J. A. McCleverty), Pergamon Press, Oxford, **1987**, chap. 54. A theoretical study of a hypothetical $[Ag(OH_2)_6]^{2+}$ ion has been performed c) R. Åkeson, L. G. M. Pettersson, M. Sandström, U. Wahlgren, *J. Am. Chem. Soc.* **1994**, *116*, 8691.

[24] B. Žemva, R. Hagiwara, W. J. Casteel, Jr., K. Lutar, A. Jesih, N. Bartlett, *J. Am. Chem. Soc*. **1990**, *112*, 4846.

[25] R. Hagiwara, F. Hollander, C. Maines, N. Bartlett, *Eur. J. Solid State Inorg. Chem.* **1991**, *28*, 855.

[26] G. M. Lucier, C. Shen, W. J. Casteel, Jr., L. Chacon, N. Bartlett, *J. Fluorine Chem*. **1995**, *72*, 157.

[27] B. Žemva, *C. R. Acad. Sci. Ser. II C* **1998**, *1*, 151.

[28] G. M. Lucier, J. Münzenberg, W. J. Casteel, Jr., N. Bartlett, *Inorg. Chem*. **1995**, *34*, 2692.

[29] W. J. Casteel, Jr., G. M. Lucier, R. Hagiwara, H. Borrmann, N. Bartlett, *J. Solid State Chem*. **1992**, *96*, 84.

[30] S. H. Elder, G. M. Lucier, F. J. Hollander, N. Bartlett, *J. Am. Chem. Soc*. **1997**, *119*, 1020.

[31] J. M. Whalen, G. M. Lucier, L. Chacón, N. Bartlett, *J. Fluorine Chem*. **1998**, *88*, 107.

[32] It is known that large vibronic coupling is connected with orbital mixing involving strongly bonding or strongly antibonding levels. For details, see the excellent review: T. Bally, W. T. Borden in *Reviews in Computational Chemistry*, *Vol. 13* (Eds.: K. B. Lipkowitz, D. B. Boyd), Wiley, New York, **1999**, p. 1.

[33] Mixed-valence compounds have been divided by Robin and Day into three classes: class I (disproportionated compounds, with completely localized electrons), class III (comproportionated compounds, completely delocalized electrons) and class II (an intermediate between I and III; dynamic comproportionation at vibrational frequencies may exist in this interesting class). See: M. B. Robin, P. Day, *Adv. Inorg. Chem. Radiochem.* **1967**, *10*, 247.

[34] $CsAgMnF_7$ exists, being presumably the first member of the quaternary $M^IAg^{II}(M')^{IV}F_7$ series (see short mention in B. G. Müller, R. Hoppe, *Z. Anorg. Allg. Chem*. **1973**, *395*, 239).

[35] R. Fischer, B. G. Müller, *Z. Anorg. Allg. Chem*. **1997**, *623*, 1729.

[36] D. Gantar, I. Leban, B. Frlec, J. H. Holloway, *J. Chem. Soc. Dalton Trans*. **1987**, 2379.

[37] M. S. R. Cader, F. Aubke, *Can. J. Chem*. **1989**, *67*, 1700.

[38] "$Ag[MF_6]_2$ (M = Nb, Ta), Ternary Fluorides of Divalent Silver": B. G. Müller, *Angew. Chem*. **1987**, *99*, 685; *Angew. Chem. Int. Ed. Engl.* **1987**, *26*, 689.

[39] B. G. Müller, R. Hoppe, *Z. Anorg. Allg. Chem*. **1972**, *392*, 37. Note added in proof (July 20, 2001): in the meantime a study of $AgM^{IV}F_6$ (M = Sn, Ti, Pb, Pd, Pt, Rh) was published. R. Fischer, B. G. Müller, *Z. Anorg. Allg. Chem.* **2001**, *627*, 445.

[40] R. Hoppe, B. G. Müller, *Naturwissenschaften* **1969**, *56*, 35.

[41] O. Graudejus, S. H. Elder, G. M. Lucier, C. Shen, N. Bartlett, *Inorg. Chem.* **1999**, *38*, 2503.

[42] R. Hoppe, G. Siebert, *Z. Anorg. Allg. Chem*. **1970**, *376*, 261.

[43] G. Siebert, R. Hoppe, R. Homann, *Naturwissenschaften* **1971**, *58*, 95.

[44] B. G. Müller, *Z. Anorg. Allg. Chem*. **1987**, *553*, 196. It is noteworthy that Cu, Ni, Zn, or Mg may substitute one Ag(1) atom, while Ca, Cd, or Hg may substitute two Ag(2) atoms.

[45] D. Koller, B. G. Müller, *Z. Anorg. Allg. Chem*. **2000**, *626*, 1429.

[46] B. G. Müller, *Z. Anorg. Allg. Chem*. **1987**, *553*, 205.

[47] Many other families of ternary and quaternary $Cu^{II}$ fluorides, for example $M^I_3Cu_3M^{IV}F_{12}$ ($M^I$ = Cs, $M^{IV}$ = Zr, Hf), are known (M. Müller, B. G. Müller, *Z. Anorg. Allg. Chem.* **1995**, *621*, 993); however, $Ag^{II}$ analogues have not been prepared so far.

[48] The large negative value of $\Theta$ for $AgTiF_6$ probably comes from impurities, i.e. $AgF_2$, because the former compound can only be synthesized with difficulties by high-pressure fluorination (B. G. Müller, personal communication, **2000**).

[49] The only exception occurs for $Ag_3Hf_2F_{14}$, where Ag(2) is found in 4+4 coordination.

[50] G. C. Allen, R. F. McMeeking, R. Hoppe, B. G. Müller, *J. Chem. Soc. Chem. Commun.* **1972**, 291.

[51] One should not exclude that the postulated diamagnetic form of "$Ag[SbF_6]_2$" is in fact $Ag[Sb_2F_{11}]$, an $Ag^I$ compound (N. Bartlett, personal communication, **2000**).

[52] Details of the crystal structure might also reveal the order of the F-abstracting strength of two very hard Lewis acids, $Ag^{III}$ and $Sb^V$.

[53] W. Dukat, D. Naumann, *Rev. Chim. Miner.* **1986**, *23*, 589.

[54] The $[Ag_2F_3]^+$ unit also may be expected in the $2\,AgF_2 \cdot AsF_5$ adduct, similar to analogous $Sn^{II}$ and $Xe^{II}$ compounds. For details, see: B. Frlec, D. Gantar, J. H. Holloway, *J. Fluorine Chem.* **1982**, *20*, 385.

[55] $[Ag_3F_9]^{3-}$ ions, analogous to the $[Cu_3F_9]^{3-}$ triangular ions with F bridges between Cu centers,[47] are not known; neither are $Ag^{II}$ analogues of the $KCu^{II}MF_7$ family (M = Zr, Hf), see: M. Kraus, B. G. Müller, *Z. Anorg. Allg. Chem.* **2000**, *626*, 1929.

[56] $[AgF]^+[W_2O_2F_9]^-$ is probably the only oxofluoride material containing infinite $[AgF]^+$ chains (Y. Katayama, R. Hagiwara, Y. Ito, *J. Fluorine Chem.* **1995**, *74*, 89). It is a very strong oxidizer, similar to other compounds in this class. Its structure is not known. Although it oxidizes Xe to $Xe^{II}$ in HF at room temperature, this compound does not liberate a peroxide anion from its structure. Most probably, oxygen atoms are not directly neighboring the Ag center in this compound.

[57] See also a review on bonding in crystals containing 1D bridged and unbridged Group 11 and 12 ($d^{10}$) linear, zigzag, and helical chains: C. X. Cui, M. Kertesz, *Inorg. Chem.* **1990**, *29*, 2568. Silver fluorides are not covered by this review.

[58] D. Gantar, B. Frlec, D. R. Russell, J. H. Holloway, *Acta Crystallogr. Sect. C* **1987**, *43*, 618.

[59] a) B. Frlec, D. Gantar, J. H. Holloway, *J. Fluorine Chem.* **1982**, *20*, 217; b) B. Frlec, D. Gantar, J. H. Holloway, *J. Fluorine Chem.* **1982**, *20*, 385. $[AgF_2]_2[AsF_5]$ has also been claimed, but no reliably pure samples of this compound were available for detailed investigation of its physical properties.

[60] O. Graudejus, B. G. Müller, *Z. Anorg. Allg. Chem*. **1996**, *622*, 1549.

[61] B. G. Müller, *J. Fluorine Chem*. **1981**, *17*, 317.
[62] B. G. Müller, R. Hoppe, *Z. Anorg. Allg. Chem*. **1973**, *395*, 239.
[63] Note that diamagnetic behavior might also imply superconducting properties of some impurity present in all samples.
[64] There are also some transition metal fluorides with infinite [MF] chains, but with an elongated octahedral coordination of the M atom, $Tl_2MnF_5 \cdot H_2O$ is a good example (P. Nuñez, A. Tressaud, J. Darriet, P. Hagenmuller, G. Hahn, G. Frenzen, W. Massa, D. Babel, A. Boireau, J. L. Soubeyroux, *Inorg. Chem.* **1991**, *31*, 770).
[65] We could not recreate the crystal structure of $[AgF]^+[RuF_6]^-$ as given in ref. [28] from the unit cell coordinates, probably because of an error in the crystal coordinates of the Ag or F(1) atom.
[66] R. H. Odenthal, R. Hoppe, *Monatsh. Chem*. **1971**, *102*, 1340.
[67] R. H. Odenthal, D. Paus, R. Hoppe, *Z. Anorg. Allg. Chem*. **1974**, *407*, 151.
[68] A. I. Popov, Yu. M. Kiselev, *Russ. J. Inorg. Chem. Engl. Transl.* **1988**, *33*, 965. It cannot be excluded that $Na_2AgF_4$ contains $[AgF_3]^-$ 1D chains rather than 2D $[AgF_2]$ planes, by analogy to $Na_2CuF_4$.
[69] R. H. Odenthal, D. Paus, R. Hoppe, *Z. Anorg. Allg. Chem*. **1974**, *407*, 144.
[70] R. H. Odenthal, R. Hoppe, *Z. Anorg. Allg. Chem*. **1971**, *385*, 92.
[71] R. H. Odenthal, R. Hoppe, *Naturwissenschaften* **1970**, *57*, 305.
[72] An interesting pressure-induced transition from a ferromagnetic to an antiferromagnetic state has been studied for analogous $Cu^{II}$ compounds (T. Kawamoto, N. Suzuki, *J. Phys. Soc. Jpn.* **1997**, *66*, 2487). There are no such studies for $Ag^{II}$ compounds.
[73] C. Friebel, D. Reinen, *Z. Anorg. Allg. Chem.* **1975**, *413*, 51.
[74] Similar tetragonally compressed octahedra occur for several $Cu^{II}$ fluorides, such as $KCuF_3$: a) A. Okazaki, *J. Phys. Soc. Jpn.* **1969**, *26*, 870; b) A. J. Edwards, R. D. Peacock, *J. Chem. Soc.* **1959**, 4126; $K_2CuF_4$: c) K. Knox, *J. Chem. Phys.* **1959**, *30*, 991; d) M. Kaneko, G. Kubawara, A. Misu, *Solid State Commun.* **1976**, *18*, 1085; and for isolated $Cu^{2+}$ ions in one of crystallographic positions in a $Ba_2ZnF_6$ host lattice: e) G. Steffen, D. Reinen, H. Stratemeler, M. J. Riley, M. A. Hitchman, H. E. Matthies, K. Recker, F. Wallrafen, J. R. Niklas, *Inorg. Chem.* **1990**, *29*, 2123. This relatively rare environment of $d^9$ systems has been predicted to occur in an ionic environment: f) A. D. Liehr, C. J. Ballhausen, *Ann. Phys. NY* **1958**, *3*, 304.
[75] Square-planar coordination of the $Ag^{II}$ center is also found in the $[Ag^{II}(py)_4]$ cation (py = pyridine). Similar square-planar coordination of $Cu^{II}$ centers is rare in fluoride systems. $SrCuF_4$ and $CaCuF_4$ with a Cu–F bond length of 1.88 Å are probably the only two examples known (H. G. von Schnering, B. Kolloch, A. Kolodziejczyk, *Angew. Chem.* **1971**, *83*, 440; *Angew. Chem. Int. Ed. Engl.* **1971**, *10*, 413). Isolated $Cu^{2+}$ ions also adopt a square-planar $F_4$ coordination in a $Ba_2ZnF_6$ host lattice in one crystallographic position.[38]
[76] G. C. Allen, R. F. McMeeking, *J. Chem. Soc. Dalton Trans.* **1976**, 1063.
[77] H. G. von Schnering, *Z. Anorg. Allg. Chem*. **1973**, *400*, 201.
[78] O. Ruff, M. Giese, *Z. Anorg. Allg. Chem*. **1934**, *219*, 143.
[79] P. Charpin, A.-J. Dianoux, H. Marquet-Ellis, C. Nguyen-Nghi, *C. R. Seances Acad. Sci. Ser. B* **1966**, *263*, 1359.
[80] E. A. Baturina, Yu. A. Lukyanychev, L. N. Rastorguev, *Zh. Strukt. Khim*. **1966**, *7*, 627.
[81] Yu. M. Kiselev, A. I. Popov, A. A. Timakov, K. V. Bukharin, V. F. Sukhoverkhov, *Russ. J. Inorg. Chem. Engl. Transl.* **1988**, *33*, 708.
[82] A. Jesih, K. Lutar, B. Žemva, B. Bachmann, S. Becker, B. G. Müller, R. Hoppe, *Z. Anorg. Allg. Chem*. **1990**, *588*, 77.
[83] The high-pressure black form of $AgF_2$ (B. G. Müller, *Naturwissenschaften* **1979**, *66*, 519) has a Curie temperature of 160 K.
[84] There has been much controversy over the magnetic behavior of $\alpha$-$AgF_2$. The oldest contributions (a) E. Gruner, W. Klemm, *Naturwissenschaften* **1937**, *25*, 59, and ref. [78]), suggest strong paramagnetism of $AgF_2$ or emphasize ferromagnetic properties of $AgF_2$ (with a Curie temperature of 163 K). More recent studies (ref. [79] and b) D. Paus, R. Hoppe, *Z. Anorg. Allg. Chem.* **1977**, *431*, 207) suggest ferrimagnetism of $AgF_2$. Müller discusses ferromagnetism.[83] Fischer et al. have noted a small ferromagnetic component perpendicular to the $AgF_2$ sheets and a long-range antiferromagnetic ordering below the Curie temperature of 163 K.[15] Finally, Bastow et al. assigned antiferromagnetic properties to $AgF_2$ and give a Neél temperature $T_N = 163$ K; c) T. J. Bastow, H. J. Whitfield, R. W. Cockman, *Solid State Commun.* **1981**, *39*, 325. Perhaps the uncertain magnetic properties of $AgF_2$ are caused by the nonstoichiometry of this compound. In our paper we follow the results of Fischer's et al. careful study.
[85] Citation taken from ref. [15b) ].
[86] R. Bougon, T. Bui Huy, M. Lance, H. Abazli, *Inorg. Chem*. **1984**, *23*, 3667.
[87] F. W. Einstein, P. R. Rao, J. Trotter, N. Bartlett, *J. Chem. Soc. A* **1967**, 478.
[88] N. Bartlett, *Gold Bull.* **1998**, *31*, 22.
[89] Compare the decomposition temperature of $AgF_3$ to the value for $CuF_3$ (−40 °C) and the sublimation temperature of $AuF_3$ (+300 °C). Compounds of $Ag^{III}$ and also $AgF_2$ have been used as fluorinating agents in organic and inorganic synthesis, see for example: a) T. Nakajima, Y. Matsuo, B. Žemva, A. Jesih, *Carbon* **1996**, *34*, 1595; b) T. Nakajima, M. Koh, V. Gupta, B. Žemva, K. Lutar, *Electrochim. Acta* **2000**, *45*, 1655; c) P. R. Slater, J. P. Hodges, M. G. Francesconi, P. P. Edwards, C. Greaves, I. Gameson, M. Slaski, *Physica C* **1995**, *253*, 16; d) G. B. Peacock, I. Gameson, M. Slaski, J. J. Capponi, P. P. Edwards, *Physica C* **1997**, *289*, 153; e) Z. Bugarceic, S. Novokmet, Z. Senic, Z. Bugarceic, *Monatsh. Chem.* **2000**, *131*, 799; f) S. Takubo, A. Sekiya, *J. Fluorine Chem.* **1998**, *87*, 105. Compounds of $Mn^{IV}$, $Cu^{IV}$, $Ni^{IV}$, $Pt^{VI}$, $Tb^{IV}$, and $M^{VI}$ (M = U, Mo, W) are other popular solid pure fluorine gas generators, see: g) K. O. Christe, R. D. Wilson, *Inorg. Chem.* **1987**, *26*, 2554; h) N. S. Chilingarov, J. V. Rau, L. N. Sidorov, L. Bencze, A. Popovic, V. F. Sukhovernikov, *J. Fluorine Chem.* **2000**, *104*, 291.
[90] Isoelectronic $Cu^{III}$ ion sometimes adopts an octahedral coordination in fluoride complexes, for example in cryolite $NaK_2CuF_6$ (C. S. Gopinath, *J. Chem. Soc. Faraday Trans.* **1996**, *92*, 3605). Octahedral coordination is also found in many $Pd^{II}$ fluorides, such as $PdMF_6$ (M = Ti, Sn, Pt), although square-planar $Pd^{II}$ is also known in fluoride environments (e.g. in $K_2PdF_4$, or $CaPdF_4$). Octahedral coordination has been suggested for $Ag^{III}$ only in $Cs_2KAgF_6$.
[91] R. Hoppe, *Z. Anorg. Allg. Chem.* **1957**, *292*, 29.
[92] A. I. Popov, Yu. M. Kiselev, V. F. Sukhoverkhov, V. I. Spitsyn, *Dokl. Akad. Nauk SSSR* **1987**, *296*, 424.
[93] K. Lutar, S. Milicev, B. Žemva, B. G. Müller, B. Bachmann, R. Hoppe, *Eur. J. Solid State Inorg. Chem*. **1991**, *28*, 1335.
[94] G. M. Lucier, J. M. Whalen, N. Bartlett, *J. Fluorine Chem.* **1998**, *89*, 101.
[95] K. Lutar, A. Jesih, B. Žemva, *Rev. Chem. Miner.* **1986**, *23*, 565.
[96] K. Lutar, A. Jesih, I. Leban, B. Žemva, N. Bartlett, *Inorg. Chem.* **1989**, *28*, 3467.
[97] a) U. Engelmann, B. G. Müller, *Z. Anorg. Allg. Chem*. **1990**, *589*, 51; b) U. Engelmann, B. G. Müller, *Z. Anorg. Allg. Chem*. **1992**, *618*, 43; c) U. Engelmann, B. G. Müller, *Z. Anorg. Allg. Chem*. **1993**, *619*, 1661; d) R. Schmidt, B. G. Müller, *Z. Anorg. Allg. Chem*. **1999**, *625*, 602; e) O. Graudejus, B. G. Müller, *Z. Anorg. Allg. Chem*. **1996**, *622*, 187.
[98] B. G. Müller, *Z. Anorg. Allg. Chem*. **1987**, *555*, 57.
[99] U. Engelmann, B. G. Müller, *Z. Anorg. Allg. Chem*. **1991**, *598/599*, 103.
[100] The stability of $CsAgF_4$ in the $NaAlF_4$ structure should be significant, because $R$(Cs–F) (ca. 3.0 – 3.2 Å) > $\sqrt{2}\,R$(Ag–F) ($R$(Ag–F) ≈ 1.9 Å).
[101] R. Hoppe, R. Homann, *Naturwissenschaften* **1966**, *53*, 501.
[102] B. G. Müller, personal communication, **2000**.
[103] $Cs_2Ag^{III}_{0.5}Ag^{V}_{0.5}F_6$ and related $Cs_2Ga_{0.5}Ag^{V}_{0.5}F_6$ seem to be the only claims of $Ag^{V}$ compounds: P. Sorbe, J. Grannec, J. Portier, P. Hagenmuller, *J. Fluorine Chem*. **1978**, *11*, 243.
[104] Attempts to synthesize another mixed-valence fluoride, $Ag^{I}$-$Ag^{II}Zr_2F_{11}$, did not succeed: D. Koller, B. G. Müller, *Z. Anorg. Allg. Chem*. **2000**, *626*, 1426.
[105] J. T. Wolan, G. B. Hoflund, *Appl. Surf. Sci*. **1998**, *125*, 251.
[106] Hypothethical mixed-valence $Ag^{II}/Ag^{I}$ fluorides are interesting in the context of isoelectronic $Cu^{II}/Cu^{I}$ oxides. The latter are often mixed- and not intermediate-valence compounds. See for example: a) S. J. Hibble, J. Köhler, A. Simon, S. Paider, *J. Solid State Chem.* **1990**, *88*, 534; b) G. Tams, H. Müller-Buschbaum, *J. Alloys Compd.* **1992**, *189*, 241.
[107] A fascinating description of Prof. Bartlett's adventure with fluorine chemistry may be found in N. Bartlett in *Fluorine Chemistry at the*

*Millennium - Fascinated by Fluorine* (Ed.: E. Banks), Elsevier, Oxford **2000**, chap. 3, p. 29.
[108] Note that despite Jahn–Teller distortion, "an average $Ag^{II}$–$F^-$ distance" of 2.22–2.30 Å is preserved in pseudooctahedral complexes of $Ag^{II}$. For similar properties of $Cu^{II}$ compounds see: a) J. Gažo, I. B. Bersuker, J. Garaj, M. Kabešova, J. Kohout, H. Langfelderova, M. Melník, M. Serator, F. Valach, *Coord. Chem. Rev.* **1976**, *19*, 253; b) I. B. Bersuker, *J. Coord. Chem.* **1995**, *34*, 289.
[109] G. Kresse, J. Farthmuller, *Phys. Rev. B* **1993**, *47*, 558.
[110] G. Kresse, J. Farthmuller, *Comput. Mater. Sci.* **1996**, *6*, 15.
[111] Unfortunately, this is not as easy a matter to evaluate as one might imagine. The VASP program requires that one choose certain Wigner–Seitz radii for the atoms in the lattice; the electrons within a certain radius sphere are then integrated. There are two problems that arise: 1) the choice of the radius of the sphere (should it be the same for $Ag^I$, $Ag^{II}$, $Ag^{III}$, or for F and $F^-$?), and 2) what about the electrons in the interstices between the spheres? We would like to emphasize that the raw computed atomic contributions do not quite add up to the total DOS. To divide the total DOS into atomic (on-site) contributions we have used the following Wigner–Seitz radii [Å]: Ag (1.503), F (0.714), K (2.275), Rb (2.418), Cs (2.831), B (0.905). Such a choice leaves no more than 15% of total electron density located in interstices between atomic spheres. The % atomic contributions to the electron density have been rescaled for each compound to add up to 100% (proportionally to the atomic contributions computed by VASP). Assumption of too large a radius for Ag and/or too small a radius of F may lead to overestimation of the covalency of the Ag–F bonds.
[112] M. R. Hayns, J.-L. Calais, *J. Phys. C* **1973**, *6*, 2625.
[113] R. C. Birtcher, P. W. Deutsch, J. F. Wendelken, A. B. Kunz, *J. Phys. C* **1972**, *5*, 562.
[114] N. J. M. Geipel, B. A. Hess, *Chem. Phys. Lett.* **1997**, *273*, 62.
[115] V. C. Jain, J. Shanker, *Pramana* **1979**, *13*, 31.
[116] From here on we will drop the principal quantum number in describing F, Ag, and Cu states.
[117] a) A. P. Marchetti, G. L. Bottger, *Phys. Rev. B* **1971**, *3*, 2604; b) M. G. Mason, *J. Electron Spectrosc. Relat. Phenom.* **1972**, *52*, 591; c) W. B. Fowler, *Phys. Status Solidi* **1972**, *52*, 591. Interestingly, both direct and indirect band gaps do not appear to scale properly in going from AgCl to AgF; that is, gaps increase and then decrease in the order AgBr → AgCl → AgF.
[118] Since the ligand s, p levels lie lower than the metal d levels, bands originating essentially from the ligand levels should be metal–ligand bonding, and bands originating from the latter should be metal–ligand antibonding.
[119] Unfortunately, the bonding index in the computational code available to us, the Crystal Orbital Overlap Population (T. Hughbanks, R. Hoffmann, *J. Am. Chem. Soc.* **1983**, *105*, 3528), is too sensitive to the choice of Wigner–Seitz radii to allow a reliable bonding assesement.
[120] In principle we should carry out spin-polarized calculations on $AgF_2$, but we have chosen not to do so, because our primary aim is to compare $AgF_2$ with other silver fluorides so as to determine the approximate position of Ag(d) and F(p) states. The Curie temperature of $AgF_2$ is rather low, and results of a precise spin-polarized calculation should not be substantially different from the ones obtained by us. Similar reasoning is valid for antiferromagnets with low Neél temperatures, such as $CsAgF_3$ and $Cs_2AgF_4$.
[121] Discussions of the degree of covalency, and on generating holes in the F(p) band by tetravalent lanthanide cations (strong oxidizers, similarly to trivalent Ag centers) may be found in: a) Z. Hu, E. J. Cho, G. Kaindl, B. G. Müller, *Phys. Rev. B* **1995**, *51*, 7514; b) Z. Hu, G. Kaindl, B. G. Müller, *J. Alloys Compd.* **1997**, *246*, 177.
[122] In the context of superconductivity, it is of great interest whether holes might be generated in the F(p) band in the hole-doped $Ag^{II}$ fluorides which create extended 1D and 2D nets. We will consider this problem further on in this paper, and in separate work.
[123] The distorted $MF_2$ layers occur also in pseudo-3D antiferromagnetic $TlMnF_4$ (P. Nuñez, A. Tressaud, J. Grannec, P. Hagenmuller, W. Massa, D. Babel, A. Boireau, J. L. Soubeyroux, *Z. Anorg. Allg. Chem.* **1992**, *609*, 71).
[124] The very narrow F(s) bands at about −25 eV and rather broad Ag(s,p) bands at +5 to +8 eV are not shown in the Figures. The very sharp DOS peak at about −9 eV (so narrow that it almost does not contribute to DOS integration) is puzzling. It is probably an artifact of the calculation.
[125] The Ag–F nonbonding states may be recognized both by their dominant F(p) character, and by kinks in the integration of the total DOS.
[126] Indication of energetic proximity of Ag(d) (in $Ag^{II}$) and F(p) orbitals is provided also by electronic and ESR spectra,[326, 328] and by electrochemistry. The reduction potential of $Ag^{II}/Ag^I$ in *liquid* HF is +2.27 V, rather close to the $F_2/F^-$ potential (+2.71 V). The $Ag^I/Ag^0$ redox pair is left far behind, at +0.88 V (see: *Comprehensive Inorganic Chemistry* (Eds.: J. C. Bailar, H. J. Emeleus, R. Nyholm, A. F. Trotman-Dickenson), Pergamon, Oxford, **1973**, p. 1053, and refs therein). Values of redox potentials in *aqueous* solutions are lower, but still very positive: +2.0 V for $[AgO]^+/Ag^I$, +2.1 V for $[AgO]^+/Ag^{II}$, +1.98 V for $Ag^{II}/Ag^I$, and +0.80 V for $Ag^I/Ag^0$ (see: J. W. Laist, *Comprehensive Inorganic Chemistry*, *Vol. 2* (Eds.: M. C. Sneed, J. L. Maynard, R. C. Brasted), D. Van Nostrand, Toronto, **1954**, p. 144).
[127] There are two strong Ag–F bonds in 1D compounds, in contrast to four strong bonds in 2D compounds with an elongated octahedral configuration of F atoms around Ag atoms. Hence, one needs to divide the value of $Ag_{tot}/F_{tot}$ obtained for a linear chain in 1D $[AgF][BF_4]$ by a factor of 2, to compare it with respective values for $AgF_2$ sheets in 2D substances.
[128] Based on $E_F$ criterion only.
[129] F. A. Cotton, G. Wilkinson, *Advanced Inorganic Chemistry*, *5th ed.*, Wiley, New York, **1988**.
[130] Data obtained from http://www.webelements.com/.
[131] We use the term "metallic" here focusing on electronegativity values, rather than the electric conductivity in elementary Ag, Cu, and Au. Metals in this classical definition have small electronegativity values and easily form cations; nonmetals have large electronegativity and act mostly as anions in compounds.
[132] The Mulliken–Jaffe EN here is calculated using a weighted average over valence s and p orbitals.
[133] "The elements Cu, Ag, and Au lie on the border between transition metals and Main Group metals ("meta-metals"), but are "true" transition metals in the narrower sense insofar as, in contrast to the elements Zn, Cd, and Hg, d electrons can still be involved in their bonding. […] The fluorides are of particular importance insofar as they are the only compounds in which certain oxidation states can exist." Citation from ref. [1a].
[134] $Au^{III}$ is found in several complexes of Au containing organic ligands, such as $[(C_2H_5)_2AuBr]_2$. Also, $Au(OTeF_5)_3$, an oxyfluoride of $Au^{III}$, exists (P. Huppmann, H. Hartl, K. Seppelt, *Z. Anorg. Allg. Chem.* **1985**, *524*, 26).
[135] Exotic paramagnetic $Cu^{IV}$ occurs in orange-red compounds with formula $M_2CuF_6$ (M = Cs, Rb), which crystallize in the $K_2PtCl_6$ structure. For details, see: a) W. Harnischmacher, R. Hoppe, *Angew. Chem.* **1973**, *85*, 590; *Angew. Chem. Int. Ed. Engl.* **1973**, *12*, 582; b) P. Sorbe, J. Grannec, J. Portier, P. Hagenmuller, *C. R. Hebd. Seances Acad. Sci. Ser. C* **1976**, *282*, 663; c) D. Kissel, R. Hoppe, *Z. Anorg. Allg. Chem.* **1988**, *559*, 40; d) W. Carl, D. Kissel, R. Hoppe, *Eur. J. Solid State Inorg. Chem.* **1990**, *27*, 5. The presence of $Au^{IV}$ in $Sn_{1-x}Au_xF_4$ (e) M. Bork, R. Hoppe, A. Hofstaetter, A. Scharmann, F. E. Wagner, *Z. Anorg. Allg. Chem.* **1996**, *622*, 1721) has not been confirmed by others.
[136] F. G. Herring, G. Hwang, K. C. Lee, F. Mistry, P. S. Phillips, H. Willner, F. Aubke, *J. Am. Chem. Soc.* **1992**, *114*, 1271.
[137] N. R. Walker, R. R. Wright, P. E. Barran, A. J. Stace, *Organometallics* **1999**, *18*, 3569.
[138] a) T. J. Bergendahl, J. W. Waters, *Inorg. Chem.* **1975**, *14*, 2556; b) T. Mori, H. Inokuchi, *Solid State Commun.* **1987**, *62*, 525; and ref. [97d].
[139] Plenty of "pseudo-$Au^{II}$" compounds exist, $Cs_2[Au^ICl_2][Au^{III}Cl_4]$ is a classical example.
[140] Very recently, $[AuXe_4]^{2+}\{[Sb_2F_{11}]^-\}_2$, a so-far unique Au–Xe compound, has been obtained (S. Seidel, K. Seppelt, *16th International*

*Symposium on Fluorine Chemistry*, Durham, UK, **2000**). Also $[F_3AsAu]^+[SbF_6]^-$, another compound containing a rare $Au^I$–$As^{III}$ bond, exists (R. Küster, K. Seppelt, *Z. Anorg. Allg. Chem.* **2000**, *626*, 236).
[141] K. Leary, N. Bartlett, *J. Chem. Soc. Chem. Commun.* **1972**, 903.
[142] A. J. Edwards, W. E. Falconer, J. E. Griffiths, W. A. Sunder, M. J. Vasile, *J. Chem. Soc. Dalton Trans.* **1974**, 1129.
[143] G. Kaindl, K. Leary, N. Bartlett, *J. Chem. Phys.* **1973**, *59*, 5050.
[144] M. J. Vasile, T. J. Richardson, F. A. Stevie, W. E. Falconer, *J. Chem. Soc. Dalton Trans.* **1976**, 351.
[145] P. Sorbe, J. Grannec, J. Portier, P. Hagenmuller, *J. Fluorine Chem.* **1978**, *11*, 243.
[146] For ionic radii of $M^V$ and hypothetical $M^{IV}$ see: A. I. Popov, N. S. Kopelev, Yu. M. Kiselev, *Dokl. Akad. Nauk. SSSR* **1988**, *301*, 623.
[147] R. Schmidt, B. G. Müller, *Z. Anorg. Allg. Chem.* **1999**, *625*, 605.
[148] Chemistry has adopted, at least in colloquial usage, a traditional term of alchemy, "affinity" or "chemical affinity". A strong affinity of certain elements for each other (such as Hg or Ag for S) has been known for millennia. A relationship may be drawn between an "affinity" of two elements and the strength of bonding between them. Extended systems with a net of strong, covalent bonds (such as diamond) are usually less volatile than systems having weaker bonds (such as metallic sodium); the latter melt, sublime, or decompose easier than the former.
[149] Fluorine adsorbs easily on the surface of metallic Ag (in contrast to metallic Au). However, this is because of a redox reaction, and AgF is formed (M. A. Loudiana, J. T. Dickinson, A. Schmid, E. J. Ashley, *Appl. Surf. Sci.* **1987**, *28*, 311).
[150] A. B. Kunz, *Phys. Rev. B* **1982**, *26*, 26.
[151] B. N. Onwuagba, *Solid State Commun.* **1996**, *97*, 267.
[152] http://www.lbl.gov/LBL-Programs/CSD/HTMLFiles/Chem-Eng_htmls/Bartlett_HighEngOx.html.
[153] M. Ilias, P. Furdik, M. Urban, *J. Phys. Chem. A* **1998**, *102*, 5263.
[154] M. Seth, F. Cooke, P. Schwerdtfeger, J.-L. Heully, M. Pelissier, *J. Chem. Phys.* **1998**, *109*, 3935.
[155] V. G. Solomonik, J. E. Boggs, J. F. Stanton, *J. Mol. Struct. (THEOCHEM)* **2000**, *496*, 213.
[156] J. K. Laerdahl, T. Saue, K. Faegri, Jr., *Theor. Chem. Acc.* **1997**, *97*, 177.
[157] J. K. Laerdahl, T. Saue, K. Faegri, *Theor. Chem. Acc.* **1997**, *97*, 177.
[158] H. Wang, J. L. Gole, *J. Chem. Phys.* **1993**, *98*, 9311.
[159] A. Ramirez-Solis, J. Schamps, *J. Chem. Phys.* **1995**, *102*, 4482.
[160] A. Ramirez-Solis, J. P. Daudey, *J. Chem. Phys.* **2000**, *113*, 8580.
[161] The existence of the AuF molecule has been controversial for years. Only very recently has it been confirmed. See: a) C. J. Evans, M. C. L. Gerry, *J. Am. Chem. Soc.* **2000**, *122*, 1560; b) S. Andreev, J. Belbruno, *Chem. Phys. Lett.* **2000**, *329*, 490.
[162] B. Reffy, M. Kolonits, A. Schulz, T. M. Klapotke, M. Hargittai, *J. Am. Chem. Soc.* **2000**, *122*, 3127.
[163] Relativistic bond length contraction is even more pronounced for $Au^0$ than for $Au^I$. For example, it is about 0.35 Å for the Au–Au bond in the $Au_2$ molecule a) P. Pyykkö, J.-P. Desclaux, *Acc. Chem. Res.* **1979**, *12*, 276); and "only" 0.28 Å for the Au–H bond in the AuH molecule (b) K. S. Pitzer, *Acc. Chem. Res.* **1979**, *12*, 271).
[164] a) P. Schwerdtfeger, M. Dolg, W. H. E. Schwarz, G. A. Bowmaker, P. D. W. Boyd, *J. Chem. Phys.* **1989**, *91*, 1762; b) P. Schwerdtfeger, P. D. W. Boyd, A. K. Burrell, W. T. Robinson, *Inorg. Chem.* **1990**, *29*, 3593.
[165] The term "valence tautomerism" is often used for quinone complexes of Fe, Co, or Mn in the solid state, with respect to the transfer of electrons between metal center and quinone moiety. See for example: a) C. G. Pierpont, C. W. Lange, *Prog. Inorg. Chem.* **1994**, *41*, 331; b) D. Ruiz-Molina, J. Veciana, K. Wurst, D. N. Hendrickson, C. Rovira, *Inorg. Chem.* **2000**, *39*, 617. The term also has a long history in the organic chemistry of olefins, and molecular rearrangements.
[166] P. Schwerdtfeger, P. D. W. Boyd, S. Brienne, A. K. Burrell, *Inorg. Chem.* **1992**, *31*, 3411.
[167] A. L. Hector, W. Levason, M. T. Weller, E. G. Hope, *J. Fluorine Chem.* **1997**, *86*, 105.
[168] C. Friebel, *Solid State Commun.* **1974**, *15*, 639.
[169] S. Deibele, J. Curda, E.-M. Peters, M. Jansen, *Chem. Commun*. **2000**, 679.
[170] M. Hidaka, T. Eguchi, I. Yamada, *J. Phys. Soc. Jpn.* **1998**, *67*, 2488.
[171] A. I. Popov, Yu. M. Kiselev, *Russ. J. Inorg. Chem. Engl. Transl.* **1988**, *33*, 1307.
[172] M. Kaneko, G. Kubawara, A. Misu, *Solid State Commun.* **1976**, *18*, 1085.
[173] A compressed octahedral geometry is often adopted by $Cu^{II}$ and $Ag^{II}$ in host fluoride lattices (lattice strain often dominates over Jahn–Teller effect).
[174] "FCu[$AuF_4$], an Unusual Copper(II) Fluoroaurate(III)": B. G. Müller, *Angew. Chem*. **1987**, *99*, 685; *Angew. Chem. Int. Ed. Engl.* **1987**, *26*, 688.
[175] T. Fleischer, R. Hoppe, *Z. Anorg. Allg. Chem.* **1982**, *492*, 76.
[176] Several compounds of $Ag^{III}$ with organic ligands are known: $Ag^{III}$ octaethylporphyrin perchlorate a) D. Karweik, N. Winograd, D. G. Davis, K. M. Kadish, *J. Am. Chem. Soc.* **1974**, *96*, 591; [Ag(ttp)], ttp = tetratolylporphyrin; b) J.-L. Du, G. R. Eaton, S. S. Eaton, *J. Magn. Reson. A* **1996**, *119*, 240; $[Ag(py)_4(NCMe)](MoF_6)_3$ and $[Ag(py)_2(NCMe)_3](UF_6)_3$ c) J. Iqbal, D. W. A. Sharp, J. M. Winfield, *J. Chem. Soc. Dalton Trans.* **1989**, 461; and $Ag(CF_3)_3 \cdot CH_3CN$ d) D. Naumann, W. Tyrra, F. Trinius, W. Wessel, T. Roy, *J. Fluorine Chem.* **2000**, *101*, 131. Unfortunately, the structures of these compounds have not been determined. There are also many compounds of $Au^{III}$ with organic ligands; see for example: e) S. Komiya, S. Meguro, A. Shibue, S. Ozaki, *J. Organomet. Chem.* **1987**, *328*, C40.
[177] An oxoaurate [$AuO_4$] unit occurs for example in $M^{II}Au^{III}[Au^{III}O_4]$, M = Ca, Sr, Ba, see: a) G. Krämer, M. Jansen, *J. Solid State Chem.* **1995**, *118*, 247; b) J.-H. Park, J. B. Parise, *Chem. Mater.* **1995**, *7*, 1055; in $Bi_2AuO_5$ and $Bi_4AuO_9$: c) J. Geb, M. Jansen, *J. Solid State Chem.* **1996**, *122*, 364; in $LnAu_2O_9$ (Ln = Nd, Gd): d) C. Steiner, M. Andratschke, K.-J. Range, *Z. Naturforsch. B* **1996**, *51*, 811; and in interesting $La_4LiAuO_8$, which crystallizes in the $Nd_2CuO_4$ structure: e) W. Pietzuch, S. A. Warda, W. Massa, D. Reinen, *Z. Anorg. Allg. Chem*. **2000**, *626*, 113.
[178] B. G. Müller, *Z. Anorg. Allg. Chem*. **1987**, *553*, 196.
[179] a) P. Gómez-Romero, E. M. Tejada-Rosales, M. Rosa Palacín, *Angew. Chem.* **1999**, *111*, 544; *Angew. Chem. Int. Ed.* **1999**, *38*, 524; b) J. Köhler, *Nachr. Chem.* **2000**, *48*, 254.
[180] See three excellent papers on crystal and electronic structure of oxocuprates: a) H. Müller-Buschbaum, *Angew. Chem.* **1989**, *101*, 1503; *Angew. Chem. Int. Ed. Engl.* **1989**, *28*, 1472; b) B. Raveau, M. Hervieu, C. Michel, D. Groult, J. Provost, *Eur. J. Solid State Inorg. Chem.* **1990**, *27*, 25; c) J. K. Burdett, G. V. Kulkarni, *Phys. Rev. B* **1989**, *40*, 8908.
[181] As a referee correctly reminds us, there are some differences between $O^{2-}$ and $F^-$ ions with respect to their capability to transport charges. Linear bridges, a probable prerequisite for the electron delocalization required for superconductivity, are much more frequent in oxides than in fluorides.
[182] See also the excellent review on bonding in crystals containing 1D bridged and unbridged Group 11 and 12 linear, zigzag, and helical chains: C. X. Cui, M. Kertesz, *Inorg. Chem.* **1990**, *29*, 2568.
[183] J. K. Burdett, S. Serov, *J. Am. Chem. Soc.* **1995**, *117*, 12788.
[184] K.-T. Park, D. L. Novikov, V. A. Gubanov, A. J. Freeman, *Phys. Rev. B* **1994**, *49*, 4425.
[185] L. H. Tjeng, M. B. J. Meinders, J. van Elp, J. Ghijsen, G. A. Savatzky, R. L. Johnson, *Phys. Rev. B* **1990**, *41*, 3190.
[186] M. T. Czyzyk, R. A. de Groot, G. Dalba, P. Fornasini, A. Kiesiel, F. Rocca, E. Burattini, *Phys. Rev. B* **1989**, *39*, 9831.
[187] A. Deb, A. K. Chatterjee, *J. Phys. Condens. Matter* **1998**, *10*, 11719.
[188] K. Heidebrecht, M. Jansen, S. Krause, A. M. Bradshaw, *J. Solid State Chem.* **1990**, *89*, 60.
[189] D. Vogel, P. Krüger, J. Pollmann, *Phys. Rev. B* **1998**, *58*, 3865.
[190] T. Kawamoto, N. Suzuki, *J. Phys. Soc. Jpn.* **1997**, *66*, 2487.
[191] Z. Hu, G. Kaindl, S. A. Warda, D. Reinen, F. M. F. de Groot, B. G. Müller, *Chem. Phys.* **1998**, *232*, 63.
[192] R. Zimmermann, P. Steiner, R. Claessen, F. Reinert, S. Hufner, P. Dufek, *J. Phys. Condens. Matter* **1999**, *11*, 1657.
[193] R. Zimmermann, P. Steiner, R. Claessen, F. Reinert, S. Hufner, *J. Electron Spectrosc. Relat. Phenom.* **1998**, *96*, 179.

[194] J. C. Parlebas, M. A. Khan, T. Uozumi, K. Okada, A. Kotani, *J. Electron Spectrosc. Relat. Phenom.* **1995**, *71*, 117.
[195] a) G. Keindl, O. Strebel, O. Kolodziejczyk, A. Schäfers, W. Kiems, R. Lösch, S. Kemmler-Sack, R. Hoppe, H. P. Müller, D. Kissel, *Physica B* **1989**, *158*, 446; b) T. Mizokawa, H. Nataname, K. Fujimori, H. Akeyama, H. Kondoh, H. Hurada, N. Kosugi, *Phys. Rev. Lett.* **1991**, *67*, 1638.
[196] S. Kim, R. S. Williams, *Phys. Rev. B* **1987**, *35*, 2823.
[197] H.-C. Hsueh, J. R. Maclean, G. Y. Guo, M.-H. Lee, S. J. Clark, G. J. Ackland, J. Crain, *Phys. Rev. B* **1995**, *51*, 12216.
[198] C. R. Aita, N. C. Tran, *J. Vac. Sci. Technol. A* **1991**, *9*, 1498.
[199] T. Ishii, R. Sekine, T. Enoki, E. Miyazaki, T. Miyamae, T. Miyazaki, *J. Phys. Soc. Jpn.* **1997**, *66*, 3424.
[200] A. P. Wilkinson, L. K. Templeton, D. H. Templeton, *J. Solid State Chem.* **1995**, *118*, 383.
[201] J. Zaanen, G. A. Sawatzky, J. W. Allen, *Phys. Rev. Lett.* **1985**, *55*, 418.
[202] The energy of Au(d) levels is very strongly influenced by relativistic effects; it may even happen that the d orbitals of Au are *above* the d orbitals of Ag (in a certain oxidation state).
[203] Y.-Q. Zheng, H. Borrmann, Y. Grin, K. Peters, H. G. von Schnering, *Z. Anorg. Allg. Chem*. **1999**, *625*, 2115.
[204] G. M. Lucier, C. Shen, S. H. Elder, N. Bartlett, *Inorg. Chem.* **1998**, *37*, 3829.
[205] For details of thermal decomposition, see Table 3 in ref. [92].
[206] J. Bardeen, L. N. Cooper, J. R. Schrieffer, *Phys. Rev.* **1957**, *108*, 175.
[207] In principle, "BCS theory lacks material aspect".[207b] There has been much effort to translate BCS predictions to chemical language. We note here the work of three groups with a chemical and physical orientation: a) K. A. Müller in *Phase Separation in Cuprate Superconductors, Proceedings* (Eds.: E. Sigmund, K. A. Müller), Springer, Berlin, **1993**, p. 1; b) A. Simon, *Angew. Chem.* **1997**, *109*, 1879; *Angew. Chem. Int. Ed. Engl.* **1997**, *36*, 1788; c) A. W. Sleight, *Acc. Chem. Res.* **1995**, *28*, 103.
[208] The largest values of the Ag–F stretching frequencies are about 650 $cm^{-1}$ for $Ag^{V}$, 600 $cm^{-1}$ for $Ag^{III}$, 450 $cm^{-1}$ for $Ag^{II}$, and about 170–320 $cm^{-1}$ for $Ag^{I}$ compounds, thus uniformly dropping with decrease of formal oxidation state of silver. See a) R. A. Nyquist, R. O. Kagel, *Infrared Spectra of Inorganic Compounds*, Academic Press, New York, **1971**, p. 362; b) S. Milicev, *Croat. Chim. Acta* **1992**, *65*, 125; c) G. L. Bottger, A. L. Geddes, *J. Chem. Phys.* **1972**, *56*, 3725; and refs. [13] and [205]. The stretching frequency for the AgF molecule (515 $cm^{-1}$) is significantly larger than in $Ag^{I}$ fluorides in the solid state: d) J. Hoeft, F. J. Lovas, E. Tiemann, T. Törring, *Z. Naturforsch. A* **1970**, *25*, 35. The largest Cu–O stretching frequencies for oxocuprate superconductors ("oxygen modes") are typically about 580–630 $cm^{-1}$ see, for example e) F. Gervais, R. Lobo, *Z. Phys. B* **1997**, *104*, 681; f) N. Watanabe, N. Koshizuka, *Eur. Phys. J. B* **2000**, *15*, 29; g) B. Roughani, L. C. Sengupta, S. Sundaram, W. C. H. Joiner, *Z. Phys. B* **1992**, *86*, 3.
[209] Usually, an increase in covalency induces an increase of the vibronic coupling constant. However, examples are known when a decrease of covalency is connected with increase of vibronic coupling: a) J. A. Aramburu, M. Moreno, K. Doclo, C. Daul, M. T. Barriuso, *J. Chem. Phys.* **1999**, *110*, 1497; b) J. A. Aramburu, M. T. Barriuso, M. Moreno, *J. Phys. Condens. Matter* **1996**, *8*, 6901. This fact is rationalized in a simple model: c) K. Wissing, M. T. Barriuso, J. A. Aramburu, M. Moreno, *J. Chem. Phys.* **1999**, *111*, 10217. We have not computed the electron–phonon coupling constant for Ag–F systems; for that exact calculations of the phonon spectrum would be required, and this is beyond our capabilities.
[210] The $T_C$ values are taken in part from the Beilstein inorganic compounds database: a) Beilstein Information, vers. 4.0 (Build 11), Copyright© 1995–1998 Beilstein Informationssystems GmbH. We also used b) C. N. R. Rao, B. Raveau, *Transition Metal Oxides*, *2nd ed.*, Wiley, New York, **1998**.
[211] The metallic character of $AgF_2$ computed here might be erroneous because of the nonpolarized spin-character of our calculations ($AgF_2$ is a spin-canted ferromagnet). For example, metallic character is obtained for $CaCuO_2$ in nonpolarized spin calculations, contrary to experiment (R. V. Kasowski, S.-I. Hatta, W. Y. Hsu, *Solid State Commun.* **1993**, *85*, 837).
[212] a) J. A. Aramburu, M. Moreno, M. T. Barriuso, *J. Phys. Condens. Matter* **1992**, *4*, 9089; b) R. Valiente, J. A. Aramburu, M. T. Barriuso, M. Moreno, *J. Phys. Condens. Matter* **1994**, *6*, 4515; c) R. Valiente, J. A. Aramburu, M. T. Barriuso, M. Moreno, *Internat. J. Quant. Chem.* **1994**, *52*, 1051.
[213] $T_C = 166$ K (−111 °C) at elevated pressure (L. Gao, Y. Y. Xue, F. Chen, Q. Ziong, R. L. Meng, D. Ramirez, C. W. Chu, J. H. Eggert, H. K. Mao, *Phys. Rev. B* **1994**, *50*, 4260). Since 1994 this 1223 compound holds the world record of critical superconducting temperature.
[214] a) A. Schilling, O. Jeandupeux, J. D. Guo, H. R. Ott, *Physica C* **1993**, *216*, 6; b) C. W. Chu, L. Gao, F. Chen, Z. J. Huang, R. L. Meng, Y. Y. Xue, *Nature* **1993**, *365*, 323; c) C. W. Chu, *IEEE Trans. Appl. Supercond.* **1997**, *7*, 80.
[215] J. Yu, S. Massidda, A. J. Freeman, *Physica C* **1988**, *152*, 273.
[216] D. L. Novikov, V. A. Gubanov, A. J. Freeman, *Physica C* **1993**, *210*, 301.
[217] S. N. Putilin, E. V. Antipov, O. Chmaissen, M. Marezio, *Nature* **1993**, *326*, 226.
[218] P. Strange, J. M. F. Gunn, *J. Phys. Condens. Matter* **1989**, *1*, 6843.
[219] T. Jarlborg, *Solid State Commun.* **1988**, *67*, 297; Compare also: B. Szpunar, V. H. Smith, Jr., *Phys. Rev. B* **1988**, *37*, 7525.
[220] D. Bhattacharya, D. K. Pandya, S. C. Kashyap, L. C. Pathak, S. Mishra, D. Sen, K. L. Chopra, *Physica C* **1990**, *170*, 245.
[221] D. L. Novikov, V. A. Gubanov, A. J. Freeman, *Physica C* **1993**, *210*, 301. Also compare to: H. Wu, Q. Zheng, X. Gong, H. Q. Lin, *J. Phys. Condens. Matter* **1999**, *11*, 4637.
[222] Y. Shimakawa, J. D. Jorgensen, J. F. Mitchell, B. A. Hunter, H. Shaked, D. G. Hinks, R. L. Hitterman, *Physica C* **1994**, *228*, 73.
[223] W. J. Yu, Z. Q. Mao, X. M. Liu, M. L. Tian, G. E. Zhou, Y. H. Zhang, *Physica C* **1996**, *261*, 27.
[224] K. Takegahara, H. Harima, A. Yanase, *Jpn. J. Appl. Phys.* **1987**, *26*, L352.
[225] D. Reefman, F. J. M. Benschop, H. B. Brom, R. A. de Groot, J. M. van Ruitenbeek, *Physica C* **1992**, *201*, 119.
[226] A Ta analogue of this Nb compound, $Nd_{2-x}Ce_xSr_2Cu_2TaO_{10}$, is also superconducting for $x = 0.5$ with $T_C = 28$ K.
[227] L. F. Mattheiss, *Phys. Rev. B* **1992**, *46*, 11171.
[228] Y. Tokura, H. Tagaki, S. Uchida, *Nature* **1989**, *337*, 345.
[229] a) L. F. Mattheiß, D. R. Hamann, *Phys. Rev. Lett.* **1988**, *60*, 2681; b) R. J. Cava, B. Batlogg, J. J. Krajewski, R. Farrow, L. W. Rupp, A. E. White, K. Short, W. F. Peck, T. Kometani, *Nature* **1988**, *332*, 814. Numerical data taken from ref. [80a].
[230] G. K. Wertheim, J. P. Remeika, D. N. E. Buchanan, *Phys. Rev. B* **1982**, *26*, 2120.
[231] H. Fukuoka, T. Isami, S. Yamanaka, *Chem. Lett.* **1997**, *8*, 703.
[232] J. P. Julien, D. A. Papaconstantopoulos, F. Cyrot-Lackmann, A. Pasturel, *Phys. Rev. B* **1991**, *43*, 2903.
[233] M. Robin, K. Andres, T. H. Geballe, N. A. Kuebler, D. B. McWhan, *Phys. Rev. Lett.* **1966**, *17*, 917.
[234] There is evidence for unique triplet Cooper pairs in this compound.
[235] T. Oguchi, *Phys. Rev. B* **1995**, *51*, 1385.
[236] $Rb_2CsC_{60}$ with $T_C = 33–35$ K holds the $T_C$ record among fullerides. Values of $T_C = 40$ K for $Cs_3C_{60}$ (a) T. T. M. Palstra, O. Zhou, Y. Iwasa, P. E. Sulewski, R. M. Fleming, B. R. Zegarski, *Solid State Commun.* **1995**, *93*, 327) and $T_C = 45$ K for $Tl_{2.2}Rb_{2.7}C_{60}$ (b) Z. Iqbal, R. H. Baughman, B. L. Ramakrishna, S. Khare, N. S. Murthy, H. J. Bornemann, D. E. Morris, *Science* **1991**, *254*, 826) have not been confirmed.
[237] a) R. C. Haddon, *Acc. Chem. Res.* **1992**, *25*, 127; b) O. Zhou, D. Cox, *J. Phys. Chem. Solids* **1992**, *53*, 11.
[238] S. Yamanaka, H. Kawaji, K. Hotehama, M. Ohashi, *Adv. Mater.* **1996**, *8*, 771.
[239] a) S. Yamanaka, K.-I. Hotehama, H. Kawaji, *Nature* **1998**, *392*, 580; b) S. Yamanaka, *Annu. Rev. Mater. Sci.* **2000**, *30*, 53.
[240] L. F. Mattheiß, L. R. Testardi, W. W. Yao, *Phys. Rev. B* **1978**, *17*, 4640.
[241] B. M. Klein, L. L. Boyer, D. A. Papaconstantopoulos, L. F. Mattheiß, *Phys. Rev. B* **1978**, *18*, 6411.
[242] M.-Z. Huang, Y.-N. Xu, W. Y. Ching, *J. Chem. Phys.* **1992**, *96*, 1648.
[243] D. L. Novikov, V. A. Gubanov, A. J. Freeman, *Physica C* **1992**, *191*, 399.
[244] Value under high pressure. This is the largest $T_c$ value among the pure elements.
[245] S. P. Rudin, A. Y. Liu, *Phys. Rev. Lett.* **1999**, *83*, 3049, and refs therein.

[246] L. F. Mattheiß, *Phys. Rev. B* **1994**, *49*, 13279.
[247] J. I. Lee, T. S. Zhao, I. G. Kim, B. I. Min, S. J. Youn, *Phys. Rev. B* **1994**, *50*, 4030.
[248] a) H. Kawaji, K. Hotehama, S. Yamanaka, *Chem. Mater.* **1997**, *9*, 2127; b) S. Ya. Istomin, J. Köhler, A. Simon, *Physica C* **1999**, *319*, 219; c) I. Hase, Y. Nishihara, *Phys. Rev. B* **1999**, *60*, 1573.
[249] The largest $T_C$ among organic charge-transfer complexes.
[250] J. Lu, L. Zhang, *Solid State Commun.* **1998**, *105*, 99, and refs therein.
[251] a) V. Balbarin, R. B. Van Dover, F. J. Disalvo, *J. Phys. Chem. Solids* **1996**, *57*, 1919; b) H. Smolinski, W. Weber, *Z. Phys. B* **1997**, *104*, 741.
[252] D. A. Papaconstantopoulos, L. L. Boyer, B. M. Klein, A. R. Williams, V. L. Moruzzi, J. F. Janak, *Phys. Rev. B* **1977**, *15*, 4221.
[253] T. Jarlborg, A. J. Freeman, *Phys. Rev. B* **1980**, *22*, 2332.
[254] S. Yamanaka, E. Enishi, H. Fukuoka, M. Yasukawa, *Inorg. Chem.* **2000**, *39*, 56.
[255] D. H. Gregory, M. G. Baker, P. P. Edwards, M. Slaski, D. J. Siddons, *J. Solid State Chem.* **1998**, *137*, 62.
[256] K. Ahn, B. J. Gibson, R. K. Kremer, H. Mattausch, A. Stolovits, A. Simon, *J. Phys. Chem. B* **1999**, *103*, 5446.
[257] T. F. Fässler, S. Hoffmann, *Z. Anorg. Allg. Chem.* **2000**, *626*, 106.
[258] H. Kamerlingh-Onnes, *Commun. Phys. Lab. Univ. Leiden Suppl.* **1913**, *34*.
[259] a) J. H. Schön, Ch. Kloc, B. Batlogg, *Nature* **2000**, *406*, 702; b) P. Phillips, *Nature* **2000**, *406*, 687.
[260] R. Schumann, M. Richter, L. Steinbeck, H. Eschrig, *Phys. Rev. B* **1995**, *52*, 8801.
[261] M. I. Eremets, K. Shimizu, T. C. Kobayashi, K. Amaya, *J. Phys. Condens. Matter* **1998**, *10*, 11519.
[262] T. Inoshita, Y. Nishihara, *Phys. Rev. B* **1998**, *58*, R1707.
[263] C. K. Jørgensen, *Mol. Phys.* **1959**, *2*, 309.
[264] H. So, M. T. Pope, *Inorg. Chem.* **1972**, *11*, 1441.
[265] A. K. Bridson, J. H. Holloway, E. G. Hope, P. J. Townson, W. Levason, J. S. Ogden, *J. Chem. Soc. Dalton Trans.* **1991**, 3127.
[266] The electronegativity of $Ag^{II}$ is so large that an unpaired electron resides more on the ligands than on the metal in $[AgCl_6]^{4-}$ (M:L = 45:58) and $[AgBr_6]^{4-}$ ions (30:70). See SCCEH results in ref. [212c].
[267] a) *Phase Separation in Cuprate Superconductors* (Eds.: E. Sigmund, K. A. Müller), Springer, Berlin, **1993**; b) R. S. Markiewicz, *Physica C* **1989**, *162–164*, 215.
[268] In looking at the literature we have found that $Tl^{II}$ (very rare because of its tendency to disproportionation) introduces holes into a $Cl^-$ band, just like $Ag^{II}$ centers do (see: a) U. Rogulis, J.-M. Spaeth, I. Cabria, J. A. Aramburu, M. T. Barriuso, *J. Phys. Condens. Matter* **1998**, *10*, 6473; b) I. Cabria, M. Moreno, J. A. Aramburu, M. T. Barriuso, U. Rogulis, J.-M. Spaeth, *J. Phys. Condens. Matter* **1998**, *10*, 6481). It should not be then excluded that $Tl^{III}$ would be able to oxidize $F^-$ ions, just like $Ag^{III}$. However, OEN of $Tl^{II}$ (2.1) is much smaller than that of $Ag^{II}$ (2.8); and the redox potential of the $Tl^{III}/Tl^{I}$ redox pair is less positive by about 0.8 V from that of the $Ag^{II}/Ag^{I}$: c) A. F. Clifford, W. D. Pardieck, M. W. Wadley, *J. Phys. Chem.* **1966**, *70*, 3241.
[269] A. C. Gossard, D. K. Hindermann, M. B. Robin, N. A. Kuebler, T. H. Geballe, *J. Am. Chem. Soc.* **1967**, *89*, 7121.
[270] W. S. Graaf, H. H. Stadelmeier, *J. Electrochem. Soc.* **1958**, *105*, 446.
[271] J. A. McMillan, *Chem. Rev.* **1962**, *62*, 65.
[272] a) M. B. Robin, K. Andres, T. H. Geballe, N. A. Kuebler, D. B. McWhan, *Phys. Rev. Lett.* **1966**, *17*, 917; b) K. Andres, N. A. Kuebler, M. B. Robin, *J. Phys. Chem. Solids* **1966**, *27*, 1747.
[273] A. B. Neiding, I. A. Kazarnovskii, *Dokl. Akad. Nauk. SSSR* **1951**, *78*, 713.
[274] M. Jansen, S. Vensky, *Z. Naturforsch. B* **2000**, *55*, 882.
[275] There are also other conducting Ag–O cluster compounds, such as $Ag[Ag_3O_4]_2[NO_3]$. See for example: B. E. Breyfogle, R. J. Phillips, J. A. Switzer, *Chem. Mater.* **1992**, *4*, 1356.
[276] Several other Ag-containing superconductors are known, for example: LaAg alloy with $T_C = 1.1$ K a) J. S. Schilling, S. Methfessel, R. N. Shelton, *Solid State Commun.* **1977**, *24*, 659; b) organic $[et]_2Ag[CF_3]_4[tce]$ (et = bis(ethylenedithio)tetrathiafulvalene, tce = 1,1,2-trichloroethane) with $T_C = 11.1$ K, J. A. Schlueter, K. D. Carlson, U. Geiser, H. H. Wang, J. M. Williams, W. K. Kwok, J. A. Fendrich, U. Welp, P. M. Keane, J. D. Dudek, A. S. Komosa, D. Naumann, T. Roy, J. E. Schirber, W. R. Bayles, B. Dodrill, *Physica C* **1994**, *233*, 379; and many Ag-doped oxocuprates, e.g. $Bi_{1.6}Pb_{0.4}Sr_2Ca_3(Cu_{1-x}Ag_x)_4O_{12+x}$: c) J. E. Rodriguez, A. Marino, *Phys. Rev. B* **1999**, *60*, 9845. There is also a large family of halogen- (including fluorine-) doped cuprates, e.g. d) M. Al-Mamouri, P. P. Edwards, C. Greaves, M. Slaski, *Nature* **1994**, *369*, 382; e) I.-G. Chen, S. Sen, D. M. Stefanescu, *Appl. Phys. Lett.* **1988**, *52*, 1355; f) S. D'Arco, M. S. Islam, *Phys. Rev. B* **1997**, *55*, 3141; g) S. Adachi, T. Tatsuki, T. Kamura, K. Tanabe, *Chem. Mater.* **1998**, *10*, 2860).
[277] a) J. K. Burdett, *Inorg. Chem.* **1993**, *32*, 3915. It is significant that avoided crossing seems to be important for such different superconducting materials as oxocuprates and samarium sulphide SmS: b) C. M. Varma, *Rev. Mod. Phys.* **1976**, *48*, 218. Independent calculations confirm the hypothesis of dual character of the wavefunction for oxobismuthates, as well: c) N. C. Pyper, P. P. Edwards in *Polarons and Bipolarons in High-$T_C$ Superconductors and Related Materials* (Eds.: E. K. H. Salje, A. S. Alexandrov, W. Y. Liang), Cambridge University Press, Cambridge, **1995**.
[278] The phenomenon of multiple charge-transfer excitation is a source of "valence tautomerism",[165] and of the "mnemon effect". For the latter see: a) L. Z. Stolarczyk, L. Piela, *Chem. Phys.* **1984**, *85*, 451; b) N. Guihery, G. Durand, M.-B. Lepetit, J.-P. Malrieu, *Chem. Phys.* **1994**, *183*, 61; c) Y. Toyozawa in *Relaxations of Excited States and Photo-Induced Structural Phase Transitions* (Ed.: K. Nasu), Springer, Berlin, **1997**, p. 17.
[279] S. Ernst, V. Kasack, W. Kaim, *Inorg. Chem.* **1988**, *27*, 1146.
[280] Note here some similarity of Burdett's approach to a "resonance" formalism, used by the "resonating valence bond" theory of superconductivity in the solid state: a) P. W. Anderson, *Science* **1987**, *235*, 1196; b) P. W. Anderson, G. Baskaran, Z. Zou, T. Hsu, *Phys. Rev. Lett.* **1987**, *58*, 2790; c) G. Baskaran, Z. Zou, P. W. Anderson, *Solid State Commun.* **1987**, *63*, 2790.
[281] Much attention has been paid to the role of peroxide anions (generated presumably in the process: $2O^{-\bullet} \rightarrow O_2^{2-}$) for superconductivity. See e.g. a) G. Tavčar, B. Ogorevč, V. Hudnik, S. Pejovnik, *Physica C* **1991**, *175*, 607; b) J.-H. Choy, D.-Y. Jung, S.-J. Kim, Q. W. Choi, G. Damazeau, *Physica C* **1991**, *185–189*, 763; and a recent discussion: c) A. R. Anderson, Murakami, G. J. Russell, *Physica C* **2000**, *334*, 229.
[282] See also an interesting article on symmetry breaking: H. Genz, *Interdiscip. Sci. Rev.* **1999**, *24*, 129.
[283] H. Tajima, M. Inokuchi, S. Ikeda, M. Arifuku, T. Naito, M. Tamura, T. Ohta, A. Kobayashi, R. Kato, H. Kobayashi, H. Kuroda, *Synth. Met.* **1995**, *70*, 1035.
[284] D. L. DeLaet, D. R. Powell, C. P. Kubiak, *Organometallics* **1985**, *4*, 954.
[285] R. D. Feltham, G. Elbaze, R. Ortega, C. Eck, J. Dubrawski, *Inorg. Chem.* **1985**, *24*, 1503.
[286] A. M. Bradford, E. Kristof, M. Rashidi, D.-S. Yang, N. C. Payne, R. J. Puddephatt, *Inorg. Chem.* **1994**, *33*, 2355.
[287] M. Ganesan, S. S. Krishnamurthy, M. Nethaji, *J. Organomet. Chem.* **1988**, *570*, 247.
[288] J. A. Jenkins, M. Cowie, *Organometallics* **1992**, *11*, 2767.
[289] B. R. Sutherland, M. Cowie, *Organometallics* **1985**, *4*, 1637.
[290] P. Sharrock, M. Melnik, *Can. J. Chem.* **1985**, *63*, 52.
[291] F. Valach, M. Tokarcik, T. Maris, D. J. Watkin, C. K. Prout, *Z. Kristallogr.* **2000**, *215*, 56.
[292] For example $CsAuCl_3$ is disproportionated to $Au^{I}$ and $Au^{III}$ a) N. Elliott, L. Pauling, *J. Am. Chem. Soc.* **1938**, *60*, 1846, and may be metallized at an external pressure of 60 kB b) R. Keller, J. Fenner, W. B. Holzapfek, *Mater. Res. Bull.* **1974**, *9*, 1664; c) P. Day, C. Vettier, G. Parisot, *Inorg. Chem.* **1978**, *17*, 2319.
[293] On coexistence of CDW (charge density wave), SDW (spin density wave), and superconductivity, see, for example: a) H. Tajima, M. Inokuchi, S. Ikeda, M. Arifuku, T. Naito, M. Tamura, T. Ohta, A. Kobayashi, R. Kato, H. Kobayashi, H. Kuroda, *Synth. Met.* **1995**, *70*, 1035; b) C.-H. Du, W. J. Lin, Y. Su, B. K. Tanner, P. D. Hatton, D. Casa, B. Keimer, J. P. Hill, C. S. Oglesby, H. Hohl, *J. Phys. Condens. Matter* **2000**, *12*, 5361. On CDW for underdoped cuprates see: c) A. Mourachkine, *Supercond. Sci. Technol.* **2000**, *13*, 1378.
[294] $AgF_2$, a ferromagnet with Curie temperature of 163 K, also exhibits the strongest antiferromagnetic coupling among $Ag^{II}$ compounds. Isoelectronic and isostructural $CuF_2$ has a Curie temperature of 69 K.

[295] Interestingly, the order of the $T_N$ versus size of cationic dopant M is reversed for $MAgF_3$ and $M_2AgF_4$ compounds, M = K, Rb, Cs.

[296] In fact, the statistics of Cooper pairs differ from those of bosons.

[297] Bednorz and Müller refer to the Jahn–Teller effect as a possible mechanism responsible for the enhancement of the critical superconducting temperature a) J. G. Bednorz, K. A. Müller, *Z. Phys. B* **1986**, *64*, 189. Considerations based on Jahn–Teller and pseudo Jahn–Teller effect have been applied to many charge-transfer processes in condensed media, see e.g.: b) J. Ulstrup in *Lecture Notes in Chemistry, Vol. 10* (Eds.: G. Berthier, M. J. S. Dewar, H. Fisher, K. Fukui, H. Hartmann, H. H. Jaffe, J. Jortner, W. Kutzelnigg, K. Ruedenberg, E. Scrocco, W. Zeil), Springer, Berlin, **1979**; c) H. E. M. Christensen, L. S. Conrad, J. M. Hammerstadt-Pedersen, J. Ulstrup in *Condensed Matter Physics Aspects of Electrochemistry (*Eds.: M. P. Tosi, A. A. Kornyshev), World Scientific, Singapore, **1991**; d) H. A. Jahn, E. Teller, *Proc. R. Soc. London Ser. A* **1937**, *161*, 220; e) I. B. Bersuker, *The Jahn-Teller Effect and Vibronic Interactions in Modern Chemistry*, Plenum, New York, **1984**; f) R. Englman, *The Jahn-Teller Effect*, Wiley, New York, **1972**; g) M. K. Grover, R. Silbey, *J. Chem. Phys.* **1970**, *52*, 2099). Similar thinking is widespread nowadays in the literature on superconductivity, too; see e.g.: h) A. Calles, J. R. Soto, J. J. Castro, E. Yépez, *Physica C* **1997**, *282–287*, 1623; i) L. R. Falvello, *J. Chem. Soc. Dalton Trans.* **1997**, 4463; j) D. Reinen, H. O. Wellern, J. Wegwerth, *Z. Phys. B* **1997**, *104*, 595.

[298] On the actual importance of vibronic (and generally lattice–electron coupling) effects for superconductivity see: 1) oxocuprates: a) A. S. Alexandrov, P. Edwards, *Physica C* **2000**, *33*, 97 and refs therein; b) J. K. Burdett, G. V. Kulkarni, *Phys. Rev. B* **1989**, *40*, 8908; c) T. Jarlborg, *Solid State Commun.* **1988**, *67*, 297; 2) oxobismuthates: d) V. Meregalli, S. Y. Savrasov, *Phys. Rev. B* **1998**, *57*, 14453; e) O. Navarro, E. Chavira, *Physica C* **1997**, *282–287*, 1825; f) M. Shirai, N. Suzuki, K. Motizuki, *J. Phys. Condens. Matter* **1990**, *2*, 3553; 3) fullerides: g) M. Schluter, M. Lanoo, M. Needels, G. A. Baraff, D. Tomanek, *Phys. Rev. Lett.* **1992**, *68*, 526; h) R. A. Jishi, M. S. Dresselhaus, *Phys. Rev. B* **1992**, *45*, 2579; i) D. L. Novikov, V. A. Gubanov, A. J. Freeman, *Physica C* **1992**, *191*, 399; j) V. Z. Kresin, *Phys. Rev. B* **1992**, *46*, 14883; k) Y. Asai, Y. Kawaguchi, *Phys. Rev. B* **1992**, *46*, 1265; l) R. Rai, *Z. Phys. B* **1996**, *99*, 327; 4) silicide clathrates: m) K. Yoshizawa, T. Kato, T. Yamabe, *J. Chem. Phys.* **1998**, *108*, 7637; n) K. Yoshizawa, T. Kato, M. Tachibana, T. Yamabe, *J. Phys. Chem. A* **1998**, *102*, 10113; 5) borocarbides: o) F. Gompf, W. Reichardt, H. Schober, B, Renker, M. Buchgeister, *Phys. Rev. B* **1997**, *55*, 9058; 6) mercury fluoroarsenates: p) J. J. M. Slot, M. Boon, M. Weger, *Solid State Commun.* **1985**, *56*, 645. On the accuracy of BCS predictions in different classes of superconductors see: r) B. Chakraverty, T. Ramakrishnan, *Physica C* **1997**, *282–287*, 290.

[299] On the theory of vibronic coupling see: a) G. Herzberg, E. Teller, *Z. Phys. Chem. B* **1933**, *21*, 410; b) G. Herzberg, H. C. Longuet-Higgins, *Discuss. Faraday Soc.* **1963**, *35*, 77; c) H. C. Longuet-Higgins, *Proc. R. Soc. London Ser. A* **1975**, *344*, 147; d) W. Siebrand, M. Zgierski in *Excited States*, *Vol. 4* (Ed.: E. C. Lim), **1979**; e) G. Herzberg, *Molecular Spectra and Molecular Structure*, *Vol. 3*, Van Nostrand Reinhold, New York, **1966**; f) G. Fischer, *Vibronic Coupling*, Academic Press, London, **1984**; g) H. Köppel, L. S. Cederbaum, W. Domcke, *J. Chem. Phys.* **1988**, *89*, 2023; h) I. B. Bersuker, V. Z. Polinger, *Vibronic Interactions in Molecules and Crystals* (Ed.: V. I. Goldanskii), Springer, Berlin, **1983**.

[300] Relationship between the dynamic Jahn–Teller effect and superconductivity has been described in: a) D. P. Clougherty, K. H. Johnson, M. E. McHenry, *Physica C* **1989**, *162–164*, 1475. A simple theoretical approach to dynamic band-gap opening in typical low-dimensional metals may be found in: b) M. T. Green, V. Robert, J. K. Burdett, *J. Phys. Chem. B* **1997**, *101*, 10290.

[301] As the reader may note, thinking of superconductivity in connection to a stress introduced into 1D or 2D structures, we are interested mainly in *linear* chains and *nonpuckered* sheets. The obvious reason for that is that kinked chains or puckered sheets are likely to be much less resistant to strain upon introduction of stress, and are of the interest to us only if they return to higher symmetry upon doping. For relationship between $T_C$ and buckling of $CuO_2$ planes in oxocuprates, see: O. Chmaissem, J. D. Jorgensen, S. Short, A. Knizhnik, Y. Eckstein, H. Shaked, *Nature* **1999**, *397*, 45.

[302] Part 1, W. Grochala, R. Konecny, R. Hoffmann, *Chem. Phys.*, submitted.

[303] Part 2, W. Grochala, R. Hoffmann, *New J. Chem.* **2001**, *25*, 108.

[304] Part 3, W. Grochala, R. Hoffmann, *J. Phys. Chem. A* **2000**, *104*, 9740.

[305] Part 4, W. Grochala, R. Hoffmann, *Pol. J. Chem.*, in press.

[306] Part 5, W. Grochala, R. Hoffmann, P. P. Edwards, unpublished results.

[307] Similar language, of a "covalency" approach to superconductivity has been widely used by A. Sleight ref. [207c]. Also Phillips discussed covalence/ionic instabilities as an important factor in superconductivity (J. C. Phillips, *Phys. Rev. Lett.* **1972**, *29*, 1551).

[308] On correlation of antiferromagnetic and superconducting properties, see, for example: a) K. Prassides, A. Lappas, *Chem. Br.* **1994**, 725; b) T. Otsuka, A. Kobayashi, Y. Miyamoto, J. Kiuchi, N. Wada, E. Ojima, H. Fujiwara, H. Kobayashi, *Chem. Lett.* **2000**, 732; c) S. Alam, *Phys. Lett. A* **2000**, *272*, 107. On interpretation of oxobismuthates as doped Peierls insulators see: d) M. J. Rice, Y. R. Wang, *Physica C* **1989**, *157*, 192. On the relationship between ferromagnetism and superconductivity see: e) S. S. Saxena, P. Agarwal, K. Ahilan, F. M. Grosche, R. K. W. Haselwimmer, M. J. Steiner, E. Pugh, I. R. Walker, S. R. Julian, P. Monthoux, G. G. Lonzarich, A. Huxley, I. Sheikin, D. Braithwaite, J. Flouquet, *Nature* **2000**, *406*, 587; f) P. Coleman, *Nature* **2000**, *406*, 580.

[309] L. Jansen, R. Block, *Phys. A* **1999**, *271*, 169.

[310] For the necessity of subtle control of a distance between two metal centers, see the predictions of a simple model we used in ref. [302].

[311] Sometimes a "clipping" dopant may occur in a layer, which does not neighbor directly a $CuO_2$ plane; $Hg^{II}$ in $HgBa_2CuO_{4-\delta}$ is a good example.

[312] The real situation in oxocuprates is, in fact, much more complicated. Both external pressure and chemical substitutions *have* great impact on the $T_C$ of cuprate materials. But "chemical pressure" is *equivalent* to external pressure only for $La_{2-x}(Ba_{1-y}Sr_y)_xCuO_4$, see: M. Marezio, F. Licci, A. Gauzzi, *Physica C* **2000**, *337*, 195.

[313] Instead of introducing anisotropic stress in oxocuprates, see e.g.: a) Kh. A. Ziq, N. M. Hamdan, J. Schirokoff, *Physica C* **1994**, *235–240*, 1217; a method of epitaxial strain may be used to increase $T_C$: b) J.-P. Locquet, J. Perret, J. Fompeyrine, E. Mächler, J. W. Seo, G. van Tendeloo, *Nature* **1998**, *394*, 453. Both methods have their limitations for increasing $T_C$; see: c) L. Jansen, R. Block, *Nature* **1999**, *399*, 114; d) I. K. Schuller, *Nature* **1998**, *394*, 419. Stress may be also applied to increase $T_C$ or to induce superconductivity in initially nonsuperconducting non-oxocuprate materials (see for example: e) D. Agassi, T. K. Chu, *Phys. Status Solidi B* **1990**, *160*, 601; f) W. D. Gill, R. L. Greene, G. B. Street, W. A. Little, *Phys. Rev. Lett.* **1975**, *35*, 1732; g) J. E. Schirber, L. J. Azvedo, J. F. Kwak, E. L. Venturni, P. C. W. Leung, M. A. Beno, H. H. Wang, J. M. Williams, *Phys. Rev. B* **1986**, *33*, 1987; h) C. E. Campos, J. S. Brooks, P. J. M. Van Bentum, J. A. A. J. Perenboom, S. J. Klepper, P. S. Sandhu, S. Valfells, Y. Tanaka, T. Kinoshita, N. Kinoshita, M. Tokumoto, H. Anzai, *Phys. Rev. B* **1995**, *52*, R7014; i) R. Brand, W. W. Webb, *Solid State Commun.* **1969**, *7*, 19.

[314] Indeed, there are *optimal* values of $T_C$ which may be obtained when applying external pressure. For elegant experimental evidence see: a) J. Gopalakrishnan in *Thallium-Based High-Temperature Superconductors* (Eds.: A. M. Herman, J. V. Jakhmi), Marcel Dekker, New York, **1995**, p. 7; b) N. E.Moulton, E.Skeleton in *Thallium-Based High-Temperature Superconductors* (Eds.: A. M. Herman, J. V. Jakhmi), Marcel Dekker, New York, **1995**, p. 437. See also: c) "High-$T_C$ Superconductivity 1996: Ten Years After the Discovery": P. P. Edwards, G. B. Peacock, J. P. Hodges, A. Asab, I. Gameson, *NATO ASI Ser.* **1997**, *343*, 135.

[315] Disproportionated systems most often have larger molar volume than the comproportionated ones. The same feature is expected for disproportionated $Ag^I/Ag^{III}$ fluorides. Note that the average of the $Ag^I$–F and $Ag^{III}$–F bond lengths ($[2.46 + 1.88]/2 = 2.17$ Å) is *larger* than the typical $Ag^{II}$–F bond length (2.07–2.13 Å). Apparently, depopulation of the Ag–F antibonding orbitals ($d^9 \rightarrow d^8$) results in smaller shortening of the Ag–F bond length than elongation of the Ag–F bond length upon population of the Ag–F antibonding orbitals ($d^9 \rightarrow d^{10}$).

[316] A simple approach to lattice effects in conducting perovskite-type oxides may be found in: J. P. Attfiled, *Chem. Mater.* **1998**, *10*, 3239.

[317] Thus, we may easily compute that the best dopants clipping the $AgF_2$ planes (with Ag–F distances of 2.07 – 2.13 Å) should have ionic radii of 1.10 – 1.17 Å. These might be $Ac^{III}$ ($R_{ion} = 1.12$ Å), $Sr^{II}$ ($R_{ion} =$ 1.18 Å), and $Pb^{II}$ ($R_{ion} = 1.19$ Å, if not oxidized to $Pb^{IV}$). $Na^{I}$ ($R_{ion} =$ 1.02 Å), $K^{I}$ and $Ba^{II}$ ($R_{ion} = 1.39$ Å) seem less appropriate. The radii of hypothetically good dopants found in this semiempirical way are much smaller than those satisfying the corresponding condition in the perovskite structure ($R_{ion}^{opt} = 1.74 – 1.82$ Å if we assume $R_{ion}$ ($F^-$) = 1.19 Å, and $R_{ion}^{opt} = 1.57 – 1.65$ Å if we assume $R_{ion}$ ($F^-$) = 1.36 Å see Table 11 in Appendix).

[318] J. Karpinski, H. Schwer, X. Mangelschots, K. Conder, A. Morawski, T. Lada, A. Paszewin, *Physica C* **1994**, *234*, 10. We are not aware of any attempts to synthesize a I/III mixed-valence $Ca_{1-\delta}Na_{\delta}CuO_2$.

[319] Z. Hiroi, M. Takano, M. Azuma, Y. Takeda, *Nature* **1993**, *364*, 315.

[320] N. R. Walker, R. R. Wright, A. J. Stace, *J. Am. Chem. Soc.* **1999**, *121*, 4837.

[321] N. R. Walker, R. R. Wright, P. E. Barran, A. J. Stace, *Organometallics* **1999**, *18*, 3569.

[322] A small force constant for $Ag^{I}$–F stretching is indicated by the relatively broad range of $Ag^{I}$–F separations found in different compounds. For example, $Ag^{I}$–F bond lengths of 2.196 – 2.571 Å are found in $[Ag_2C_2 \cdot 8AgF]$ (G. C. Guo, G. D. Zhou, Q. G. Wang, T. C. W. Mak, *Angew. Chem.* **1998**, *110*, 652; *Angew. Chem. Int. Ed.* **1998**, *37*, 630). The shortest of these distances (2.20 Å) is still longer than a typical $Ag^{II}$–F bond length (2.07 – 2.13 Å).

[323] For example, there are no Ag–F nets in $Ag[SbF_6]$, instead there are isolated $Ag^+$ ions. $Sb^{V}$ is a too strong a F abstracting agent for $Ag^{I}$ to create a 1D $[AgF][SbF_5]$ net. On the other hand, $Ag^{II}$ is also too weak a F abstracting agent to create 1D $[AgF]^+[SnF_5]^-$ or 2D $[AgF_2][SnF_4]$ nets in $Ag^{II}[SnF_6]^{2-}$. Redox potentials and magnetic properties of dopants also have to be taken into account. For example, doping of $Ag^{II}$ compounds with $U^{V}$ usually results in the reaction: $U^{V} + Ag^{II} \rightarrow U^{VI} + Ag^{I}$ (for details, see: P. A. G. O'Hare, J. G. Malm, *J. Chem. Thermodyn.* **1984**, *16*, 753).

[324] For example, Ba levels add to $DOS_F$ in $Ba_6Si_{46}$, a clathrate Si compound, effectively increasing $T_C$ compared to Na compounds. For details, see: S. Saito, A. Oshiyama, *Phys. Rev. B* **1995**, *51*, 2628.

[325] Some IR absorption spectra have been published. See ref. [208] for details.

[326] Four older contributions should be noted here: a) C. Friebel, *Solid State Commun.* **1974**, *15*, 639, b) C. Friebel, D. Reinen, *Z. Anorg. Allg. Chem.* **1975**, *413*, 51; c) G. C. Allen, K. D. Warren, *Inorg. Chem.* **1969**, *8*, 1895; d) G. C. Allen, R. F. McMeeking, *J. Chem. Soc. Dalton Trans.* **1976**, 1063. There are also more recent data on optical spectra of $Ag^{III}$ fluoride complexes: e) A. L. Hector, W. Levason, M. T. Weller, E. G. Hope, *J. Fluorine Chem.* **1997**, *86*, 105.

[327] As far as we know, $^{19}F$ and $^{109}Ag$ NMR spectra have been published so far only for $KAgF_4$ (R. Eujen, B. Žemva, *J. Fluorine Chem.* **1999**, *99*, 139), and for $AgF_2$ (ref. [84c]).

[328] Much information has been collected on ESR and optical spectra of $Ag^{2+}$ ions isolated in fluoride hosts, see for example: a) H. Bill, D. Lovy, H. Hagemann, *Solid State Commun.* **1989**, *70*, 511; b) A. Monnier, A. Gerber, H. Bill, *J. Chem. Phys.* **1991**, *94*, 5891; c) E. Minner, D. Lovy, H. Bill, *J. Chem. Phys.* **1993**, *99*, 6378; d) D. C. Von Hoene, Dissertation, University of Cincinnati (USA), **1968**; e) M. V. Eremin, V. A. Ulanov, M. M. Zaripov, *Appl. Magn. Reson.* **1998**, *14*, 435; f) P. Bautinaud, A. Monnier, D. Lovy, H. Bill, *J. Phys. Chem. Solids* **2000**, *61*, 1663, and ref. [212]. There is also data for $Ag^{2+}$ ions in other hosts, e.g. $KNO_3$: g) K. Chandrasekharan, V. S. Murty, *Physica B* **1995**, *205*, 349; $CdCl_2$ and $CdBr_2$: h) T. Miyanaga, *J. Phys. Soc. Jpn.* **1979**, *46*, 167.

[329] Electric resistance measurements in these substances may be very difficult, because even the surface of solid Au rods might be oxidized by the sample measured, as pointed out in ref. [14].

[330] B. G. Levi, *Phys. Today* **1996**, *49*, 17.

[331] There has been much discussion on one-dimensionality in oxocuprates. It appears that there are 1D "charge stripes" in the electronic structure of the $CuO_2$ planes a) J. Zaanen, *Science* **1999**, *286*, 251). There are also 1D (in geometric and electronic sense) "ladder oxocuprates", for which the largest $T_C = 12$ K b) M. Uehara, T. Nagata, J. Akimitsu, H. Takahashi, N. Ori, K. Kinoshita, *J. Phys. Soc. Jpn.* **1996**, *65*, 2764; c) ref. [330]). For an effective exciton mechanism of superconductivity in 1D structures see: d) J. E. Hirsch, D. J. Scalapino, *Phys. Rev. B* **1985**, *32*, 117; e) Z. Tesanovic, A. R. Bishop, R. L. Martin, *Solid State Commun.* **1988**, *68*, 337. Nanoscale one-dimensionality has also been discussed. There are many advantages, but also many technical problems with the synthesis of pseudo 1D metallic wires f) P. P. Edwards, P. A. Anderson, L. J. Woodall, A. Porch, A. R. Armstrong, *Mater. Sci. Eng.* **1996**, *217*, 198; g) A. Kelly, *Sci. Am.* **1965**, *212*(*2*), 28.

[332] Our preliminary DFT computations for $[AgF][AgF_4]$ in the $[CuF]$-$[AuF_4]$ structure indicate that pressure-induced metallization might occur at several GPa.